NYO-7687

PHYSICS AND MATHEMATICS

NATURAL ALPHA RADIOACTIVITY IN MEDIUM-HEAVY ELEMENTS (Thesis)

By
Ronald D. Macfarlane

May 28, 1959

Carnegie Institute of Technology
Pittsburgh, Pennsylvania

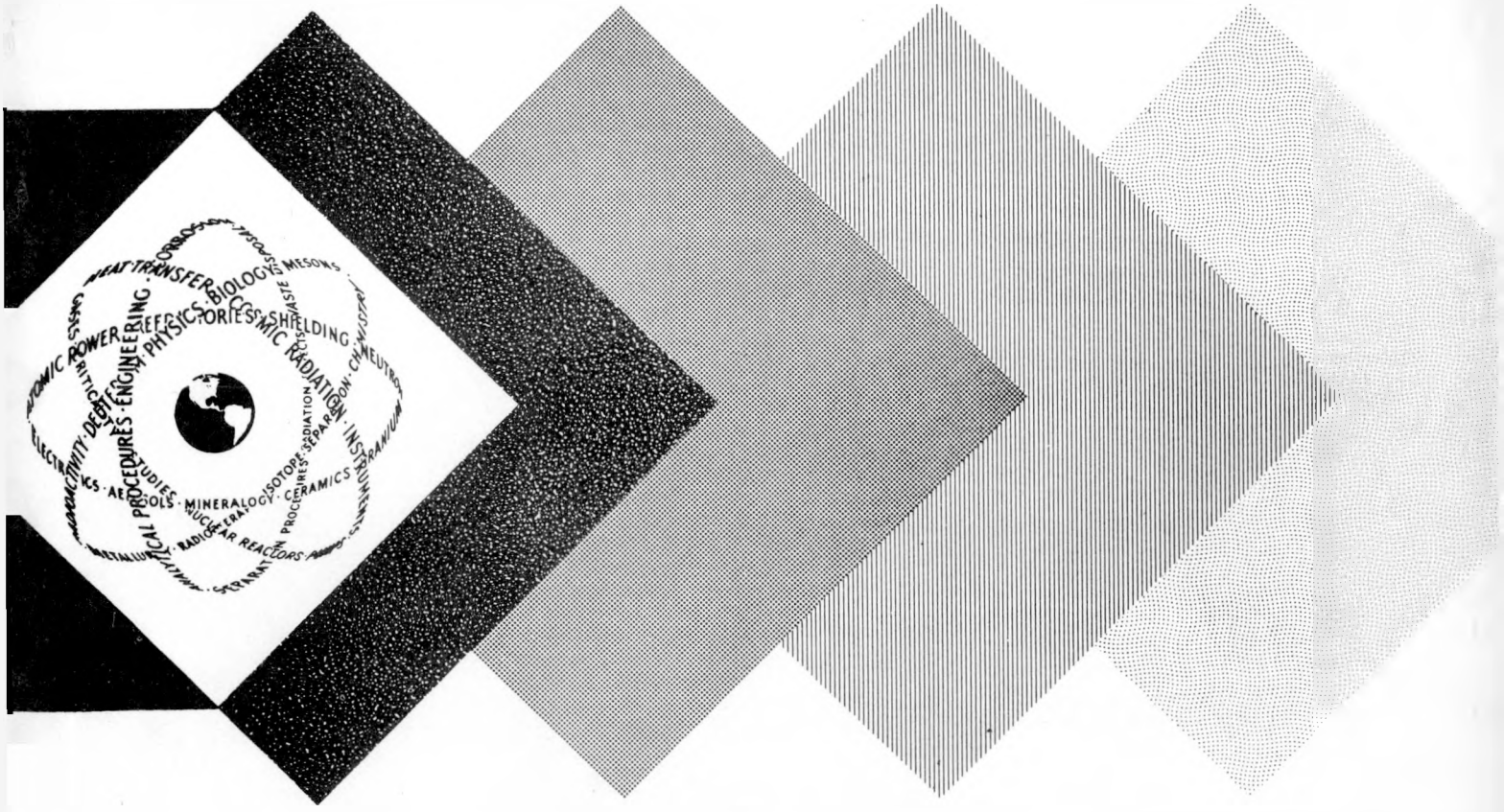

UNITED STATES ATOMIC ENERGY COMMISSION
Office of Technical Information

LEGAL NOTICE

Printed in USA. Price $2.75. Available from the Office of Technical Services, Department of Commerce, Washington 25, D. C.

USAEC Office of Technical Information Extension, Oak Ridge, Tennessee

NYO-7687

NATURAL ALPHA RADIOACTIVITY IN MEDIUM-HEAVY ELEMENTS

by

Ronald D. Macfarlane

Doctoral Dissertation

May 28, 1959

Contract No. AT (30-1)-844 with

United States Atomic Energy Commission

CARNEGIE INSTITUTE OF TECHNOLOGY

Department of Chemistry

Pittsburgh 13, Pennsylvania

Loch Sloy

TABLE OF CONTENTS

LIST OF FIGURES

LIST OF FIGURES (CON'T)

LIST OF TABLES

ACKNOWLEDGMENTS

I wish to express my appreciation to Professor Truman P. Kohman for his suggestion of this problem, his guidance during the course of the work, and for his critical evaluation of the results which were obtained. I would also like to thank Dr. Albert A. Caretto, Jr. for his guidance and supervision during the academic year 1957-58 while Professor Kohman was on leave of absence.

The invaluable assistance of Mr. Franc Mesojedec and Mr. James R. Simanton in the construction and maintenance of the electronic equipment used in this work and the contribution of my fellow graduate students through their many helpful discussions and their assistance in taking data is also greatly appreciated.

I would also like to thank the Isotopes Division of Oak Ridge National Laboratory for making available the enriched isotope samples used in this work, and the Westinghouse Atomic Power Division for the loan of the Po-Be neutron source.

I wish also to acknowledge the assistance of the Carnegie Institute of Technology Computer Center in the use of the IBM-650 computer and the staff of the Chemistry Department Machine Shop for their assistance in the construction of some of the equipment used.

Also, I am grateful to those responsible for the final preparation of the thesis: to Mrs. Thomas Becker for the preparation of the figures, to Miss Sonya Leszunov for the final typing, and to Mrs. Beverly Macfarlane for her assistance in proof-reading and compilation.

Finally, I would like to express my gratitude to the United States Atomic Energy Commission for the financial support of this research.

R. Macfarlane
May, 1959

SYNOPSIS

A large internal-sample ionization chamber was constructed and used in conjunction with a 24-channel pulse analyzer for the purpose of studying weak natural alpha radioactivities among the medium-heavy elements. The background of the counter was reduced to a low level by a careful selection of the materials used to construct the counter and by using massive shielding and anti-coincidence. A counting gas consisting of 94% argon, 5% ethylene, and 1% nitrogen was found to give good energy resolution and drift stability.

A method was developed for forming thin, uniform oxide films over a large (1200 cm^2) cylindrical surface area suitable for obtaining reasonably sharp alpha spectra.

The following nuclides were studied for the purpose of obtaining more precise values for the alpha particle energy, specific activity and half-life: Ce-142, Sm-147, Nd-144, and Pt-190. New natural alpha activities were sought in Sm-148, 149, Gd-152, Hf-174, and Hg-196. A search was made in natural Sm for the existence of Sm-146 activity, considered to be absent in nature because of a relatively short alpha half-life. Also, a sample of W enriched in W-180 was studied in order to determine whether this was the isotope responsible for the previously observed alpha activity in natural W.

The natural alpha activity of Nd-144, Sm-147, and Pt-190 was confirmed. It was not possible to detect alpha activity in Ce-142 at the level which had previously been reported. Neither was it possible to observe an activity in W-180 at the level expected assuming this to be the isotope responsible for the previously observed alpha activity in natural W. Other negative results were obtained for Sm-146, Sm-148,149, and Hg-196. New natural alpha activities were found in Gd-152 and Hf-174.

Ce-142- No new natural alpha activity was observed. A lower limit of 5.3×10^{16} years was set for the alpha half-life. This is a factor of 10 higher than the half-life which had previously been reported. The Q value has been calculated to be 1.69 ± 0.1 Mev using mass data. This energy corresponds to a theoretical half-life of 1.4×10^{18} years.

Nd-144- The alpha particle energy of Nd-144 was determined to be 1.84 ± 0.02 Mev and the alpha half-life, $(2.36 \pm 0.29) \times 10^{15}$ years.

Sm-146- No second activity was observed in natural Sm which could be attributed to Sm-146. An upper limit for the alpha half-life was set at $\leq 3 \times 10^{8}$ years and Q determined to be ≥ 2.45 Mev from theoretical considerations. Previous measurements with artificially-produced Sm-146 give Q = 2.6 Mev and the alpha half-life $\sim 5 \times 10^{7}$ years.

Sm-147- The alpha particle energy was determined to be 2.24 ± 0.02 Mev and the alpha half-life $(1.18 \pm 0.05) \times 10^{11}$ years.

Sm-148- No natural alpha activity was observed. A lower limit for the half-life was set at $\geq 2.4 \times 10^{14}$ years. Mass measurements give a Q of 1.9 ± 0.1 Mev which corresponds to a theoretical half-life of 1.2×10^{18} years.

Sm-149- No natural alpha activity was observed. A lower limit for the alpha half-life was set at $\geq 1.1 \times 10^{15}$ years. Mass measurements give a Q of 2.0 ± 0.1 Mev which corresponds to a theoretical half-life of 1.5×10^{16} years.

Gd-152- A new natural activity was observed. The alpha particle energy was determined to be 2.15 ± 0.03 Mev and the alpha half-life $(1.13 \pm 0.08) \times 10^{14}$ years.

Hf-174- A new natural alpha activity was observed. The alpha particle energy was determined to be 2.50 ± 0.03 Mev and the alpha half-life $2.0 \pm 0.4 \times 10^{15}$ years.

W-180- No alpha activity was observed. The alpha half-life was determined to be $\geq 8.8 \times 10^{14}$ years. Previous measurements with natural tungsten give 2×10^{14} years assuming W-180 to be the active isotope.

Pt-190- Alpha activity was observed in natural Pt and Pt enriched in Pt-190 and a confirmation of the previous mass assignment of the active isotope obtained. The alpha particle energy was determined to be 3.11 ± 0.03 Mev and the alpha half-life $6.9 \pm 0.5 \times 10^{11}$ years.

Hg-196- No alpha activity was observed. The alpha half-life was determined to be $> 1 \times 10^{14}$ years. From the systematics of the alpha energies (obtained from mass data) of the other Hg isotopes, Q for this nuclide was estimated to be 2.9 Mev corresponding to a theoretical alpha half-life of 1×10^{17} years.

Finally, using the available alpha decay, mass, and beta decay data and the Cameron Mass Formula, a plot was made of the alpha decay systematics of the region between Sn and Pb.

I. INTRODUCTION

A. General

The study of characteristics and peculiarities of alpha decay has unraveled many interesting facets of the nature of the structure of the nucleus and the forces which hold it together. Many properties of the nucleus, such as its size and shape, the nature of its excited states, and special stable configurations, can be elucidated from an analysis of alpha decay data.

Alpha radioactivity is a prominent mode of decay among the heavy elements where the energy available for alpha decay is large. Half-lives are observed over a large range of values from 10^{-15} seconds to 10^{11} years. For the elements below bismuth in the periodic table, alpha decay becomes a comparatively rare phenomenom.

G. Hoffmann, in 1921, was the first to detect alpha radioactivity in an element with atomic number less than 83 when he observed what he believed to be natural alpha activity in platinum. (Hof-21). Eleven years later, Hevesy and Pahl detected weak alphas arising from natural samarium. (Hev-32).

More nuclides were added to the list of medium-heavy alpha emitters in 1949 when S. G. Thompson, A. Ghiorso, J. O. Rasmussen, and G. T. Seaborg produced alpha emitters of gold, mercury, gadolinium, and dysprosium. (Tho-49). Since then, an extensive study has been made by Rasmussen and co-workers on artificially produced alpha emitters in the rare earth region. (Ras-53, Tot-58).

With the development of the nuclear emulsion technique, a very sensitive means of detecting weak alpha emitters was made available. Subsequently, by this method, new natural alpha emitters of bismuth, (Far-51, Por-52,56), tungsten (Por-53), neodymium (Wal-54, Por-54) platinum, (Por-54), cerium (Rie-57), and lead (Rie-58a) have been reported.

The data now available on medium-heavy alpha emitters show that the systematics of alpha decay in this region is analogous to that of heavy element alpha emitters; i.e. neutron deficient nuclides are more alpha labile, and nuclides decaying to or near major closed shells show an enhancement in alpha decay energy.

One property which a number of these alpha emitters possess which is not observable among the heavy elements is a very long half-life. To the experimentalist, this is a problem because he must design techniques with a very high sensitivity in order to detect these radiations. But to the theoretician, whose life's blood is the experimental result, it provides the data to test his theory in regions not before tested. It is this point which, in the author's eyes, makes the energy expended on this study of long-lived alpha emitters worthwhile.

B. Objectives of this Study

1. Development of A Technique For Studying Weak Natural Alpha Activities Using an Ionization Chamber

The first objective of this study was to develop a method for studying weak natural alpha activities using a large low-background internal-sample ionization chamber which could give a more precise measurement of alpha particle energy and specific activity than the nuclear emulsion technique. At the same time, an attempt would be made to approach the extremely high sensitivity of the nuclear emulsion technique for studying very weak alpha emitters.

2. Obtain Precise Measurements of the Alpha Energies and Half-Lives of Already Known Naturally Occurring Medium-Heavy Alpha Emitters

Included in this category are Ce-142, Nd-144, Sm-147, Pt-190, and Bi-209, and the natural tungsten alpha activity. It is important to obtain precise values of the alpha energy and half-life of these nuclides so that a

good comparison between theoretical and experimental half-lives can be made.

3. Search for New Alpha Activities in Some Naturally Occurring Medium-Heavy Nuclides

Natural alpha activity was sought in Sm-148, Sm-149, Gd-152, Hf-174, and Hg-196.

Good resolution of Sm-147 activity from the possible alpha activity of Sm-148, Sm-149, and Gd-152 is particularly important because their alpha energies are probably very close to the Sm-147 alpha energy and not resolvable by the nuclear emulsion technique. Hg-196 is a nuclide which is best studied using counters because of the effect of mercury on the silver in nuclear emulsions.

4. Search for Evidence of Sm-146 Alpha Activity in Natural Samarium

Sm-146 is beta stable but presumed missing in nature due to alpha instability. (Mat-42). This nuclide contains 84 neutrons so that it decays by alpha emission to a closed shell of 82 neutrons with an enhanced alpha energy. It has been produced by cyclotron bombardment of Nd with alpha particles and its half-life determined to be $\sim 5 \times 10^7$ years. (Dun-53). The large uncertainty in the half-life does not rule out, however, the possibility of its existence in nature.

5. Determine Whether W-180 is the Isotope Responsible for the Observed Natural Alpha Activity in Tungsten

Natural alpha activity has been observed in natural tungsten by Porschen and Riezler. (Por-53). The observed alpha particle energy (3.2 Mev) corresponds to a theoretical half-life of $\sim 10^9$ years, which, if correct, rules out any of the known natural isotopes of tungsten as being responsible for the activity. If the actual energy is considerably lower, ($\sim$ 2.6 Mev) then the alpha half-life would be much longer and the active isotope could be the lightest naturally occurring isotope, W-180.

6. Study of Alpha Energy Systematics Among the Medium-Heavy Elements

An attempt was made to obtain a clearer picture of alpha decay systematics in the medium-heavy elements using the latest available alpha decay, mass, and beta decay data.

7. Compare Theoretical and Experimental Alpha Half-Lives for the Medium-Heavy Alpha Emitters

An analysis was made of the quantum-mechanical alpha decay rate equation over large ranges of atomic number, alpha energy, and half-life, and compared where possible with experimental data. This study was made with the facilities of the IBM-650 magnetic drum calculator at the Carnegie Institute of Technology Computer Center.

C. Early Investigations of Natural Alpha Activity in the Medium-Heavy Elements

1. Introduction

The discovery of natural alpha radioactivity in samarium in 1932 (Hev-32) stimulated considerable interest in searching for alpha activity in other elements as well. All elements were considered likely possibilities and as a result specific activity limits were set for elements ranging from Be to Bi.

The first extensive survey was reported by G. von Hevesy and M. Pahl in 1934. (Hev-34). Using a Geiger counter and depositing samples internally on the walls of the counter they examined 22 elements for natural alpha activity. Negative results were obtained for La, Pr, Nd, Eu, Gd, Tb, Dy, Ho, Er, Yb, Lu, Y, Sc, Hf, Ge, Ga, Rh, Ru, Pd, Pt, Au, and Hg. Dysprosium and platinum showed slight activities but the activities were attributed to impurities. The general conclusion of the study was that none of the elements studied had a specific activity equal to or greater than samarium.

In the same year, W. F. Libby examined 5 elements for natural alpha activity using an internal sample screen wall counter. He was unable to find

alpha activity in Gd, Pr, Sn, I, and Be, and set a lower limit of 10^{14} years for the alpha half-lives of these elements. (Lib-34)

Soon afterward, J. Schintlemeister published the results of a search for the cause of reported anamolous 2-cm range pleochroic halo in certain micas. (Sch-35,36) Using an internal-sample ionization chamber in conjunction with an electrometer, he was able to obtain energy spectra and resolve activity due to uranium, thorium, and their decay products. He was unable to find the activity producing the halo but in the process established an upper limit for the specific activity of a number of elements. An upper limit of 2α/g/sec was set for the following elements: Ga, Ge, In, Tl, Se, P, Tm, Yb, Ir, Os, Re, W, Ta, Ba, Cd, Ag, Nb, Br.

In 1951, E. Broda and K. Jenkner reported their findings of a search of 13 elements for new natural alpha activities. (Jen-51). They employed the nuclear emulsion technique. Listed below are the elements studied together with the lower limit they established for the alpha half-life.

Element	Lower Limit of Half-Life (years)
Titanium	4×10^{15}
Zinc	4×10^{15}
Rubidium	17×10^{15}
Strontium	3×10^{15}
Zirconium	2×10^{15}
Molybdenum	9×10^{15}
Cadmium	6×10^{15}
Cesium	4×10^{15}
Praesodymium	4×10^{15}
Neodymium	0.3×10^{15}
Samarium (second group)	0.1×10^{15}
Lead	3×10^{15}
Bismuth	3×10^{15}

Also, using the nuclear emulsion technique, W. Porschen and W. Riezler investigated all the elements from cerium through bismuth. A summary of their results appears in a 1956 paper. (Por-56). They confirmed the results of Faraggi and Berthelot on the natural alpha activity of bismuth (Far-51) and of Waldron, Schultz, and Kohman (Wal-54) on the natural alpha activity of neodymium. They also reported new natural alpha activities in tungsten and platinum. They obtained negative results on 23 elements and reported lower limits for their alpha half-life.

Element	Lower Limit of Half-Life	
	1.5-2.5 Mev.	2.5-3.7 Mev.
Lanthanum	5×10^{15} years	7×10^{16} years
Cerium	4×10^{16} years	2×10^{17} years
Praesodymium	2×10^{16} years	3×10^{16} years
Europium	8×10^{15} years	8×10^{16} years
Gadolinium	4×10^{16} years	2×10^{17} years
Terbium	5×10^{16} years	1×10^{17} years
Dysprosium	5×10^{16} years	5×10^{16} years
Holmium	6×10^{16} years	1×10^{17} years
Erbium	1×10^{17} years	5×10^{17} years
Thulium	5×10^{16} years	2×10^{17} years
Ytterbium	1×10^{17} years	2×10^{17} years
Lutetium	1×10^{17} years	1×10^{17} years
Hafnium	2×10^{17} years	3×10^{17} years
Rhenium	2×10^{16} years	8×10^{16} years
Osmium	1×10^{17} years	1×10^{17} years
Iridium	1×10^{17} years	5×10^{17} years
Gold	3×10^{16} years	6×10^{17} years
Mercury	1×10^{13} years	1×10^{13} years
Thallium	6×10^{15} years	2×10^{16} years
Lead	2×10^{17} years	1×10^{18} years

Sufficient information concerning alpha decay systematics in the medium-heavy elements is now available from alpha decay data and atomic mass measurements so that it is possible to determine which is the element in the periodic table below which natural alpha activity cannot be observed. ($Q \leq 0$) From an analysis of the available data, which is presented later in the thesis, it appears that cerium is that element.

2. Summary of Negative Results on Natural Alpha Activity Between Cerium and Bismuth

The results of previous unsuccessful searches for natural alpha radioactivity in the medium-heavy elements are summarized in Table I. For each element, the natural isotope which is probably the most alpha labile is given and a lower limit for the half-life of that isotope calculated. Except for Nd and Ce, this isotope is what is considered to be the most neutron deficient naturally occurring isotope of that particular element. For Ce and Nd, the isotope decaying by alpha emission to the closed shell of 82 neutrons was chosen, Ce-142 and Nd-144. Also included is the upper limit for the specific activity of a natural sample of that particular element.

TABLE I

Summary of Previous Negative Results

Nuclide	Upper Limit of Specific Activity (α/gm/sec) (natural sample)	Lower Limit of Half-Life (years)	Reference
Ce-142	0.002	4.7×10^{15}	Por-56
Pr-141	100	1×10^{12}	Hev-34
	1	1×10^{14}	Lib-34
	0.023	4×10^{15}	Jen-51
	0.0047	2×10^{16}	Por-56
Nd-144	100	2.4×10^{11}	Maz-33, Yeh-33, Cur-33, Hev-34
	0.352	6.2×10^{13}	Jen-49
	0.305	7.2×10^{13}	Jen-51
	0.0183	1.2×10^{14}	Mul-52

TABLE I (CON'T)

Summary of Previous Negative Results			
Nuclide	Upper Limit of Specific Activity (α/gm/sec) (natural sample)	Lower Limit of Half-Life (years)	Reference
Eu-151	100	4.7×10^{11}	Hev-34
	0.011	3.8×10^{15}	Por-56
Gd-152	100	2×10^{9}	Hev-34
	0.84	2×10^{11}	Lib-34
	0.084	2×10^{12}	Kel-48
	0.002	8×10^{13}	Por-56
Tb-159	100	1×10^{12}	Hev-34
	0.0012	5×10^{16}	Por-56
Dy-156	100	5.2×10^{8}	Hev-34
	0.33	1.56×10^{11}	Gys-44
	0.0016	1.1×10^{13}	Por-56
	0.00000000042	1×10^{18}	Rie-58a
Ho-165	100	1×10^{12}	Hev-34
	0.0013	6×10^{16}	Por-56
Er-162	100	1.4×10^{9}	Hev-34
	0.0008	1.4×10^{14}	Por-56
Tm-169	2	3.9×10^{13}	Sch-36
	0.0016	5×10^{16}	Por-56
Yb-168	100	1.4×10^{9}	Hev-34
	2	5.5×10^{10}	Sch-36
	0.0008	1.4×10^{14}	Por-56
Lu-175	100	1×10^{12}	Hev-34
	0.00075	1×10^{17}	Por-56
Hf-174	100	1.9×10^{9}	Hev-34
	0.00074	3.8×10^{14}	Por-56
Ta-181	2	3.6×10^{9}	Sch-36
W-180	2	6.7×10^{10}	Sch-36
Re-185	2	3.6×10^{13}	Sch-36
	0.0036	7.4×10^{15}	Por-56
Os-184	2	6.5×10^{9}	Sch-36
	0.0007	1.8×10^{13}	Por-56

TABLE I (CON'T)

Summary of Previous Negative Results			
Nuclide	Upper Limit of Specific Activity (α/gm/sec) (natural sample)	Lower Limit of Half-Life (years)	Reference
Ir-191	2	1.3×10^{13}	Sch-36
	0.00069	3.8×10^{16}	Por-56
Pt-190	100	1.2×10^{8}	Hev-34
Au-197	100	1×10^{12}	Hev-34
	0.002	3×10^{16}	Por-56
Hg-196	100	1.4×10^{9}	Hev-34
	10	1.4×10^{10}	Por-56
Tl-203	0.0032	5.9×10^{15}	Por-56
Pb-204	0.021	4.5×10^{13}	Jen-49
	0.000014	7×10^{16}	Wal-53
	0.000064	1.5×10^{16}	Por-56
Bi-209	0.021	3×10^{15}	Jen-51
	0.000032	2×10^{18}	Hin-52,58

3. Summary of Positive Results on Natural Alpha Activity in the Medium-Heavy Elements

Listed in Table II are the results of previous searches for natural alpha activity in the medium-heavy elements which gave positive results. Except for some of the samarium studies and the early work of Hoffmann on the natural alpha activity of platinum all the measurements were made using the nuclear emulsion technique.

Except where indicated, all the elements studied contained their natural distribution of isotopes.

Because of the large number of investigations which have been made on samarium alpha activity, these results have been included in a separate table. (Table IIa)

TABLE II

Summary of Previous Positive Results

Nuclide	E_α(Mev)	Half-Life (years)	Specific Activity (α/gm/sec) (natural sample)	Reference
*Ce-142	1.5	5.1×10^{15}	0.002	Rie-57
Nd-144	1.9	1.5×10^{15}	0.015	Wal-54
	1.8	5×10^{15}	0.003	Por-54
*	1.8	2.2×10^{15}	0.0102	Por-56
Sm-147	See table IIa			
W (natural, isotope unknown)	3.2		0.000327	Por-53
Pt-190	3	6×10^{11}	0.01	Hof-21
	3.3	6×10^{11}	0.012	Por-54
*Pb-204	2.6	1.4×10^{17}	0.0000059	Rie-58a
Bi-209	3.2	2.7×10^{17}	0.0002	Far-51
	2.9	2×10^{17}	0.0003	Por-52
	3.0	2×10^{17}	0.0003	Por-56

*indicates that electromagnetically enriched isotopes were used.

TABLE IIa

Summary of Previous Results on Natural Alpha Activity of Samarium

Investigators	Reference	Specific Activity	E(Mev)	Method of Detection
G. V. Hevesy, M. Pahl	Hev-33	75 α/g/sec	2.20	Geiger count.
M. Herzfinkiel, A. Wroncberg	Her-34	67	3.10	ion ch
M. Curie, F. Joliot	Cur-34	88	2.80	cloud ch
G. Ortner, J. Schintlmeister	Ort-34	-	2.25	ion ch
M. Mader	Mad-34	89	2.30	ion ch
D. Lyford, J. Beardon	Lyf-34	102	2.90	ion ch
W. F. Libby	Lib-34	140	2.40	prop. count.
H. J. Taylor	Tay-35	-	2.20	nuc. emul.
R. Hosemann	Hos-36	89	2.20	nuc. emul.
L. Lewin	Lew-36	-	2.20	ion cn
P. Cuer, C. M. G. Lattes	Cue-46	94	2.20	nuc. emul.
E. Picciotto	Pic-49	133	-	nuc. emul.
Ch. Haenny, M. Najar, M. Gaillourd	Hae-49		2.20	nuc. emul.
W. P. Jesse, J. Sadauskis	Jes-50		2.18	ion ch
D. Szteinaznaider	Szt-53		2.12	nuc. emul.
G. Beard, M. Wiedenbeck	Bea-54	108	-	prop. count.
G. E. Leslie	Les-56	115	2.18	nuc. emul.
G. Beard, W. H. Kelly	Bea-58	103	-	scint. count.

4. Some Questions Concerning the Natural Alpha Activity of Samarium Solved by Previous Investigators

a. Anomalous Range Radiations in Samarium

In 1934, M. Mader reported that along with the 2.20 Mev alphas of samarium, there existed a second radiation with range 1.37 cm. (Mad-34). (The range of the 2.2 Mev alpha in air is 1.16 cm.) The specific activity of this second group, attributed to proton radiation, was reported to be 33 particles/g/sec. An attempt to verify Mader's results was made by G. Ortner and J. Schintlmeister, but they were unable to observe the second group. (Ort-34).

In 1936, H. J. Taylor and V. D. Dabholkar, using nuclear emulsions impregnated with samarium, reported the observation of a second group with a range of 3.5 cm and an intensity 1% that of the 2.2 Mev alphas. Through an examination of the grain density of these tracks, they attributed the radiation to protons. (Tay-36).

In the same year, R. Hosemann, reporting on the specific activity and range of the main alpha radiation, set a limit for a second group of less than 5% of the total activity. (Hos-36). Also, in 1936, L. Lewin reported the presence of a second group in samarium of very short range, 0.13 cm, which produced 35% as much ionization as the 2.2 Mev alpha. (Lew-36).

Using nuclear emulsions, M. Blau, in 1939, reported the presence of a second group in samarium of 2 cm range. (3.5 Mev) (Bla-39).

Eight years later, G. Frongia and N. Margongui, also using nuclear emulsions, reported that they could not find the radiations observed by Blau and Taylor. (Fro-47).

Finally, Jenkner and Broda, searched for and could not find a second radiation in samarium. (Jen-51). They set an upper limit of 0.08 particles/g/sec. for the specific activity of a second group.

b. Mass Assignment of Samarium Alpha Activity

The first attempt of a mass assignment to the samarium alpha activity was made by M. Curie and F. Joliot in 1934 (Cur-34). Utilizing the mass data of Aston, they calculated the alpha decay energy of a number of samarium isotopes and showed that Sm-148 appeared to be the likely isotope.

No further work was done on this problem until 1938 when T. R. Wilkins and A. J. Dempster separated electromagnetically and analyzed for radioactivity the various natural isotopes of samarium. In a preliminary report, they attributed the alpha activity to Sm-148. (Wil-38). The study was interrupted by the death of Professor Wilkins and not continued until 10 years later. In a paper by A. J. Dempster, he reported that the previous assignment of 148 by Wilkins and Dempster appeared to be in error and that more recent data indicated that the active isotope was 152. (Dem-48).

The possibility that Sm-146 was the active isotope was ruled out by Inghram, Hess, and Hayden when they observed with a mass spectrograph that the concentration of Sm-146 in natural samarium was less than 0.002%. (Ing-48). They pointed out that if the observed specific activity was due to Sm-146 it would correspond to a half-life of less than 2×10^7 years, a half-life too small to have survived geologic time.

After a more thorough investigation by Dempster, he reassigned the mass number of the isotope to 147. (Dem-49). This result soon afterward was confirmed by B. Weaver (Wea-50) and L. Love and W. A. Bell (Bel-50) by studying the radioactivity of each fraction of electromagnetically separated samarium isotopes.

A milligram amount of isotopically pure Sm-147 was obtained by J. O. Rasmussen, S. G. Thompson, and F. L. Reynolds as a decay product from an old Pm-147 source. The specific activity corresponded to the same order of magnitude of natural samarium assuming that Sm-147 was the active isotope (Ras-50).

5. Extinct or Nearly Extinct Beta Stable Alpha Emitters Among the Rare Earth Elements

a. Previous Investigations of the Possible Natural Occurrence of Sm-146

Sm-146 is considered to be beta stable because it lies between two stable even-even isotopes of samarium, Sm-144 and Sm-148.

It has been suggested that its apparent absence in nature is due to the fact that it has a relatively short alpha half-life (less than 10^8 years). (Mat-42).

Attempts have been made to detect Sm-146 in natural samarium with the aid of a mass spectrograph. M. Inghram, D. Hess, and R. Hayden could not detect it and set a value of less than 0.002% for the isotopic abundance. (Ing-48) T. L. Collins, F. M. Rourke, and F. A. White, employing a more sensitive spectrometer, also could not detect Sm-146. (Col-57). They set a limit of less than 0.00008% for the isotopic abundance.

Attempts have been made to produce artificially Sm-146 with the hope of being able to measure its decay properties. Long, Pool, and Kunder searched for Sm-146 activity in old neodymium targets which were bombarded with deuterons. (Lon-52) They observed an activity which might have been due to Sm-146 but the evidence did not appear to be conclusive enough. They estimated that the half-life probably lies between 10^4 and 10^6 years.

D. C. Dunlavy and G. T. Seaborg succeeded in producing a small amount of Sm-146 by an intense bombardment of neodymium with deuterons. (Dun-53). The samarium fraction, isolated from the target, was exposed for a few weeks to a nuclear emulsion plate. Ten tracks were observed with a mean range of 2.55 Mev. From the activity measured, together with estimates of the cross-section for Sm-146 production, an approximate value of 5×10^7 years was obtained for the half-life.

Considering the approximations involved in determining the half-life, the possibility that the half-life is long enough to be still present in nature cannot be ruled out. For a nuclide whose half-life is greater than 3×10^8 years it would be possible to detect it in nature by its radioactivity. (This is assuming the age of the elements to be 6.6×10^9 years.) (Bur-57).

b. Previous Investigations of the Possible Natural Occurrence of Gd-150

The situation with Gd-150 is similar to that of Sm-146. It was predicted to be beta stable (Koh-48) and is presumed missing in nature because of a short alpha half-life. ($< 10^8$ years).

D. Hess examined the mass spectrum of the natural gadolinium isotopes but could not find evidence for the presence of Gd-150. He set an upper limit of 0.005% for the isotopic abundance. (Hes-48). W. L. Leland also looked for natural Gd-150 using a mass spectrograph but obtained negative results. He set an upper limit of 0.0005% for the isotopic abundance. (Lel-50).

Recently, Collins, Rourke and White obtained a mass spectrum of the natural gadolinium isotopes. They observed a small peak in the spectrum which could be due to mass number 150, but the possibility of attributing this to an impurity ion was not ruled out. They set an upper limit of 0.002% for the isotopic abundance of Gd-150. (Col-57).

Gd-150 was produced artificially by Rasmussen, Thompson and Ghiorso in 1953 by an intense bombardment of europeum oxide with 19-Mev deuterons. (Ras-53). An alpha energy spectrum of the separated gadolinium fraction revealed the presence of a long-lived alpha emitter with an energy of $2.7 \pm .15$ Mev. The half-life was estimated to be greater than 10^5 years.

Here, as in the case of Sm-146, the uncertainty in the alpha decay energy does not exclude the possibility of the existence of Gd-150 in nature.

6. Unsettled Questions Dealing With Natural Alpha Activity in the Medium-Heavy Elements

a. The Question of the Natural Alpha Activity of Tungsten

In 1953, Porschen and Riezler reported the discovery of a very weak alpha activity in natural tungsten using the nuclear emulsion technique. (Por-53). They observed that the specific activity was 0.00032 α/gm/sec and that the track length corresponded to an alpha energy of 3.2 Mev.

Noting that the alpha energy was higher than would be expected for a natural tungsten isotope they calculated a theoretical half-life using the Gamow-Gurney-Condon formula and found that the half-life should be $\sim 6 \times 10^{8}$ years corresponding to this energy.

This relatively short half-life together with the observed specific activity rules out any of the known isotopes of tungsten as being the source of the activity.

As a possible explanation, they postulated that the activity was due to a rare isotope of tungsten, for example W-178, which is present in nature at a level too low to be detected by a mass spectrometer.

Assuming this rare isotope to have an alpha half-life of 6×10^{8} years, they (Porschen and Riezler) calculated that the present isotopic abundance of this isotope is $\sim 2.5 \times 10^{-7}$%.

In an attempt to confirm their hypothesis, Porschen and Riezler examined some samples of tungsten which were obtained from the mass 178 and 179 position of the isotope separator at Harwell. (Por-56). They were unable to observe an alpha activity in these samples. However, it is not known whether this experiment was sensitive enough to conclusively rule out the

possibility that W-178 or W-179 could be a naturally occurring alpha emitting nuclide.

The natural alpha activity of tungsten is still an open question. There is a possibility that the measured alpha energy is in error and is actually lower than 3.2 Mev, perhaps low enough to allow a mass assignment of 180, considered to be the lightest of the naturally occurring isotopes of tungsten. (Koh-54).

If the activity is due to a rare isotope, with a half-life of 6×10^8 years, the question is which isotope is it? Most probably it would be W-178 which is only two mass numbers removed from W-180. W-178 has been produced artificially and found to undergo electron capture with a 21 day half-life. (Wil-50). In order for the rare isotope to be 178, this would have to correspond to an isomeric state of W-178, the ground state being actually beta stable or having a very long beta half-life. Such long-lived isomeric states are not uncommon in this region of nuclides.

b. The Question of the Natural Alpha Activity of Bismuth

The discovery of natural alpha activity in bismuth was reported by H. Faraggi and A. Berthelot in 1951. (Far-51). Employing Ilford C-2 nuclear emulsions, they observed some tracks in a bismuth loaded emulsion corresponding to 3.2 Mev energy. The observed specific activity corresponded to a half-life of 2.7×10^{17} years for Bi-209, the only naturally occurring isotope of bismuth.

One year later, Porschen and Riezler reported their results on natural bismuth activity which were essentially in agreement with those of Faraggi and Berthelot. Also using nuclear emulsions, they observed an activity with 2.9 Mev energy and a specific activity corresponding to a half-life of 2×10^{17} years (Por-52).

Shortly afterward, Hincks and Millar published the results of their investigation of natural alpha activity in bismuth. They were unable to detect the activity reported by Faraggi and Berthelot and Porschen and Riezler. (Hin-52).

In a later paper by Porschen and Riezler, they reported finding a few more tracks in their original plate and also revised their estimate of the alpha energy to 3.0 Mev. (Por-56).

A recent paper by Hincks, Millar and Hanna gives an account of a careful analysis of their original data in which they failed to observe an activity in bismuth. They conclude that the alpha half-life is $> 2 \times 10^{18}$ years. They also calculate a value for the alpha disintegration energy of Bi-209 using nuclear reaction energy cycles and determined it to be $2.93 \pm .11$ Mev. Using this energy they obtained a theoretical range for the half-life as being between 5×10^{19} years and 5×10^{22} years.

Also, from their calculations, they found that an alpha disintegration energy of 3.22 Mev would correspond to a half-life of 2.8×10^{17} years. This energy and half-life is approximately the same as was obtained by Faraggi and Berthelot and Porschen and Riezler.

It should be possible to resolve this question of the natural alpha activity of bismuth by the use of counting techniques. With a counter of high sensitivity, the alphas of Bi-209 could be detected if the results of Faraggi and Berthelot and Porschen and Riezler are correct.

D. Methods for Determining the Energies of Unknown Alpha Emitters

General

In searching for new alpha activities, it is desirous to know approximately what the alpha decay energy is beforehand. Particularly in the case of even-even nuclides where the equations of the kinetics of alpha decay are well developed, a knowledge of the alpha decay energy enables one

to predict an approximate value for the half-life. In a study such as this, where new long-lived alpha emitters are being sought, an estimate of the alpha decay energy will determine whether a particular nuclide should have a half-life short enough to enable detection of its activity.

In this section, methods used to determine the energies of unknown alpha emitters will be discussed.

1. Mass Spectrographic Data

Recent mass measurements have been of such precision that alpha decay energies determined from them agree remarkably well with experimentally determined values. (Nie-57, Joh-57, Dem-58). These mass measurements have been used extensively in this study to evaluate alpha decay energies among the medium-heavy nuclides.

In Table III, a comparison is made between alpha energies determined from mass data and experimentally determined alpha energies. The agreement is generally quite good.

TABLE III

Comparison of Experimental with Calculated (From Mass Data) Alpha Energies

Nuclide	Q (Mev) (from mass data)	Reference	Q (Mev) (from alpha decay data)	Reference
Ce-142	1.70 ± 0.10	Nie-57	1.55 ± .20	Rie-57
Nd-144	1.80 ± 0.15	Nie-57	1.89 ± .02	this work
Sm-147	2.16 ± 0.15	Nie-57	2.30 ± .01	this work
Pb-204	2.41 ± 0.10	Dem-58	2.65 ± 0.20	Rie-58a
Bi-209	2.90 ± 0.10	Dem-58	3.2 ± .20 3.00 ± .20	Far-51 Por-56

2. The Semi-Empirical Mass Formula

On the basis of the liquid drop model of the nucleus, C. F. von Weizacker, in 1935, proposed a method for estimating the binding energy of a nucleus. (Wei-35)

The method considers the contribution of volume, surface, and coulombic effects to the total binding energy of the nucleus. Although each effect can be expressed in terms of the atomic number and mass number, coefficients for the functions must be determined empirically.

The evaluation of these coefficients has been treated by several authors utilizing nuclear decay data and data obtained from mass spectroscopic measurements (Bet-36, Fer-47, Mat-46, Fee-47, Pry-50, Ret-50, Fow-49, Gre-54).

In later developments and refinements of the mass formula, which was originally established for even-even nuclides only, a pairing term was added so that the mass formula could be valid for odd nucleon nuclides as well. (Boh-39, Sah-46) This added term has little effect, however, on the determination of alpha energies from the mass equation.

With the Weizacker-Bethe mass formula, Das (Das-50) and Pryce (Pry-50) showed that it satisfactorily described the observed trend in alpha decay energies as a function of mass number. Agreement between calculated and experimental values, however, was poor.

T. P. Kohman (Koh-49), utilizing the form of the mass formula suggested by Bohr and Wheeler, (Boh-39) determined the empirical constants in that equation with the aid of the Mattauch and Flugge packing fraction curve. With this, he obtained an estimate of the variation of alpha decay energy with mass number for the elements below bismuth.

In 1957, A. G. W. Cameron published an improved semi-empirical formula which included, among other refinements, empirical corrections in binding energy due to shell effects. (Cam-57). Alpha decay energies calculated with this formula are generally in good agreement with experimentally determined energies.

3. Energy and Mass-Energy Closed Cycles

The use of closed decay-cycle energy balances to determine the alpha decay energies of unknown alpha emitters has been used quite effectively for the heavy elements.

Unfortunately, the number of alpha emitters in the region of the medium-heavy elements is very small, so that the number of nuclides for which alpha energies can be calculated by this method is small.

By using mass data in combination with beta decay it is possible to obtain the alpha energies of a number of beta labile nuclides using a kind of mass-energy closed cycle calculation.

4. Empirical Alpha Decay Energy Formulae

When the alpha decay energy surface of the heavy elements is examined, it is immediately apparent that away from closed shells there is a systematic effect of the number of neutrons and protons on the observed alpha decay energy.

Utilizing this observation, Y. Pal Varshni developed an empirical equation relating the neutron and proton number to the alpha decay energy for the heavy elements (Var-56):

$$E\ (\text{Mev}) = 0.4\ Z - 1.795\ (N - 132)^{1/2} - 26.208\ [N > 132]$$

Varshni found that energies calculated with this formula agreed to within an average of 3.6% for the heavy elements.

Using the same format, N. K. Rama Swamy redetermined the empirical constants and established a similar equation for the medium-heavy nuclides: (Swa-56)

$$E_d = 0.36\ Z - 1.19\ (N-82)^{1/2} - 17.89 \qquad \begin{matrix}[N > 82,\\ Z < 82]\end{matrix}$$

Comparing energies calculated from this equation, Swamy found that the average fractional error was 0.053%.

Listed below are a number of nuclides for which the alpha decay energy was calculated by the Swamy formula together with the experimental alpha decay energy.

Nuclide	Q (Calculated, Mev)	Q (Experimental, Mev)	Reference
Sm^{147}	2.37	2.30	This work
Eu^{147}	3.11	2.98	Ras-53
Gd^{148}	3.47	3.27	Ras-53
Gd^{150}	2.77	2.80	Ras-53
Tb^{149}	3.83	4.08	Ras-53
Nd^{144}	2.03	1.90	This work
Pt^{190}	3.7	3.20	This work

The agreement with the experimental values is quite good for the rare earth alpha emitters. Between the rare earths and lead, however, the error appears to increase. This is probably due to the fact that there is very little information on alpha decay energies in that region which could be used in determining the parameters of an empirical equation.

When data do become available in the future, either from mass measurements or discovery of new alpha emitters, it might be possible to revise the constant in Swamy's formula so that it would give the correct energy values over a large range.

E. Theory of the Kinetics of Alpha Decay - The Bethe Formula

1. Introduction

A recent review article by I. Perlman and J. O. Rasmussen discusses the theory of alpha decay in great detail (Per-57). The reader is, therefore,

referred to this paper for a good discussion and review of the subject.

The theory, as it is developed to the present, gives good account for the kinetics of decay of even-even nuclides but the apparent complexity of the decay of odd-nucleon nuclei has not yielded to a satisfactory theoretical explanation.

Refinements of the theory of alpha decay since it was first treated as a quantum-mechanical-barrier penetration problem have been with the objective of modifying the original theory to correspond to the properties of the nucleus as we know them today. The original theory proposed by Gamow (Gam-28) and Gurney and Condon (Gur-28), however, employing a one-body model for alpha decay, is quite adequate for calculating the half-lives of even-even nuclides.

2. The Bethe Formula

In the section on the discussion of results, reference will be made to the rate formula originally derived by Gamow and later solved more exactly by Bethe. (Bet-37).

In Bethe's derivation, an expression for the decay constant is obtained in the following form:

$$\lambda = \frac{\sqrt{2}\,\pi^{2}\hbar^{2}\,e^{-2C}}{M^{3/2}R^{3}\left(2\frac{Ze^{2}}{R}-E\right)^{1/2}} \qquad \text{(IE-1)}$$

where M is the reduced mass of the alpha particle, Z and R, the charge and radius of the residual nucleus, and E the total alpha disintegration energy. The term C is the integral expression:

$$C = \left(\frac{2M}{\hbar}\right)^{1/2}\int_{R}^{R_E}\left(\frac{2Ze^{2}}{R}-E\right)^{1/2}dr \qquad \text{(IE-2)}$$

where R_E is the "classical turning point radius", defined as the distance from the nucleus where the potential and kinetic energy are equal.

The integral expression C was evaluated by Bethe in the following exact form:

$$C = \left(\frac{2M}{\hbar}\right)^{1/2} \frac{(2Ze^2)}{E^{1/2}} \left[\arccos\left(\frac{ER}{2Ze^2}\right)^{1/2} - \frac{ER}{2Ze^2}\left(1-\frac{ER}{2Ze^2}\right)^{1/2}\right] \quad \text{(IE-3)}$$

If the alpha energy E is neglected compared to the barrier height, the integral reduces simply to:

$$C = \frac{2\pi Ze^2}{\hbar v} - \frac{2e}{\hbar}(4ZMR)^{1/2}$$

where v is the reduced mass velocity of the alpha particle. This is the expression for C originally obtained by Gamow.

The quantity $\frac{\sqrt{2}\,\pi^2\hbar^2}{M^{3/2}R^3(2Ze^2/R - E)^{1/2}}$ in the decay constant formula has been interpreted as being the decay constant in the absence of a coulombic barrier, and is sometimes referred to as the frequency factor.

In order to evaluate R, the nuclear radius, different values of R are substituted into the equation until one is found which gives the correct alpha half-life.

Once R is obtained, the radius parameter, r_o, can be evaluated using the relationships, $R = r_o A^{1/3}$.

The radius parameter varies considerably in the neighborhood of a closed shell configuration, and even for nuclides far removed from closed shells there are observed small fluctuations in r_o.

Variations of the radius parameter are not necessarily associated with variations of the actual nuclear radius but may reflect inadequacies in the theory in failing to give the correct alpha decay rate for certain nuclides because of other effects, e.g. low probability for alpha particle formation due to closed shell effects.

The radius parameter has been evaluated by the author for thirty heavy even-even alpha emitters. An average value of 1.54×10^{-13} cm was calculated for the radius parameter in this region.

3. Variation of Alpha Half-Life With Energy and Atomic Number

Using equation IE-1 and IE-3, and a radius parameter of 1.54×10^{-13} cm, the alpha half-life was calculated for nuclides ranging in atomic number from 10 to 100 in intervals of 10 and for alpha energies ranging from 0.25 to 15 Mev. For each Z, the A which lies closest to the beta stability line was chosen.

The results appear in Figure I. This plot can be used to quickly obtain a rough approximation of the alpha half-life knowing the energy and Z (the variation of half-life with A for a given Z is not very large) or conversely, the alpha energy knowing the half-life and Z. Z and A refer to the parent nucleus.

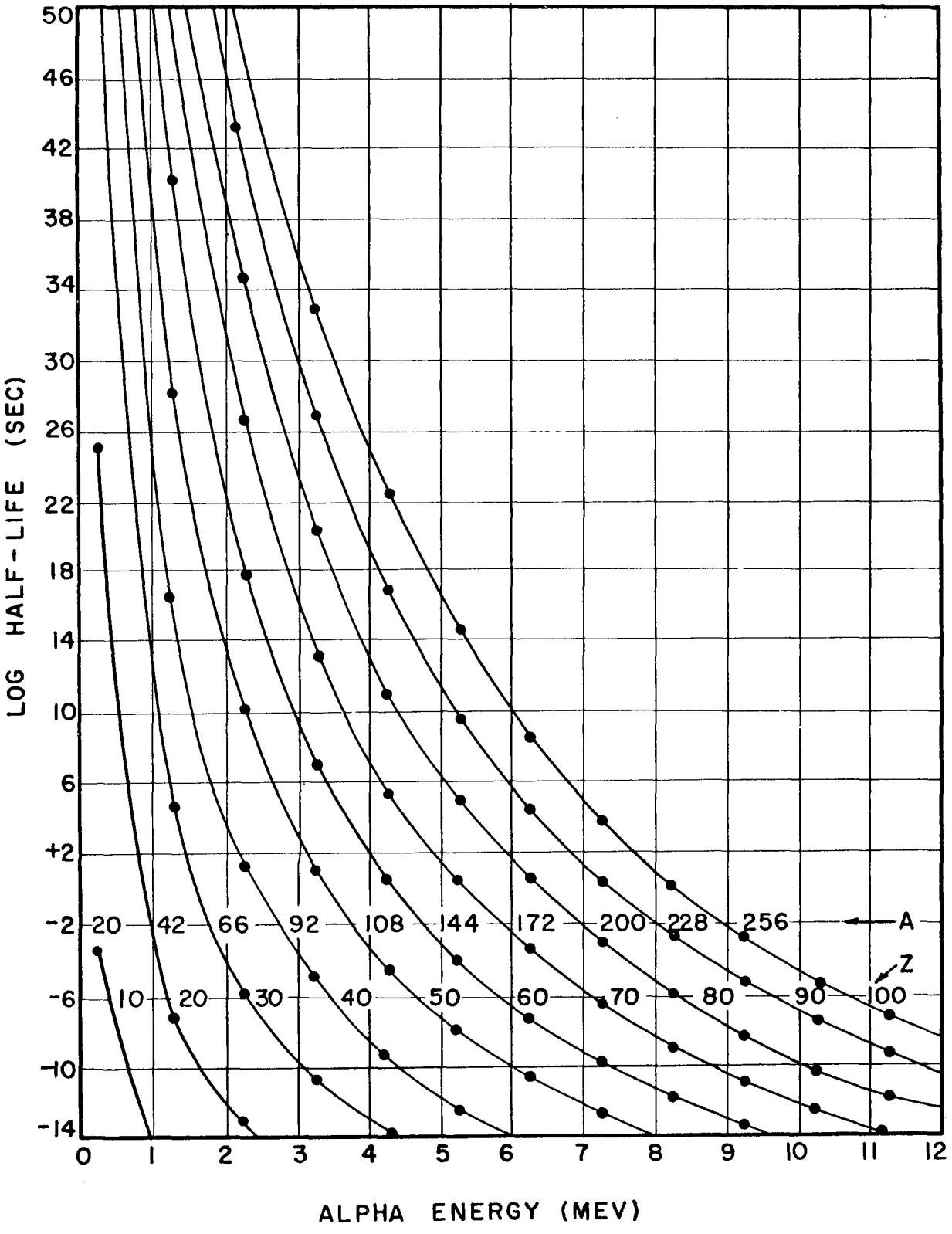

Figure I. Theoretical Alpha Half-life as a Function of Energy and Atomic Number (Bethe Formula)

II. DESCRIPTION OF APPARATUS

A. The Ionization Chamber

1. General Comments

On the basis of early investigations discussed in Section I, the level of the counting rate for the elements which were to be studied would probably be on the order of a few counts per hour to as small as fractions of a count per hour. In order to be able to detect such a small amount of of activity and obtain an energy spectrum, an ionization chamber was constructed which contained, it was hoped, the essential features for detecting these weak activities.

First, it was made fairly large. Approximately 1200 cm^2 were available inside the counter on which a sample could be deposited. Secondly, it was made as simply as possible: a metal cylinder sealed at both ends with O-ring seals and a fine wire, the collecting electrode, strung the length of the cylinder. This simplicity of design minimized the amount of surface area exposed to the sensitive volume of the counter, which aided in attaining a low background. From a practical standpoint, counter decontamination was a simple operation, as was trouble-shooting when the counter malfunctioned.

Once the counter was constructed, the next problem was to find methods for lowering the background, and developing the characteristics of the counter so that it would have a satisfactory energy resolution for alpha particles and at the same time good drift stability.

2. Description

The chamber shown in (Figure II) is a steel cylinder 51 cm long with an inside diameter of 11.2 cm and an outside diameter of 13.2 cm. The total sample area is 1200 cm^2. The anode is a 0.13 mm nickel wire strung the full length of the counter and running axially down the center. One end of the

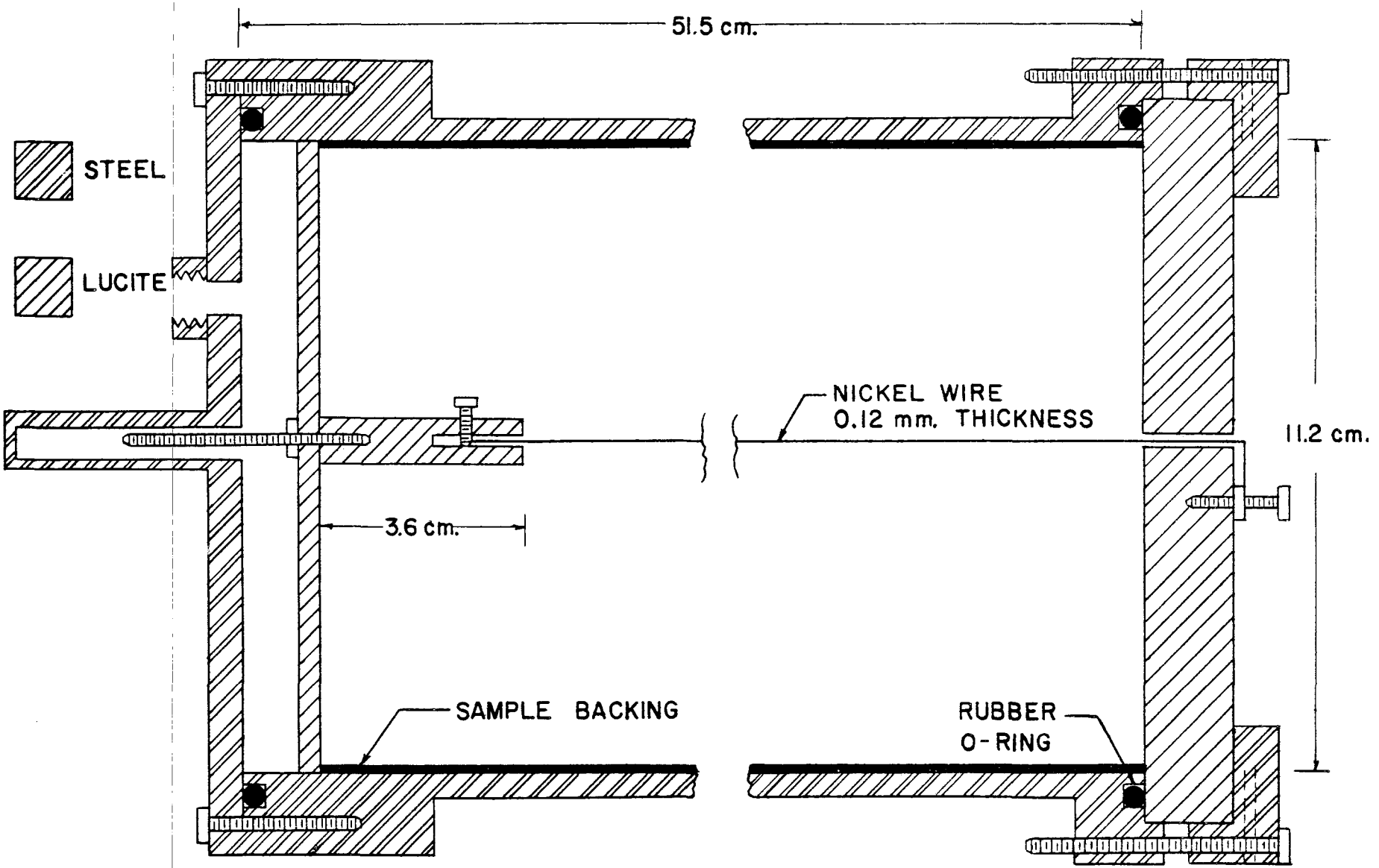

Figure II. Diagram of Ionization Chamber

wire passes through a small hole drilled through the center of a lucite end-plate and is fastened to a screw terminal on the outside surface of the plate. The hole is sealed with High Py-Seal Cement (Fisher Scientific Corp., Pittsburgh, Penna.). This is a solid resin which is particularly suited for making vacuum seals on glasses, metals, and plastics. It can be used at temperatures up to 150°C without softening. The connector for the other end of the wire is a lucite rod 3.6 cm long and 0.8 cm in diameter. Axial holes are drilled in both ends of the rod. One is to receive the nickel wire, which is then fastened into position with a set-screw; and the other, threaded, to receive a bolt which is fitted through a hole and secured with a nut to a lucite end-plate. This lucite end-plate is rectangular with the short sides rounded to fit snugly into the counter and against the sample backing. There is sufficient space between the walls of the counter and the long sides of the end-plate to allow for evacuation and filling of the chamber.

The counter is made vacuum tight at the "high voltage" end of the counter by an O-ring seal between the counter wall and the lucite disc. External pressure is applied to the seal by a metal ring which fits against the lucite end-plate and is bolted to a metal flange welded to the outside wall of the counter. The preamplifier housing is attached with screws directly to this metal ring. The seal on this end of the counter is more or less permanent and is only broken when the counter is disassembled for repairs or cleaning.

The other end of the counter is used for insertion and removal of samples. The seal on this end is made by an O-ring between the counter wall and a metal plate which is fastened to the end of the counter and against the O-ring seal with 8 screws. The valve which is used for evacuation,

filling, and sealing the counter is welded to this metal end-plate. It is a Type 493-CS two-way line-shut-off valve, manufactured by the Imperial Brass Manufacturing Co., Chicago 31, Illinois. The end open to the atmosphere is attached to a metal tube to which is clamped a ground-glass ball joint through a short piece of rubber vacuum tubing. The ball joint can be attached to a matching socket which is connected to the vacuum line.

3. Operation of the Counter

a. Introducing the Sample

The sample to be counted is deposited on a metal sheet (See section IV, C for methods of sample deposition), which is rolled into a cylinder approximately the diameter of the counter and slipped concentrically into it. The lucite end-plate is placed into position against the end of the metal sheet and at the same time the lucite rod holding the center wire fastened to it. The wire is adjusted from either end so it is taut and will not sag or vibrate. The metal end-plate is then put on and screwed tight to the O-ring. The counter is now ready for evacuation.

b. Evacuation

The chamber is attached to a glass vacuum line and pumped down to approximately 10^{-3} mm pressure using a Welch Duo-Seal mechanical fore-pump and a silicone oil diffusion pump. During the beginning of the pumping operation, the outside of the chamber is heated with a Fisher burner to speed up the degassing of the counter walls. Approximately two hours are required to reach 10^{-3} mm pressure, but this pumping operation is usually allowed to go overnight to insure good degassing.

This degassing technique is especially important when oxide samples are counted. Oxides retain small amounts of adsorbed gases which are difficult to pump off without heating. If these adsorbed gases are not removed in the evacuation operation, outgassing will continue while the sample is being counted.

This results in a gradual decrease in the size of the output pulse with time and a smearing out of the energy spectrum.

c. Counting Gas

The gas mixture that was used was a mixture of 94% argon, 5% ethylene, and 1% nitrogen.

First, a conventional gas mixture of 98% argon and 2% nitrogen was tried, and it gave good resolution for short counting periods (up to 10 hours). This is a mixture which has been used successfully by Facchini and co-workers.(Fac-56). Facchini points out that the reason for the nitrogen is to render argon less sensitive to the effects of trace amounts of oxygen, e.g. loss of pulse size and resolution, and drift.

The energy resolution for Po-210 alphas was good, ~ 6%, but the output pulse size had a tendency for an upward drift with time which amounted to as much as 16% for a three-day run. This behavior suggested that degassing was taking place in the counter resulting in the introduction of a small amount of some foreign gas or gases. The fact that the pulse size increased with time further suggested that these gases were causing the production of more ion-pairs for a given energy than for Ar-N_2 alone. Such an effect has been observed with argon mixtures where the added gas possessed an ionization potential lower than the excited metastable of argon (12.3 ev) (Ber-53, Mel-54, Jes-55). Through an interaction with an excited argon atom a molecule of this added gas is thought to de-excite the argon atom and become, itself, ionized. When other gases were tried which had an ionization potential greater than 12.3 ev no increase in pulse size was observed. With the counter used in this study, the impurity gas probably originates from the lucite end-plates.

Jesse and Sadauskis have shown that the addition to argon of a foreign gas (such as ethylene) having a lower ionization potential than the

meta-stable state of argon (10.5 ev for ethylene) increases the number of ion pairs produced for a given energy compared to pure argon. This increase becomes larger when the concentration of the added gas is increased but approaches a limit where the addition of more gas does not effect the pulse size (~ 1 part in 1000) (Jes-55). Addition of a large amount of a gas of low ionization potential to argon, then, should have the effect of stabilizing the pulse size against the addition of a trace of a gas of low ionization potential through outgassing.

Five percent ethylene was added to the mixture of 98% argon and 2% nitrogen. A 20% increase in pulse size compared to Ar-N_2 was observed for a given energy, and further, the pulse size no longer had a tendency to drift upward with time.

But, does the presence of ethylene in the gas effect the action of nitrogen in reducing the sensitivity of the gas to traces of oxygen? To test this, a gas mixture of 95% argon and 5% ethylene was tried. For a counting time of 3 days, the pulse size with this gas decreased to about 85% of its initial value, probably due to oxygen degassing. With the argon-nitrogen-ethylene mixture the pulse size decreased to about 95% of its initial value for the same period, under the same conditions. It appears, therefore, that the nitrogen is needed and the presence of ethylene does not appreciably effect the ability of nitrogen to minimize the effects of trace amounts of oxygen.

The effect of changing the relative amounts of argon, ethylene, and nitrogen was not studied. It is quite probable that a wide range of concentrations of the gases will give equally satisfactory results.

d. Operating Pressure and Anode Voltage

The performance of the counter was studied at four different pressures: 40 cm, 80 cm, 160 cm, and 240 cm. At each pressure a Sm-147 alpha

spectrum was recorded for different anode voltages in order to study the variation of output pulse size. The results appear in Figure III.

At a counter pressure of 40 cm, the output pulse size of the Sm-147 alpha is fairly constant from 160 volts to 450 volts, whereupon the pulse size rises sharply with increasing center-wire voltage due to gas multiplication. At 80 cm, the flat part of the curve is at 32 volts compared to 42 volts at 40 cm. This reduction in pulse-height is probably the result of more ion recombination at the higher pressure. This effect is also demonstrated at 160 cm and 240 cm where the pulse-height voltage in the flat part of the curve is 28 and 25 volts respectively.

At the pressures above 40 cm, there is a range of center-wire voltages where the pulse height increases slowly with voltage before it rises sharply due to proportional action. This is additional evidence for ion-electron recombination. At higher anode voltages, the field strength around the center-wire is stronger, so that when an ion-pair is formed in this field the positive and negative charges will migrate apart more quickly and the number of ion-electron recombination events reduced.

The sharpness of the Sm-147 alpha peak was approximately constant at the four pressures studied and appeared to be uneffected by changes in the anode voltage until the proportional region was reached. In the proportional region, the peak was spread out due to the statistical nature of proportional action.

A pressure of 160 cm was chosen as the operating pressure. It is advantageous to operate at a pressure greater than atmospheric because if there are very small leaks in the counter, so small that their effect is not observed when the chamber is evacuated, gas will leak out of the counter rather than air in. The latter situation would have a more serious effect on the output pulse of the chamber than if the pressure were to be decreased by some small amount.

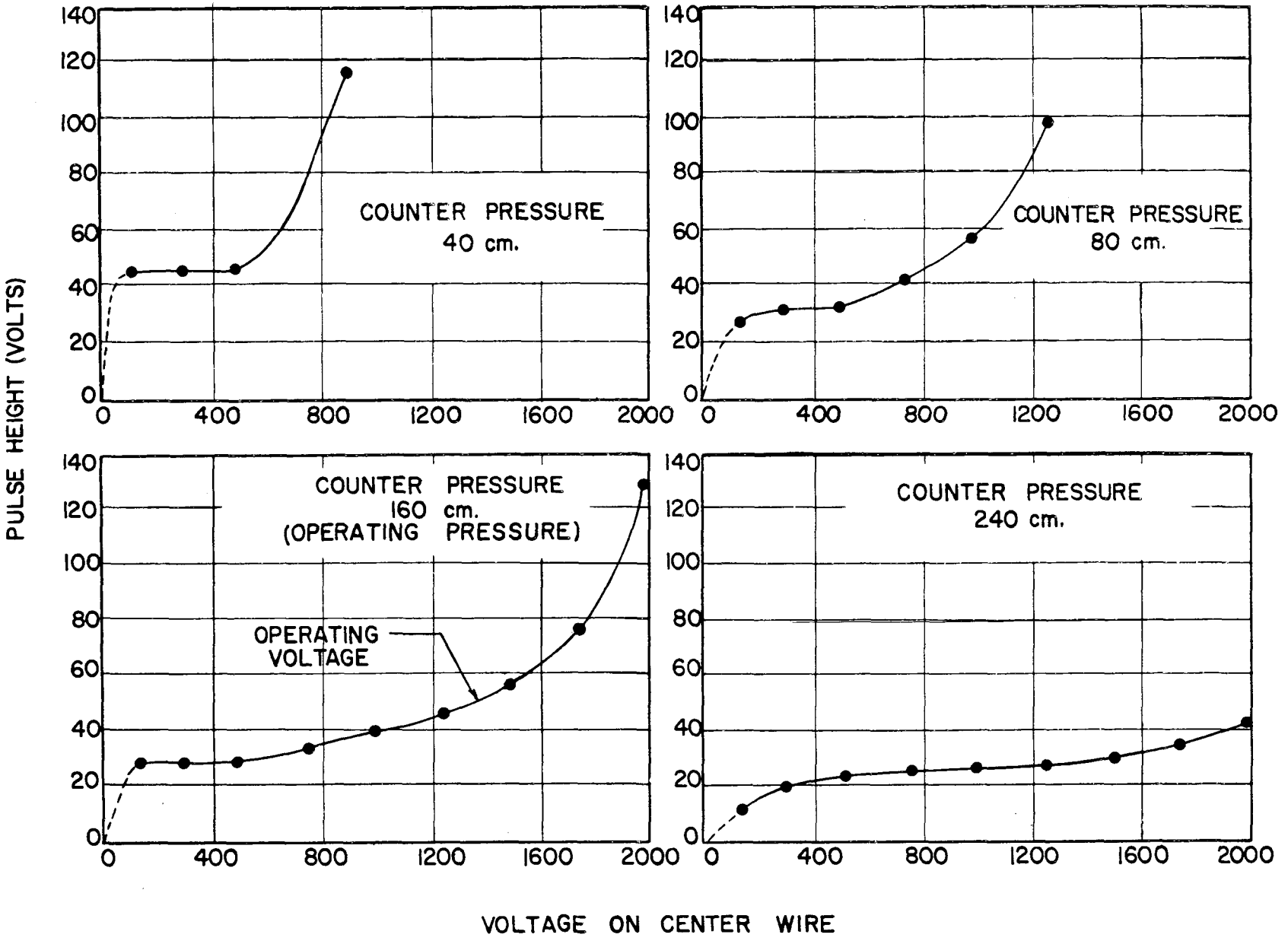

Figure III. Pulse-Height Voltage vs. Anode Voltage at Different Counter Pressures.

Some preliminary experiments were run at 80 cm but the drift stability was not quite as good as was desired. A slight decrease in the output pulse size was observed which amounted to 5% of its original value in a 3 day run. If this drift were due to oxygen outgassing from the walls of the counter, it should be possible to reduce the drift rate by increasing the amount of gas in the chamber, thus reducing the effective concentration of oxygen in the gas. At 160 cm pressure, the output pulse size was only reduced to 98% of its original value for the same counting time. Operating at still higher pressures would probably give even better drift stability, but the performance at 160 cm was considered to be quite acceptable and not warranting the extra effort involved in constructing an all metal vacuum system able to withstand high pressures.

An anode voltage of 1400 volts was chosen for the operating voltage. At 160 cm pressure, this voltage is in the region where the output pulse size varies slowly with anode voltage and is probably close to or just within the proportional region. Although at lower center-wire voltages, the output pulse is less sensitive to the anode voltage, the larger pulse size obtained at 1400 volts was necessary for obtaining precise measurements of the alpha energy.

e. Counter Performance

1. Resolution

The resolution of the counter is a property which measures the sharpness of an alpha peak in the energy spectrum. It can be expressed as the width of the peak at half-maximum divided by the pulse-height voltage corresponding to the maximum of the peak.

For a very thin (e.g. 0.01 mg/cm^2) source of Sm-147, whose alpha energy is representative of the alphas studied, a resolution of 3% has been observed for short runs up to 5 hours under the conditions of pressure and

anode voltage described above, and spreads out to ~ 6% for longer counting periods. The reason for this is that there is a small amount of counter drift plus the fact that the electronics are not completely stable. This causes a fluctuation of the output pulse height about a mean value.

2. Drift Stability

As mentioned above, for a three-day run the output pulse is reduced to only about 98% of its original value. With the electronic gain used, this amounts to a drift of about 1 channel (for 1 volt channels) for the Sm-147 alpha peak. If the run is to be counted for more than a three-day period, the counter, after the three-day run, is evacuated for 10 hours and refilled to the same pressure. The output pulse size usually returns to within half a channel of the original pulse size. If allowed to run more than three days without evacuating and refilling, the drift and resolution become progressively worse.

B. Electronic Equipment

1. Preamplifier

Pulses originating in the ionization chamber are first amplified in a standard Los Alamos Model 100 preamplifier having a gain of 150. A circuit diagram is given in the book "Electronics" (Elm-49).

The output of the ion chamber is connected to the grid of the first tube of the preamplifier through a 500-μμf high-voltage blocking capacitor rated at 20,000 volts. This capacitor, manufactured by Cornell-Dubilier (Cat. No. 3-MMU-200T5), is specially designed to withstand the effects of humidity and temperature and has been used for long periods of time without producing spurious pulses.

The output signal from the blocking capacitor is displayed to the grid of the first tube, a 6AK5, for the first stage of amplification. The second and third stage also are 6AK5 tubes. The third tube is a cathode

follower which permits the use of a long cable to transmit the pulse to the main amplifier. The preamplifier is mounted in a ventilated brass can which is bolted to one end of the chamber.

2. Main Amplifier

The signal from the preamplifier is increased further to a voltage suitable for pulse-height analysis by using an amplifier which follows rather closely the Higinbotham non-overloading design. It consists of two feedback loops involving four 12AX7 tubes followed by a 12AT7 inverter. Gain is provided by coarse and fine attenuators and by changing the feedback of the loops. The coarse attenuator located at the input advances by factors of two from 1 to 32. The fine attenuator is a divider in the plate of the 12AT7 and advances by steps of 0.1 from 0.5 to 1 of full gain.

The output of the amplifier is linear to 140 volts with a rise-time of less than 0.1 microsecond. A maximum gain of 1000 can be obtained.

3. Pulse Analyzer

The pulse analyzer was designed and constructed in this laboratory by J. R. Simanton. (See Figure IV for Block Diagram)

The output of the main amplifier is fed into an expander amplifier which subtracts a fixed voltage from the pulse and then amplifies this pulse. This expanded signal is displayed to the bank of 24 channels.

When anti-coincidence or coincidence is used, the anti-coincidence or coincidence signal is amplified in a gate amplifier. It then passes into a voltage discriminator which is adjustable to pass only those pulses which are greater than some desired threshold value. These pulses are then shaped and presented to the grids of the channel discriminators to block or pass the signal from the expander amplifier.

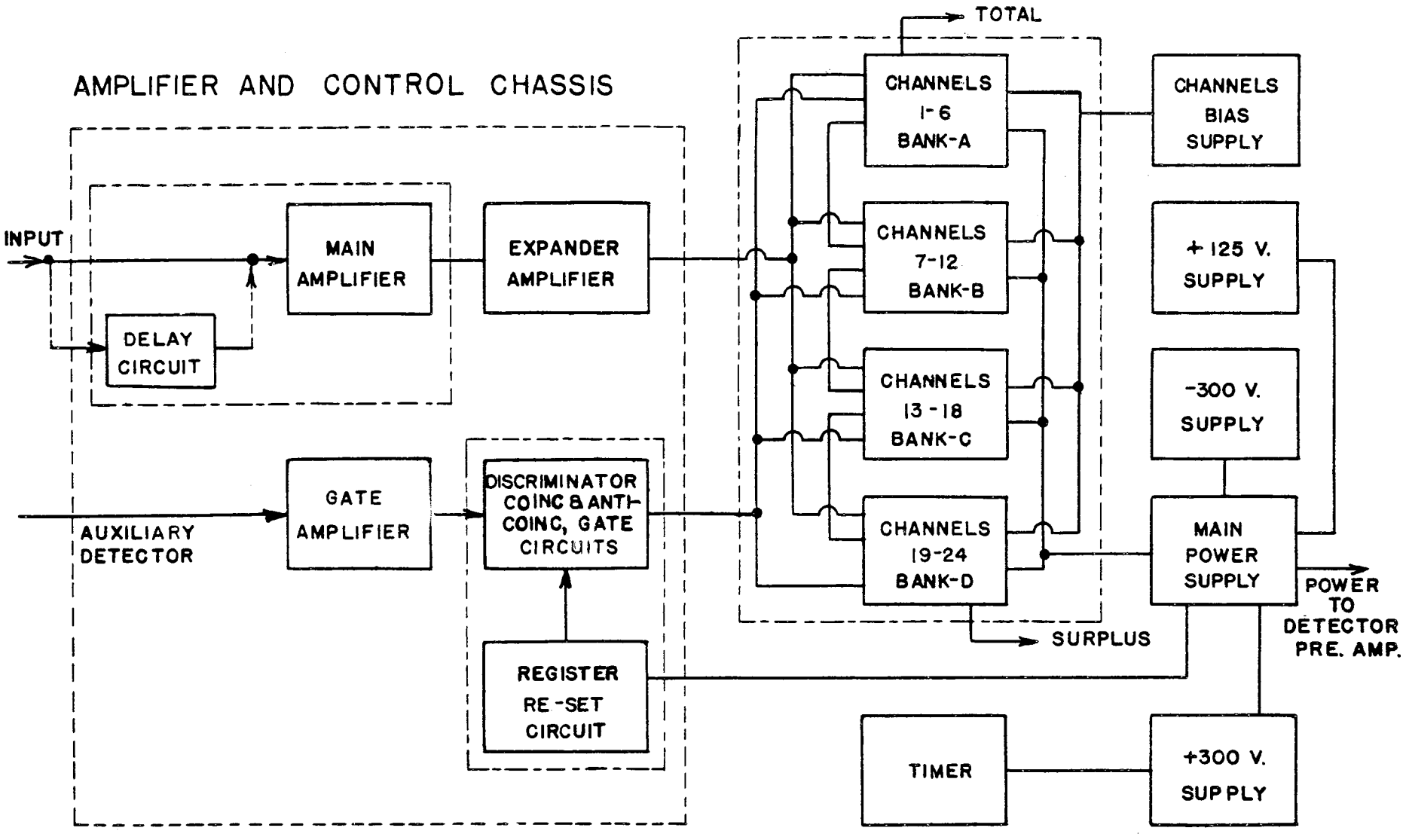

Figure IV. Block Diagram of Pulse Analyzer

4. Power Supplies

a. Preamplifier

1. Filament Supply- a B. F. Goodrich 57-plate 6-volt storage battery. With constant use, the battery is recharged every 3 days for a 10 hour period using a 6-volt Mallory tapering charger (Model 65AC6).

2. 300 volt Plate Supply- Model 28 Regulated Power Supply, Lambda Electronics Corporation.

b. High Voltage Supply for Ion Chamber - HV-2A Power Supply, 0-5000 volts, Technical Measurement Corporation. Two 50-megohm resistors are placed in series between the high voltage lead from the power supply and the high voltage connection at the ion chamber. Between the two resistors, a 0.05-microfarad Glassmike filter capacitor rated at 7500 volts is connected to ground.

c. Pulse Analyzer and Main Amplifier

1. 300-volt plate supply and 6-volt AC filament supply- Model 32 Regulated Power Supply, Lambda Electronics Corporation.

All power for the Lambda power supplies is obtained from a 110-volt AC line regulated by a 4-KVA Sola Constant-Voltage Transformer.

III. THE BACKGROUND IN THE REGION OF ALPHA ENERGIES

A. General Comments

One of the advantages the nuclear emulsion technique has over the use of an ion chamber for the study of weak alpha radioactivities is its extremely low background. This is due partly to the fact that different types of radiation can be distinguished. In a nuclear emulsion plate, a 3-Mev proton or meson can be distinguished from a 3-Mev alpha particle from the length of its track and its track density. In an ion chamber, however, if 3 Mev of energy is released, a pulse will be recorded of a certain size which is nearly independent of the nature of the ionizing radiation.

Also, with nuclear emulsions, it is possible to completely resolve alpha tracks of thorium, uranium, and their decay products. With solid-sample counting in an ion chamber, there is always some tailing of these activities into the low-energy region because of absorption of some of the radiation by the sample.

A factor limiting the sensitivity of the ion chamber for detecting weak alpha radiations is the level of the background activity. It must be reduced to a level where an activity of only fractions of a count per hour can be distinguished from the background.

In this work, the criterion for the observation of an activity was the presence of an alpha peak in the spectrum superimposed on the background. The smaller the width of the peak, (or the better the resolution), the lower is the effective background under the peak, because the peak is contained within a smaller energy interval. The resolution, therefore, is another factor effecting the sensitivity.

B. Factors Contributing to the Background

1. Natural Radioactivity of Materials of Construction

The only source of alpha radiation other than that from the sample to be studied which can contribute to the background comes from the materials used to construct the counter. Traces of uranium, thorium, and their decay products are present in all metals and plastics in varying amounts. By choosing those materials which are known to have a low alpha background, contribution of this source to the total background can be minimized. Studies conducted by McDaniel, Schaefer, and Colehour, and Grummit, Brown, Cruikshank and Fowler on the relative radioactive contamination of metals, glasses, and plastics have been a useful guide to the selection of the best materials (Dan-56, Gru-56). Among the metals, they find that steel and stainless steel have the lowest radioactive contamination. The background of plastics, however, are a factor of 50 lower than steel.

The counting gas also contributes some activity from the small amount of radon which has been introduced into the gas as a decay product of U-238 which is present in the walls of the gas cylinder. This does not present any problem, however, because these alpha particles can be easily resolved from the lower energy alphas by pulse-height analysis.

The contribution of beta and gamma radioactivity to the background is very small because the long range and low specific ionization of these radiations prevents them from depositing greater than 1.5 Mev energy in the counter.

2. Natural Radioactive Contamination of Samples

It is impossible to remove the last traces of samarium, uranium, thorium and their decay products from the samples to be studied. By using pulse-height analysis, however, the major portion of counts from these sources

can be resolved. But, because of self-absorption there is some tailing of the heavy element contamination into the low energy region. The corrections for this increase in background will be discussed in the section pertaining to the analysis of data. (Section V, B, part 3).

3. External Radiations

There will not be much contribution from the natural radioactivity of the environment close to the counter to the total background. Gamma ray sensitivity will be low but will increase slightly when high Z samples are put in the chamber for counting.

Certain components of cosmic radiation will be detected by the chamber and give pulses greater than 1 Mev energy, e.g. μ-mesons, protons, and cosmic-ray produced showers and cascades. By nuclear reactions with the counting gas and walls of the counter, the neutron component of cosmic rays will also contribute. For thermal neutrons, it is possible to produce pulses through interactions with hydrogen and nitrogen nuclei in the counting gas. Some examples of fast neutron reactions which can occur are $Ar^{40}(n,\alpha)S^{37}$, $Ar^{36}(n,\alpha)S^{33}$ from the counting gas and $Fe^{56}(n,\alpha)\ Cr^{53}$, $Fe^{57}(n,\alpha)\ Cr^{54}$ from the counter walls.

4. Electronics

For systems utilizing high electronic gain, the presence of electronic noise, pick-up, and "hum" can be a serious problem. If the level is high enough, pulses will appear which are on the order of the size of the pulses produced by alpha particles in the chamber.

To keep the level to a minimum, care was taken in the layout of the components of the preamplifier and its construction. A 6-volt storage battery for the filament supply of the preamplifier rather than an A.C. supply was found to greatly reduce the "hum" level. All plate voltage supplies used were designed to give voltages free from spurious pulses.

The first tube of the preamplifier, the major source of noise, was carefully chosen to give a low noise level, and was periodically replaced.

By careful electrical shielding of the most sensitive part of the system (the preamplifier and ion chamber) it was possible to reduce the sensitivity of the system to electrical pick-up to a negligible level.

A check on the contribution of these effects to the background was made periodically. To do this, the center wire from the chamber was disconnected from the high voltage blocking capacitor in the preamplifier. An "electronic background" was then taken at the same voltage and gain settings. With normal operation, no more than 0.1 counts per hour has been observed above the pulse-height voltage corresponding to 1 Mev.

C. Methods Used to Reduce the Background

1. Copper Plating of Sample Backing

The largest area exposed to the sensitive volume of the chamber is the metal sheet on which the sample is deposited. A large decrease in the background would be expected if the number of alphas emitted by the sample backing could be greatly reduced. These alphas are emitted by uranium and thorium impurities distributed throughout the metal so that their alpha spectrum has the shape of an infinitely-thick sample, i.e. an even distribution of activity throughout the energy spectrum, at least up to 4 Mev. By covering the surface with a material containing fewer radioactive impurities, it should be possible to reduce somewhat the overall background.

A reduction was observed when the sample backing (Type 304, stainless steel) was covered with a thick coat of freshly electroplated copper. (100 mg/cm^2) (See section IV, C, part 3 for a description of the plating technique.) The background counting rate between 1 and 4 Mev was reduced from 28 to 16 counts per hour with the decrease occurring fairly uniformly over the entire spectrum. The counter pressure was 160 cm and anticoincidence cancellation was used.

What part of the residual background was actually due to the sample backing was not known so it was not possible to quantitatively evaluate the effectiveness of the plating technique in reducing the contribution of the sample-backing to the total background. One can say, however, that a significant reduction is affected.

Unfortunately, the copper plating technique could only be used in those cases where it was not required to flame the sample backing. When heated with a Fisher burner, copper forms a loose non-adherent layer of copper oxide. In later experiments, a different type of stainless steel was found which gave almost the same background bare as the copper plated Type 304 stainless. This second type is 302 stainless. It is not known why the Type 302 stainless should have a smaller level of contamination. The nickel and chromium contents are approximately the same but the carbon content of the 304 is larger by a factor of 2. Possibly the difference is due to the fact that they might have been manufactured by different companies.

2. Massive Shielding

Surrounding the ion chamber with massive shielding does not offer a very great reduction in the background above 1 Mev. (See Figure V). This is not surprising because the radiations which are effectively absorbed by massive shielding, betas and gammas, do not contribute appreciably to the background in this region. That part of the background which can be reduced by massive shielding is probably due to the soft component of cosmic rays and the very small number of gammas which give pulses large enough to be counted.

3. Shielding Arrangement

The shield consists of a steel chest with walls 5.1 cm thick, 45.5 cm high, 51 cm wide, and 10 cm long. The ends of the chest are closed off by steel doors 5.1 cm thick. The chest is surrounded by a layer of

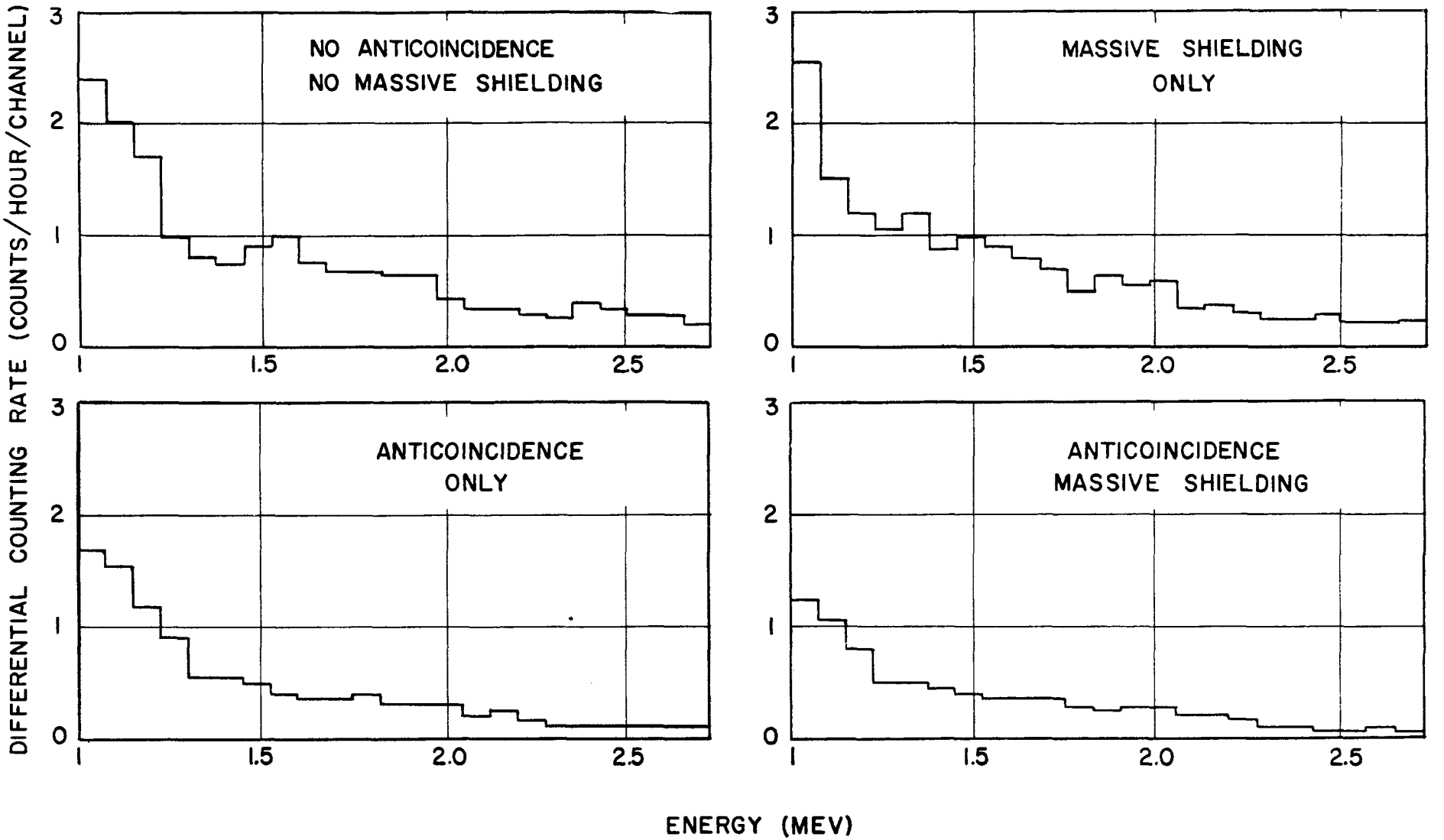

Figure V. Effect of Massive Shielding and Anti-Coincidence on the Alpha Background.

lead bricks 10 cm thick on top, 7.6 cm along the sides, and 5.1 cm on the bottom. Additional shielding is provided by a cylindrical mercury shield which fits inside the chest. It is made from two concentric steel tubes 66 cm long and connected at each end by iron rings 1.2 cm thick welded to the two cylinders. The inside diameter of the smaller cylinder is 12.7 cm. The annular space of 1.2 cm is filled with triple-distilled mercury.

4. Anti-coincidence Cancellation

The effectiveness of anticoincidence guard tubes for reducing the background of Geiger and proportional counters has been clearly demonstrated by many workers. Anti-coincidence cancellation has never been used in conjunction with alpha decay studies, probably because very low level alpha activities have never been studied before using counters.

The only radiations which can be cancelled by anti-coincidence are those which are ionizing and are capable of passing through massive shielding, producing at least one ion pair in the Geiger guard tubes, and releasing greater than 1 Mev energy in the ion chamber, e.g. the μ mesonic component of cosmic rays, protons, showers, and cascades.

5. Arrangement of Anti-coincidence Guard Tubes

The guard tubes are Model No. B32A20S commercial tubes obtained from H. W. Leighton Laboratories. The tubes measure 76 cm in length with an outside diameter of 5.1 cm. For the counting gas, a mixture of argon and ethyl alcohol is used at a pressure of 16 cm. Operating voltage is 1200 volts.

Fifteen tubes are packed tightly around the circumference of the mercury shield and are themselves shielded by the steel chest and lead bricks. The anodes of the tubes are connected in parallel, and voltage is applied to this electrode. The total counting rate of this arrangement is 2500 counts per minute.

6. Summary of the Effect of Massive Shielding and Anti-coincidence on the Background Above 1 Mev

The background study which has been referred to above and is represented in Figure V was made at a counter pressure of 160 cm with 94% argon-4% ethylene-1% nitrogen as the gas. The sample backing covering the entire surface of the counter was a bare Type 302 stainless steel sheet, the same type as was used for a large number of the measurements.

The integral counting rate for each of the runs represented in Figure V is given in Table IV for different regions of the spectrum.

TABLE IV

Effect of Massive Shielding and Anti-coincidence on the Background Above 1 Mev

Conditions	Counting Rate (Counts/hour)			
	1-1.5 Mev	1.5-2 Mev	2-2.5 Mev	2.5-3 Mev
No anti-coincidence, no massive shielding	8.9 ± 0.5	3.6 ± 0.4	2.5 ± 0.3	1.9 ± 0.2
Massive Shielding Only	7.7 ± 0.7	3.2 ± 0.5	2.9 ± 0.4	1.4 ± 0.3
Anti-coincidence Only	6.3 ± 0.6	2.6 ± 0.4	1.9 ± 0.3	1.0 ± 0.2
Anti-coincidence plus Massive Shielding	4.2 ± 0.4	2.4 ± 0.2	1.7 ± 0.2	0.8 ± 0.1

From these measurements, the conclusion is that massive shielding contributes only slightly to the lowering of the background and most of the effect is in the low energy region ($<$1.5 Mev). Anti-coincidence cancellation lowers the background still further in the low energy region and also has a significant effect between 1.5 and 3 Mev, the region covering the alphas studied, lowering it by a factor of 1.5.

IV. SAMPLE PREPARATION

A. Source of Samples and Isotopic Composition

1. Natural Samples

Samarium- A sample of samarium oxide of 99.9% purity was obtained from the Lindsay Chemical Company, West Chicago, Illinois.

Platinum- The natural platinum sample which was studied was obtained in the form of a metal sheet from the chemical stock room of Carnegie Institute of Technology. The original source is unknown.

2. Enriched Isotope Samples

All the enriched isotope samples used in this study were obtained from the Isotope Division of the Union Carbide and Carbon Corporation, Oak Ridge, Tennessee.

Listed in Table V are the isotopic analyses which were given for each sample.

TABLE V

Isotopic Composition of Enriched Isotope Samples

Element	Isotope	Atomic Percent	Enrichment Factor
Cerium	136	<0.01	
	138	<0.01	
	140	9.92 ± 0.06	0.11
	142*	90.08 ± 0.06	8.13
Neodymium	142	1.06 ± 0.057	0.04
	143	1.18 ± 0.078	0.10
	144*	62.62 ± 0.299	2.62
	145	2.80 ± 0.068	0.34
	146	31.51 ± 0.252	1.83
	148	0.66 ± 0.107	0.12
	150	0.17 ± 0.042	0.03

Samarium	144	0.1 ± 0.02	0.03
	147	6.4 ± 0.2	0.43
	148*	83.1 ± 0.3	7.42
	149	7.3 ± 0.1	0.53
	150	1.2 ± 0.1	0.16
	152	1.3 ± 0.1	0.05
	154	0.6 ± 0.06	0.03
	147	1.0 ± 0.05	0.07
	148	4.0 ± 0.1	0.36
	149*	88.8 ± 0.1	6.43
	150	3.5 ± 0.1	0.47
	152	1.9 ± 0.05	0.07
	154	0.9 ± 0.05	0.04
Gadolinium	152*	14.96 ± 0.28	74.8
	154	9.75 ± 0.13	4.53
	155	27.26 ± 0.27	1.85
	156	19.32 ± 0.19	0.94
	157	10.08 ± 0.18	0.69
	158	11.67 ± 0.21	0.47
	160	6.97 ± 0.24	0.32
Tungsten	180*	6.95 ± 0.02	49.6
	182	42.16 ± 0.03	1.61
	183	14.15 ± 0.04	1.69
	184	22.22 ± 0.06	0.72
	186	14.52 ± 0.03	0.51
Platinum	190*	0.76 ± 0.02	67.9
	192	5.80 ± 0.03	7.43
	194	45.32 ± 0.19	1.38
	195	29.64 ± 0.14	0.88
	196	15.63 ± 0.11	0.62
	198	2.85 ± 0.03	0.40
Hafnium	174*	10.14 ± 0.10	56.3
	176	19.28 ± 0.13	3.71
	177	28.87 ± 0.17	1.56
	178	21.72 ± 0.06	0.80
	179	7.14 ± 0.06	0.52
	180	12.86 ± 0.08	0.37
Mercury	196*	1.46 ± 0.01	9.74
	198	7.48 ± 0.06	0.75
	199	9.03 ± 0.04	0.53
	200	13.15 ± 0.07	0.57
	201	7.87 ± 0.04	0.60
	202	25.24 ± 0.09	0.85
	204	35.78 ± 0.09	5.25

* indicates enriched isotope

B. Radiochemical Purity of Samples

The level of radioactive contamination in the samples which were studied was checked by obtaining an alpha energy spectrum in the region of 1-6 Mev and determining whether the level was low enough to enable easy detection of the activity under examination. The major part of the activity due to uranium, thorium, and their decay products is resolved by pulse-height analysis, but some of the activity from these alpha emitters appears in the low energy region (1.5-3 Mev) due to sample-thickness effects. For the rare earth alpha emitters, only a very small amount of samarium contamination can be tolerated because the Sm-147 alpha energy is nearly the same as the energies of the rare earth alpha emitters studied. Fortunately, the level of alpha emitting contaminants in the samples which were examined was low enough so that no radiochemical purification was required.

C. Sample Deposition

1. General Comments

One of the thorniest problems in this work was the problem of developing a technique for uniform sample deposition over a large area (1200 cm^2).

In alpha particle spectroscopy where it is desirous to obtain sharp spectra in order to determine alpha energies precisely, the condition of the sample plays an important role: it must be thin and uniform.

Electrodeposition of the sample onto the sample backing affords the kind of deposit required and gives a good deposit over a large area. Unfortunately, however, the number of elements in this study which could be electroplated was only one: platinum. Practically all the other elements were electropositive and did not lend themselves to a convenient electrodeposition technique. It, therefore, became necessary to develop another method for the deposition of these samples.

The method developed consisted of spreading an alcohol solution containing the sample as an alcohol soluble salt, evaporating off the alcohol, and finally igniting the residue to the oxide.

In cases where it was not possible to prepare an alcohol soluble salt, an alcohol slurry was prepared and spread over the sample backing.

The techniques and experimental conditions employed are described in detail in the following section.

2. Preparation of Sample Backings

a. General Comments

In the section pertaining to techniques used in reducing the alpha background. (Section III, C), it was demonstrated that a low background could be obtained if proper care was taken to minimize the contribution of the sample backing. A stainless steel backing whose inside surface was freshly electroplated with a thick coat of copper gave the lowest background which was obtained. This sample backing was used effectively for the enriched tungsten, mercury, and platinum runs.

However, for the rare earth studies, where it was necessary to heat the sample backing to red heat, it was not possible to use a copper coated sample backing because of the formation of a loose, scaly copper oxide deposit when the backing was heated to red heat.

Fortunately, a stainless steel backing was found whose level of activity was almost as low as copper coated stainless steel. This backing was used for the rare earth studies.

b. Preparation of Copper-Coated Stainless Steel Backing

The stainless steel backing was a sheet measuring 34.3 cm wide, 48.3 cm long, and 0.045 cm thick. It was a Type 304 stainless steel obtained from Williams and Co., Inc., Pittsburgh, Penna.

First, the sheet was rolled into a cylindrical shape 48.3 cm long and approximately 11.4 cm in diameter. A sheet metal roller was used to obtain a uniform cylindrical shape.

To remove grease and other foreign materials from the surface, the sheet was thoroughly cleaned first with benzene, then followed by alcohol.

A thick coat of copper (100 mg/cm^2) was then electroplated on the inside surface of the cylindrical sheet.

c. Copper Plating Bath

The plating bath was a standard sulfuric acid–copper sulfate formulation. (Gra-53).

(1) Bath Formula–

Copper Sulfate– 188 g/liter

Sulfuric Acid– 74 g/liter

(2) Total Volume of Bath– 7.5 liters

(3) Anode– Cold Rolled Electrolytic copper rod, 2.5 cm diameter, 50 cm long; obtained from Williams and Co., Inc., Pittsburgh, Penna.

(4) Cathode– Stainless Steel Sheet– 1500 cm^2 area

(5) Cathode Current Density– 0.001 amperes/cm^2

(6) Plating Time– 24 hours

d. Preparation of Stainless Steel Backing

The stainless steel backing which was used for the rare earth studies was a sheet measuring 34.3 cm wide, 48.3 cm long, and 0.045 cm thickness. It was a Type 302 stainless steel obtained from Williams and Co., Inc., Pittsburgh, Penna.

The sheet was first rolled into a cylindrical shape 48.3 cm long and approximately 11.4 cm in diameter.

It was cleaned by washing with benzene and then with ethyl alcohol.

The sheet was then heated to red heat by slowly passing a Fisher burner over the entire surface. This forms an adherent oxide layer on the surface of the stainless steel which facilitates the wetting of the surface of the stainless steel by the alcohol solution of the rare earth nitrate.

3. Specific Sample Deposition Techniques

a. Cerium, Neodymium, Samarium, Gadolinium, Hafnium

This method was used successfully for preparing thin, uniform oxide films of these elements. Sample weights varied from 15 mg to 100 mg. Films were formed over an area of 1200 cm^2.

Procedure

1. The sample, in oxide form, was placed in a 50 ml beaker and 5 ml of concentrated nitric acid added. (In the case of cerium, and hafnium, the sample was in the hydroxide form.)
2. After the sample had dissolved in the acid, the solution was evaporated to dryness using an infra-red heat lamp.
3. Five ml of distilled water was added and the solution evaporated to dryness again. (This removes a large part of the excess nitric acid.)
4. The glassy residue was then dissolved in about 20 ml of absolute ethyl alcohol.
5. The sample backing. (Type 302, stainless steel), measuring 34.3 cm wide, 48.3 cm long, and 0.045 cm thickness, was rolled into the shape of a cylinder 48.3 cm long and placed inside a tube having the same dimensions as the ion chamber used for the measurements. The edges of the sheet were overlapped to prevent loss of solution when it was put on the sample backing. The tube containing the sample backing was then placed in a horizontal position on a wooden stand which consisted of a base and two end pieces with deep V-shaped grooves on which the tube was placed.

6. The alcohol solution containing the sample was drawn into a 25 ml pipette and the solution distributed evenly over the sample backing located on the inside of the cylinder. This was done by moving the pipette up and down the length of the cylinder and manually rotating the cylinder at the same time.
7. When all the solution was transferred to the sample backing, heat lamps were placed at both ends and the cylinder rotated until the solution had evaporated to a lacquer-like residue.
8. The sample backing was then baked for an hour with the heat lamps.
9. In the final step, the sample backing was removed from the cylinder and the entire surface ignited to red heat with a Fisher burner. Upon ignition, the nitrate is converted to the final form for counting as the oxide.

b. Tungsten and Mercury

The procedure for the deposition of WO_3 and HgS was modified from the above procedure because of inherent difficulties with tungsten and mercury. In the case of tungsten, no alcohol soluble salt of tungsten is known which can be ignited to a stable form (such as WO_3). For mercury, an alcohol soluble salt can be prepared, but ignition to the oxide is not possible because of the volatility of mercury and its salts. Electrodeposition on a copper surface is not possible because of rapid diffusion of mercury into the copper.

The modification to the procedure merely involved deposition of WO_3 and HgS as an alcohol slurry rather than as a solution.

Procedure

1. A 100 mg sample of WO_3 or HgS, as a very fine powder, was slurried with 20 ml of absolute ethyl alcohol.

2. The slurry was transferred with a pipette to the sample backing, a copper plated stainless steel sheet rolled into a cylindrical shape and fitted into the tube described above.
3. Heat lamps were placed at both ends and the cylinder rotated until the alcohol had evaporated.
4. In the final operation, the cylinder was baked for an hour. The sample backing was then removed from the cylinder and put in the ion chamber for counting.

c. Platinum

This element was conveniently electroplated using the plating bath of Pfanhauser (Gra-53). Samples were deposited over an area of 1000 cm^2 with thicknesses ranging from 0.05 to 2 mg/cm^2 on a Type 304 stainless steel backing, on which had been electroplated a thick coat of copper.

Procedure

1. The platinum sample was first dissolved in a 3:1 mixture of hydrochloric acid and nitric acid. (aqua regia).
2. The solution was evaporated to near dryness and then diluted to 200 ml volume with distilled water.
3. Twenty grams each of diammonium phosphate and disodium phosphate were then added and the resulting orange colored solution boiled until a change to a pale yellow color was observed. ($\sim$ 3 hours). (The color change is due to the formation of a complex amino phosphate of platinum.)
4. The solution was then poured into a cylindrical glass container 45 cm high, 15 cm in diameter having a capacity of 8 liters. The volume of the solution was increased to 7.5 liters by dilution with hot distilled water.

5. The platinum was electrolyzed on the sample backing using the conditions described below.

4. Conditions for Electroplating Platinum

Cathode- copper coated stainless steel sheet. Area- 1000 cm^2.

Anode- platinum gauze ribbon, 45 cm long, 0.92 cm wide.

Current- 2 amperes, D.C.

Duration of Electrolysis- 15 hours

Plating Bath- Bath described above. Bath temperature about 80 C. for first 2 hours cooling to room temperature for remainder of electrolysis.

D. Assay of Amount of Sample Deposited

1. General Comments

In order to determine the specific activity and half-life from the measured counting rate, an accurate assay of the amount of sample which was counted must be known.

As described above, only two methods of sample deposition were employed: (1) the spreading out of slurry or solution on the sample backing and, (2) electroplating, the technique used for platinum.

2. Method Involving the Evaporation of a Solution or Slurry

With the first method, an accurately weighed amount of sample was used to prepare the solution or slurry. Transfer of the solution or slurry to the sample backing was done taking care to insure a quantitative transfer. That the technique employed was indeed quantitative was checked by preparing weighed samples of samarium oxide, depositing them on the sample backing, and determining whether the observed counting rate corresponded to the expected counting rate for that particular weight sample. For the several runs made with samarium oxide, it was evident that the transfer of sample to the sample backing had been quantitative. Further discussion of this matter will be

deferred to the section dealing with the determination of specific activity from counting data.

3. Method Involving Electrodeposition of Platinum

Even though initially a known amount of platinum was used to prepare the plating bath, it was not certain that the electrolysis would give a quantitative deposition of the platinum. As it turned out, it was found that for amounts greater than 1 g about 80% of the platinum was plated out on the backing. The other 20% either stayed in solution or sank to the bottom of the electrolysis container as a fine powder.

In order to find out how much platinum was plated out, the sample backing containing the platinum was immersed in 10 M nitric acid for a couple of days. The copper layer underneath the platinum eventually dissolved leaving the platinum behind as a loose deposit which could be taken off the sheet, washed, dried, and weighed. In the Pt-190 enriched isotope run in which was used a 50 mg sample of Pt a quantitative recovery of the material was affected indicating that no significant amount of Pt is dissolved by the nitric acid.

V. ANALYSIS OF DATA

Introduction

In cases where alpha activity was observed an analysis of the data gave the alpha particle energy and the specific activity of the sample counted. From these, the alpha decay energy, half-life, and the specific activity of the nuclide emitting the alphas as well as the specific activity of the natural element can be calculated.

A. Measurement of Alpha Particle Energy

1. Introduction

When an alpha particle is emitted from the sample into the sensitive volume of the ion chamber, it leaves in its path a large number of excited and ionized atoms and molecules in the gas. In the presence of an electric field originating at the center wire, the electrons formed in this event are attracted to the center wire and a small voltage drop is experienced throughout the wire. This voltage drop is the origin of the pulse which is finally detected and analyzed in the 24-channel pulse analyzer. The magnitude of the voltage drop is dependent upon a number of fixed properties of the counter and associated electronics and the number of electrons or ionizations produced along the path of the alpha particle. The number of electrons produced by the alpha particle is a function of the energy of the alpha particle and the average energy required to produce an ion pair.

The question of the variation with energy of the average energy required to produce an ion pair in a gas has been subject to some question in recent years. T. E. Cranshaw and J. A. Harvey, in 1948, using a fast ion chamber with electronic pulse-height analysis investigated the effect of the energy required to produce an ion pair (W) in argon over a range of alpha energies from 5 to 9 Mev.(Cra-48). They found an energy dependence which

could be described by the following empirical relationship,

$$W = 27.5 + 1.9\ E^{-1/2} \qquad V\text{-}1$$

where W is the average energy required to produce an ion pair (in electron volts) and E is the alpha particle energy (in Mev). They reported that a plot of ionization pulse size vs. alpha energy showed a linear but not proportional relationship between the two quantities, the curve intersecting the energy axis at 85 kev.

According to equation V-1, the curve actually is not linear throughout the entire energy range but becomes non-linear at low energies due to the effect of the $E^{-1/2}$ dependence. At higher energies, ($>$1.5 Mev) this term makes a negligible contribution and the ionization vs. voltage curve is essentially linear.

Two years later, W. P. Jesse, H. Forstat, and J. Sadauskis (Jes-50) also investigated the ionization vs. energy relationship for argon taking the measurements down to 1.5 Mev, the alpha energy of the $B^{10}(n,\alpha)\ Li^{7}$ reaction. Their measuring apparatus involved the use of a slow ionization chamber with a vibrating reed electrometer for the pulse measuring device. Their results indicated that the ionization vs. energy relationship was linear <u>and</u> proportional, in apparent disagreement with the results of Cranshaw and Harvey.

In the same year, G. C. Hanna also reported the results of an investigation of the ionization vs. energy relationship for argon (Han-50). His instrument was a fast ionization chamber connected to fast electronics and an electronic pulse analyzer. He also extended the measurements into the low energy region by using the alpha from the $B^{10}(n,\alpha)Li^{7}$ reaction. The results obtained by Hanna were the same as those of Cranshaw and Harvey: ionization vs. energy is linear but not proportional.

Hanna suggested that the apparent discrepancy existing between the results of Jesse, Forstat, and Sadauskis, and the results of Cranshaw and

Harvey and himself might be explained in the following manner: "Along with Cranshaw and Harvey, we [Hanna] are measuring only the immediately available electronic component of the ionization. Jesse, Forstat, and Sadauskis, using a slow recorder, measure the total ionization. It is possible that in pure argon, atoms in metastable states of excitation can release delayed secondary electrons from the electrodes of the ionization chamber, an effect which might not unreasonably be expected to increase in relative importance for the slower ionizing particles. Such electrons would be missed if fast electron collection were employed. The magnitude of such an effect would, however, seem to be too small."

No additional work has been reported on this problem either with pure argon or mixtures of other gases with argon.

Numerous studies have been made on the effect of adding small amounts of different gases to argon on the energy required to produce an ion pair, but none investigate the effect on the ionization vs. energy relationship.

The first question which had to be answered before alpha energies could be determined in this work was, "What is the nature of the pulse-height voltage vs. energy curve for the gas used, a mixture consisting of 94% argon, 5% ethylene, and 1% nitrogen?"

2. Determination of the Pulse-Height Voltage vs. Energy Curve

a. General Comments

With the ionization chamber, amplifiers, and pulse analysis system used in this study, the amount of ionization produced by an alpha particle is measured as a pulse height in terms of volts. The absolute value of the pulse-height voltage is arbitrary, depending not only on the amount of ionization produced in the chamber but also on the electronic magnification of the pulse in the amplifiers.

By measuring the pulse-height voltage of certain alpha emitters and comparing with their known alpha energies, the pulse-height voltage vs. energy relationship was obtained. Points for the high energy region ($>$ 4 Mev) were obtained by studying the spectra of thorium and its alpha-emitting decay products. Below 4 Mev, points for the curve were obtained by measuring the alpha and triton spectra of the $B^{10}(n,\alpha)Li^7$ and $Li^6(n,\alpha)H^3$ thermal neutron reactions.

Listed in Table VI are the particle energies which were used in the calibration.

TABLE VI

Particle Energies Used in Energy Calibration

Emitter	Particle Energy (Mev)	Branching Fraction	Weighted Average Energy for Peak (Mev)	Reference
Po-126	6.77	0.99	6.77	Bri-54
Em-220	6.28	0.99	6.28	Bas-53
Ra-224	5.68	0.95	5.68	Asa-53
Th-228	5.42 5.34	0.71 0.28	5.40	Ste-57
Th-230	4.68 4.61	0.76 0.24	4.67	Hum-56
Th-232	4.01 4.00	0.76 0.24	4.01	Har-57
$Li^6(n,\alpha)H^3$				
α	2.05	1	2.05	Mat-56
H^3	2.74	1	2.74	Mat-56
$B^{10}(n,\alpha)Li^{7*}$				
α	1.47	0.96	1.47	Mat-56

For Ra-224, the second group at 5.44 Mev actually appears in the peak attributed to Th-228. The Ra-224 peak was considered then to include only one energy alpha and the Th-228 peak three energies, two from Th-228 itself and one from Ra-224.

In the $B^{10}(n,\alpha)$ reaction 96% of the reactions leave the Li-7 nucleus in an excited state, the remainder going directly to the ground state. The alpha emitted in the later reaction is higher by 0.3 Mev and does not contribute significantly to the main peak. This higher energy group was not observed in the spectrum because of its low intensity.

b. Experimental Details

1. Preparation of Calibrating Sample

The sample used for calibrating the counter for energy consisted of 5 mg of Li as Li_2O, 0.2 mg of B as B_2O_3, and 0.1 mg of Th as ThO_2. It was deposited on a stainless steel sheet over an area of 1100 cm^2. The method of sample deposition, which is the same as described in detail in section IV, C, Part 3, involved the preparation of an alcohol solution of lithium acetate, boric acid, and thorium nitrate. This solution was spread over the sample backing, evaporated to dryness and heated with a Fisher burner to form the oxides of these elements.

2. Neutron Moderator and Source

A Po-Be neutron source was obtained on loan from Bettis Atomic Power Division of Westinghouse Electric Corporation. The source, 20 millicuries in strength, was contained in a steel capsule measuring 4.5 cm in length and 0.8 cm in diameter.

The moderator used to reduce the neutrons to thermal energies consisted of a 48-gallon steel drum filled with water. The ion chamber containing the Li, B, Th, source was placed in a vertical position in the center of the drum and held in position by two iron rings clamped to a ring

stand. The neutron source was then lowered on a string to a point midway between the ends of the chamber and touching the counter wall.

c. Results of Energy Calibration

In Figure VI, the spectra of the low energy alphas arising from the $B^{10}(n,\alpha)Li^7$ and $Li^6(n,\alpha)H^3$ reactions are plotted together with the alphas of Th^{232} and five members of the thorium chain. Also included is the 2.74 Mev H^3 peak which is produced in the thermal neutron lithium reaction.

From these spectra, the pulse-height voltage corresponding to the various particle energies was determined by estimating the position of the maximum for each individual pulse distribution.

In Figure VII, the pulse-height voltage is plotted against the corresponding particle energies. As shown in this figure, the relation between pulse-height voltage and energy is linear but not proportional, the curve intercepting the energy axis at 158 kev. A least-squares analysis of the data gives the following equation for the curve:

$$E = (0.0830 \text{ Mev/volt})\ V + 0.158 \text{ Mev.}$$

V = pulse-height (volts)

E = alpha particle energy (Mev) V-2

The first term in equation V-2 is dependent on the apparatus used, i.e. the electronic gain, counter capacitance, while the second term, the energy intercept, should be dependent only on the nature of the counting gas, and should be independent of electronic gain. That the relationship is linear and not proportional is in agreement with the findings of Cranshaw and Harvey (Cra-48) and Hanna (Han-50). Their observation that the energy intercept fell at 85 kev is not in disagreement with the value observed in this work. It is quite possible that there are some small differences in the ionization properties of an argon-nitrogen-ethylene mixture compared to pure argon which could explain this difference.

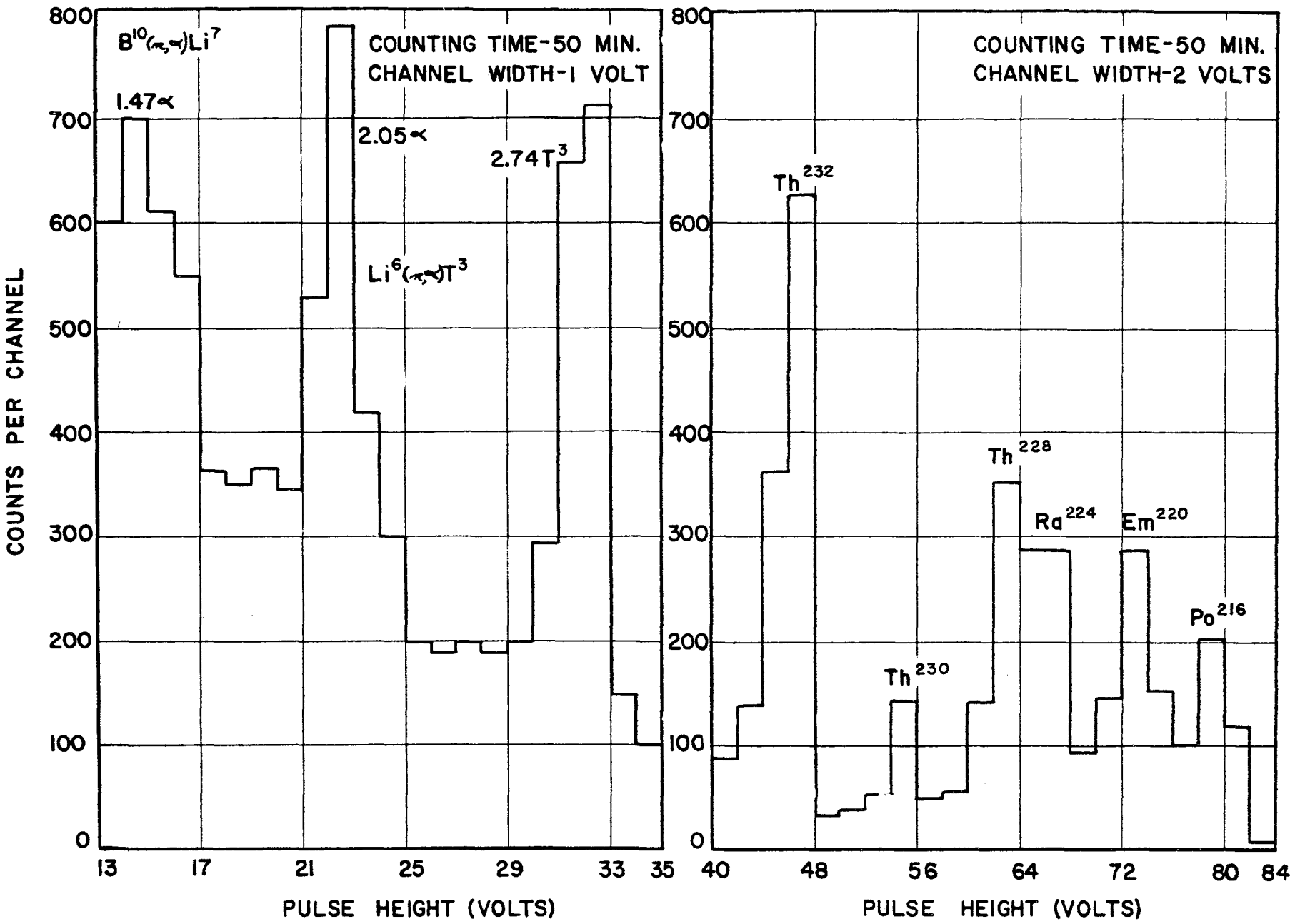

Figure VI. Spectra Used for Energy Calibration of Counter

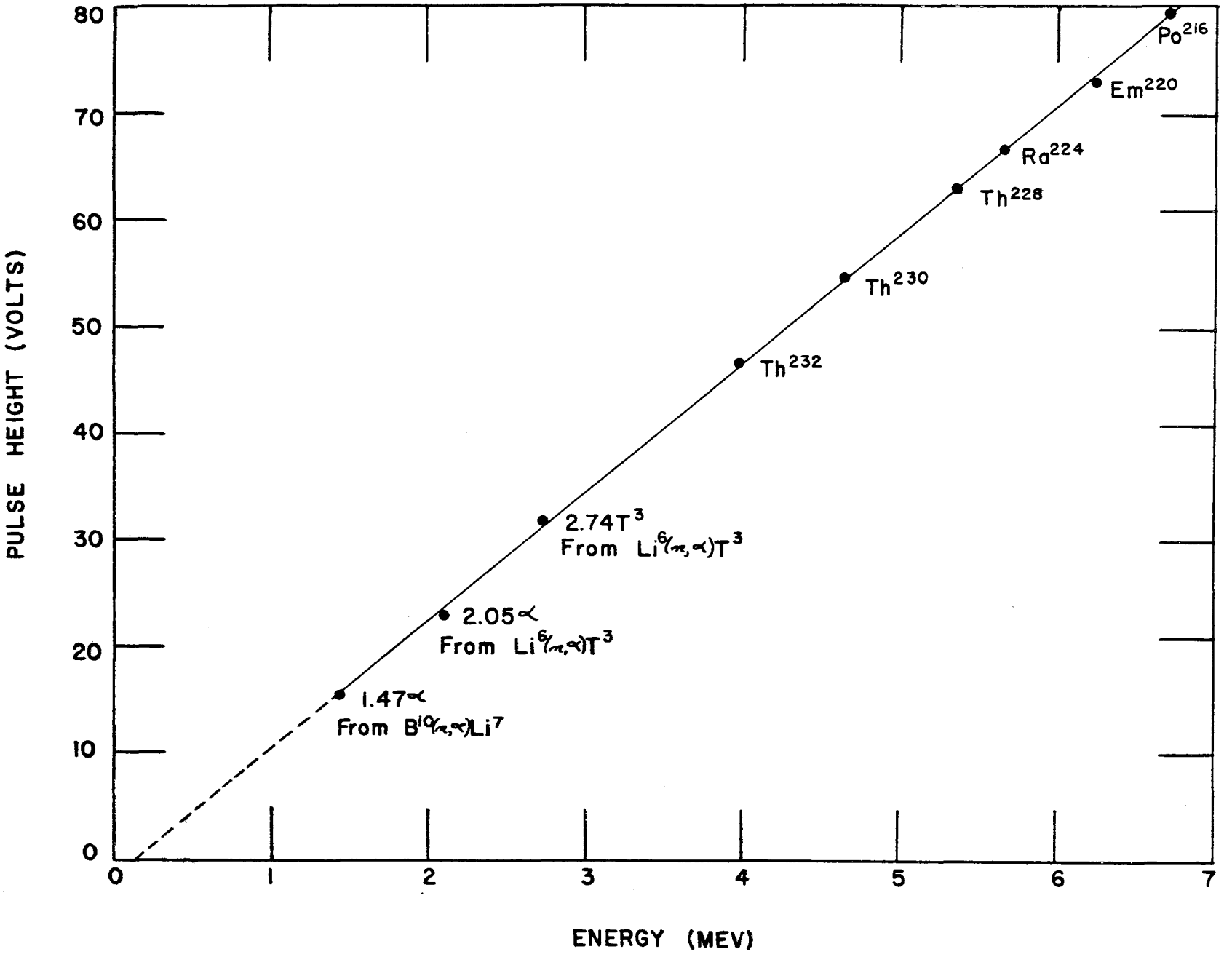

Figure VII. Energy vs. Pulse-Height Voltage Calibration Curve

3. Demonstration of the Constancy of the Energy Intercept for Various Electronic Gains

a. General Comments

In the previous section, the value of the energy intercept was determined to be 158 kev. This was based on measurements run at an electronic gain of 30,000, which is a factor of two lower than the gain used for the sample measurements. This lower gain was chosen in order that the high energy alphas used in the calibration would give a pulse-height voltage within the range of the linearity of the amplifiers.

In order to test whether the energy intercept was independent of gain, a series of measurements was made in which the pulse-height voltages corresponding to the alphas of Sm-147 and Th-232 were determined at four different gains.

b. Results

Figure VIII shows the relationship between pulse-height voltage and alpha energy at electronic gains of 7,500, 15,000, 30,000, and 60,000. The energy intercept, which was accurately determined by previous measurement, was assumed to be known. For each gain setting, it was possible to draw a straight line through the two points corresponding to Sm-147 and Th-232 and have the curve intercept at the position on the energy axis corresponding to 158 kev. This substantiates the fact that the energy intercept is independent of the slope of the pulse-height voltage vs. energy curve. Actually, this is the expected result if the value of the energy intercept is a function of the counting gas only. If it was found that the energy intercept varied with gain, it would be an indication that the amplification system was non-linear.

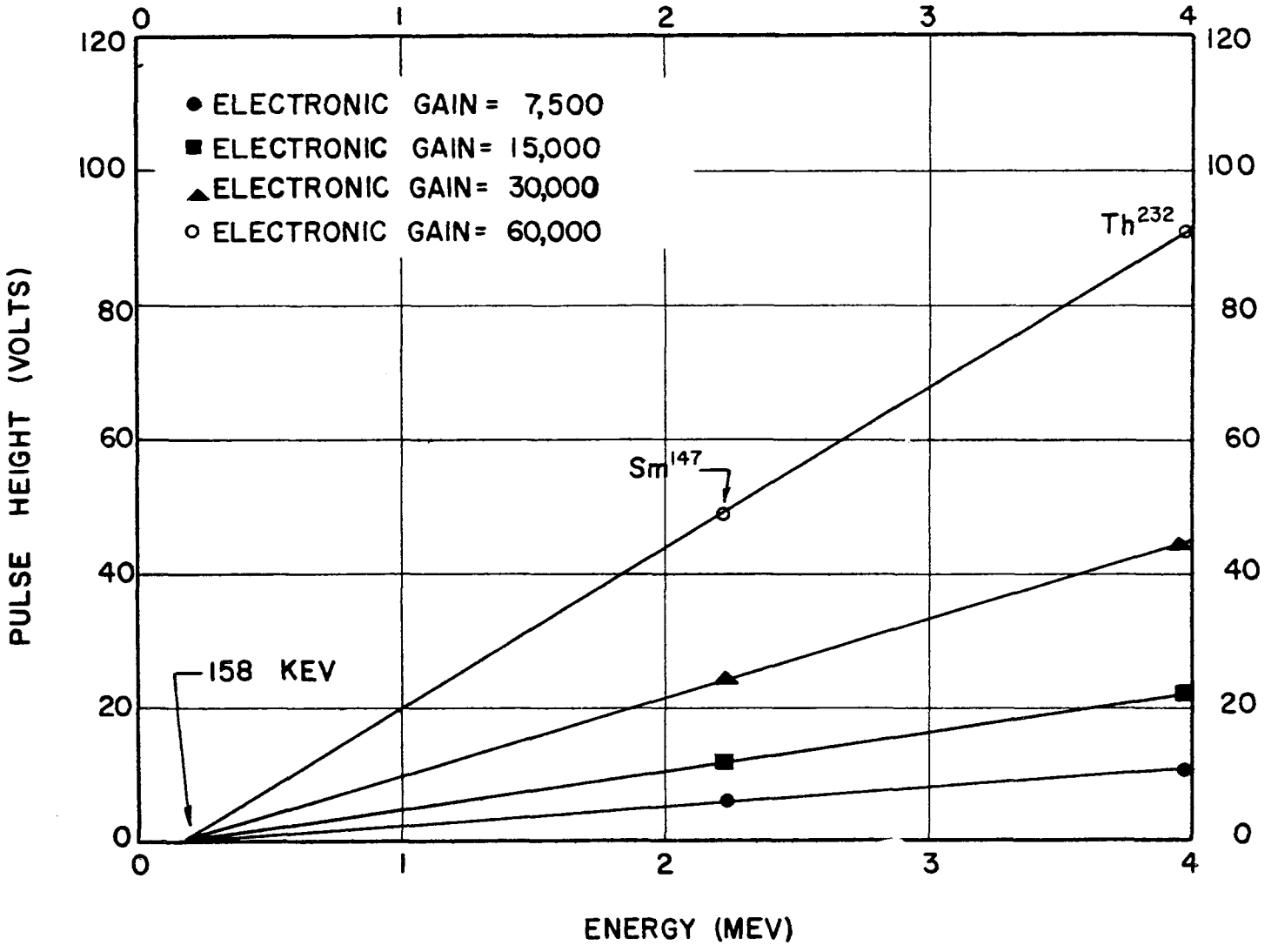

Figure VIII. Effect of Electronic Gain on the Energy Calibration Curve

4. Method Used to Determine Alpha Particle Energies

a. General Procedure

The first step in the procedure for determining the alpha particle energy of a particular alpha emitter was to obtain an alpha spectrum of the alpha emitter in the presence of an alpha group for which the energy is accurately known. This "energy standard" was either a separate source placed on top of the sample being studied or intimately mixed with the sample. Careful measurements employing both techniques have shown either method to be equally valid provided certain precautions are taken. (See Section VI, the results of the Gd-152 measurements)

Once an alpha spectrum was obtained of the "unknown" group and the standard, the spectrum was plotted in histogram form. The peaks from each of the alpha groups, the unknown and standard, were usually distributed over two or three channels. The actual position of the peak on the voltage scale was determined by observing the relative number of counts in each of the channels over which the peak was spread and visually estimating the position of the maximum of the distribution.

After the pulse-height voltage of the standard and "unknown" was determined, the slope of the pulse-height voltage vs. energy curve for that particular measurement was calculated using the value of the energy and pulse-height voltage of the standard and the energy intercept of the original curve calculated in the previous section.

With the slope determined, the equation for the calibration curve can be written; hence, the energy of the "unknown" alpha emitter can be obtained from the observed pulse-height voltage of the unknown.

$$V-V_o = \frac{V_o}{E_o-E^*} \times (E-E_o)$$

regrouping, and solving for E

$$E = E^* + (E_o - E^*) \times \frac{V}{V_o} \qquad V-3$$

E_o = alpha particle energy of standard

V_o = pulse-height voltage of standard

E = alpha particle energy of unknown

V = pulse-height voltage of unknown

E^* = energy-intercept = 158 kev.

B. Determination of Specific Activity

1. Introduction

The specific activity of a particular emitter is defined as the absolute disintegration rate per unit weight of the sample. In order to convert the counting rate which is experimentally observed into the absolute rate, the counting yield, or number of counts per disintegration, must be evaluated. The several factors which contribute to the counting yield in this study are discussed in the following section.

2. Factors Contributing to the Counting Yield (Y)

a. Counting Geometry Factor (G)

In this study, where the sample was spread out, essentially, on the counter wall, one half of the alphas emitted by the sample are not detected because they enter into the counter wall without losing any energy in the counting gas. There is also some loss at the ends of the counter but this is minimized by spreading the sample only to within about an inch from the end of the counter.

b. Self-Absorption Factor (S)

The fraction of alphas lost in a sample due to self-absorption has been calculated by B. B. Cunningham, A. Ghiorso, and A. H. Jaffey (Cun-49a)

to be $\frac{t}{2R}$ where t = sample thickness, and R = the range of the alpha for that particular sample. The self-absorption factor, S, which was used for the calculations in this work is defined as:

$$S = 1 - \frac{t}{2R} \qquad V-4$$

where t and R are in mg/cm^2.

In this work, the sample thicknesses which were used were no more than 0.05 the alpha particle range. This corresponds to a maximum loss of activity due to self-absorption of 2.5%. Although this is not a significant contribution, it is, nevertheless, a systematic loss and is corrected for.

1. Range-Energy Relationship for Alpha Particles and Variation With Atomic Number

Appearing in the self-absorption factor is the range of the alpha in the particular sample being counted. The experimental determination of alpha ranges in various elements has been, over the years, scanty and contradictory. Recent work on determining range-energy relationships for alphas has been done by G. W. Gobeli who measured the range of alphas in Al, Si, Cu, Ge, Ag, and Au over the range 1.5-5 Mev (Gob-56). It was decided to use his data in order to obtain the alpha ranges for the elements of interest.

Gobeli obtains, from his data, a curve for the range-energy relationship for each of the elements he studied. In order to arrive at an expression which gives the range-energy relationship as a function of Z, the range for each element at 2 Mev was divided by the corresponding range in air and a plot of this ratio vs. atomic number of the absorber made using Gobeli's data. The points gave a rough fit to a straight line which can be expressed analytically as:

$$\frac{R_Z}{R_a} = 0.053\ Z + 0.64 \qquad V-5$$

where R_Z is the alpha range in an element of atomic number Z and R_a the range in air both in mg/cm^2. The range-energy relationship for air was that calculated by Livingston and Bethe (Bet-37, Wil-49).

When the ratio of ranges was determined for energies greater than 2.5 Mev and less than 1.7 Mev, different values for the ratio were obtained. The equation is, therefore, restricted to this region.

The range-energy relationship used in the Pt^{190} results was assumed to be close enough to the values obtained by Gobeli for gold foils.

c. Backscattering Factor (B_S)

The work of B. B. Cunningham, A. Ghiorso, and J. C. Hindman on determining the specific activity of Pu^{239} (Cun-49b) has given experimental evidence that alpha backscattering can be significant. This problem was given theoretical scrutiny by J. A. Crawford, who derived an expression relating the dependence of the amount of backscattering as a function of the atomic number of the scatterer and the energy of the alpha particle. Crawford derives the ratio of backscattering of alphas of a certain energy (E_α) in a sample to that of a standard (for which the backscattering factor has been experimentally determined) which can be expressed as

$$\frac{\phi}{\phi_s} = \frac{\Sigma N_i A_i^2}{A_s^{3/2} \Sigma N_i A_i^{1/2}} \qquad \text{V-6}$$

where ϕ = the fraction of alphas backscattered by the sample backing

ϕ_s = the fraction of alphas backscattered by the standard backing

N_i = weight fraction of the "i"th component of the sample

A_i = atomic weight of the "i"th component of the sample

A_s = atomic weight of the standard backing

The equation expressing the energy (or range) dependence Crawford shows to be

$$\frac{\phi_{E_\alpha}^2}{\phi_{E_s}^2} = \frac{\left(R_{E_s}\right)_s}{\left(R_{E_\alpha}\right)_s} \qquad \text{V-7}$$

E_α = the fraction of alphas of energy E_α backscattered by the "standard" backing

E_s = the fraction of alphas of energy E_s backscattered by the "standard" backing

$\left(R_{E_\alpha}\right)_s$ = range of alphas of energy E_α in standard backing (mg/cm^2)

$\left(R_{E_s}\right)_s$ = range of alphas of energy E_s in standard backing (mg/cm^2)

For the standard, the fraction of the alphas from U-234 with an energy of 4.76 Mev backscattered from platinum has been found by B. B. Cunningham, A. Ghiorso, and J. C. Hindman to be ~ 0.03 (Cun-49b).

By combining V-6 and V-7, an equation for calculating the backscattering factor for any sample backing and any energy is obtained.

$$B_s = 1 + 2 \times \left(\frac{R_{E_s}}{R_{E_\alpha}} \right)_s^{1/2} \times \frac{\Sigma N_i A_i^2}{A_s^{3/2} \Sigma A_i N_i^{1/2}} \times \phi^* \qquad V\text{-}8$$

ϕ^* = backscattering fraction for standard (4.76 Mev alpha on Pt)=0.03

A_s = atomic weight of standard backing (platinum) = 195.09

R_{E_s} = range of standard alpha energy (4.76 Mev) in Pt = 15.2 mg/cm^2

In this study, the backscattering medium is predominantly the sample backing. There is some backscattering from the sample itself but because only very thin samples are used, this will be considered a negligible contribution.

Ranges of alphas in Pt were considered to be the same as for gold, for which experimental data are available (Gob-56).

The stainless steel backing which was used for most of the measurements was comprised of ~ 69% Fe, ~ 18% Ni, and ~ 8% Cr.

Using the information given above, V-8 can be written as

$$B_s = 1 + 2x \left[\frac{15.2 \text{ mg/cm}^2}{R_{E_\alpha}} \right]^{1/2} \times \frac{\left[0.69(55.85 \text{ g/mole Fe})^2 + 0.18(58.71 \text{ g/mole Ni})^2 + 0.08(52.01 \text{ g/mole Cr})^2 \right] \times 0.03}{(195.08 \text{ g/mole Pt})^{3/2} \left[0.69(55.85 \text{ g/mole Fe})^{1/2} + 0.18(58.71 \text{ g/mole Ni})^{1/2} + 0.08 (52.01 \text{ g/mole Cr})^{1/2} \right]}$$

$$= 1 + \frac{0.092 \text{ mg}^{1/2}/\text{cm}}{\left(R_{E_\alpha}\right)^{1/2}_{Pt}} \qquad \text{V-9}$$

(for a stainless steel sample backing)

For an alpha emitter of 2 Mev energy (range in Pt = 6 mg/cm^2) deposited on a stainless steel backing, the backscattering factor is

$$1 + \frac{0.092 \text{ mg}^{1/2}/\text{cm}}{(6 \text{ mg/cm}^2)^{1/2}} = 1.037.$$

d. Coincidence Loss Factor (C)

Because anticoincidence guard tubes are used to reduce the background, it is possible that there will be a loss of counting rate due to a near simultaneous formation of a pulse in the ion chamber due to the sample and in one or more of the guard tubes from an event of external origin. When this occurs, the pulse from the ion chamber is electronically cancelled.

The probability that such an event will happen is equal to the fraction of the time that the counting system is insensitive to radiations due to the formation of an anticoincidence pulse.

1. Calculation of "Dead Time" of the Counting System due to Anticoincidence Cancellation

The square-wave pulse which is used to blank the incoming pulse from the ion chamber in the anticoincidence circuit is of 40 μ seconds duration and occurs ~ 40 times per second. (The counting rate of the Geiger bank is ~ 2500 counts/minute.) This means that for every second, 40 x 40 μ sec. or 0.0016 seconds are not available to receive a pulse from the ion chamber. The fractional loss of activity, then, due to this coincidence effect should be just 0.0016, a negligible effect.

2. Experimental Verification

In order to determine, experimentally, whether coincidence loss is significant, the counting rate of a moderately strong source was determined with and without anti-coincidence cancellation, and the counting rates were compared.

Experimental Details

At the time this experiment was performed it was more convenient to use an external Na-22 source and operate the counter in the proportional region rather than put an intense alpha source in the counter. The source was taped to the body of the counter and put inside the mercury shield which separates the Geiger guard tubes from the ion chamber. No significant increase in the counting rate of the Geiger bank was observed. A count was made with the source in this position recording all counts above a certain fixed pulse-height voltage, with and without anti-coincidence. The source was then removed and a background taken under the same conditions with and without anti-coincidence. The results appear in Table VII.

TABLE VII

Coincidence Loss due to Anti-Coincidence Cancellation

Conditions	Counting Rate (Counts per minute)
(1) No anticoincidence, with source	6290 ± 5
(2) Anti-coincidence, with source	6215 ± 5
(3) No anti-coincidence, without source	521 ± 1
(4) Anti-coincidence, without source	465 ± 0.78
(5) Coincidence Counts, with source (1) - (2)	75 ± 7
(6) Coincidence Counts, without source (3) - (4)	56 ± 1.3
(7) Coincidence Loss (5) - (6)	21 ± 7

The fraction of the activity of the sample lost due to coincidence with pulses from the Geiger guard tubes is $\frac{21 \pm 7}{6290} = 0.003 \pm 0.001$, which is in reasonable agreement with the calculated value of 0.0016.

e. Counting Yield (Y)

The counting yield is the fraction of alphas detected by the ion chamber per alpha disintegration of the nuclide being studied. It is calculated by taking the product of the counting geometry (G) which is 0.5 for this work, the self-absorption factor (S) (equation V-4), the backscattering factor, B_S (equation V-7, 8), and the coincidence loss factor which is considered to be unity.

$$Y = G \times S \times B_S \times C \qquad \text{V-9}$$

3. Determination of the "Net Counting Rate"

a. General Comments

The term "net counting rate" is defined as the integral counting rate (corrected for background) of the sample from zero to the maximum energy of the alpha being studied. The determination of the net counting rate from the data obtained in the measurement involves, then, a resolution of the activity from the background activity and an extrapolation of the data from the low energy cut-off of the spectrum to zero energy.

Each of the nuclides studied presented its own peculiar problems in resolving the effective background activity and in extrapolating the spectrum to zero energy. This discussion will, therefore, be limited to a general description of the method of attack, and the specific details referred to the individual results.

b. Extrapolation of the Spectrum to Zero Energy

For reasons which include the noise level of the electronics, the high background at low energies, and the lack of a sufficient number of channels in the pulse analyzer to cover the region of interest at the desired

energy interval, the differential counting rate spectrum for each of the samples measured was cut off at some arbitrary low energy. Because of this, a correction for a loss of counts having energies below the threshold energy must be made.

When the counting rate is much larger than the background level, as in the case of Sm-147 and Pt-190, it is a simple matter to visually extrapolate the energy spectrum to zero energy and estimate the number of counts between zero and the threshold energy.

The situation for counting rates which are comparable to or even lower than the level of the background calls for a different approach. The level of activity due to the sample at an energy not too far removed from the main peak has been reduced to such a low level that to use it to extrapolate from threshold to zero energy would indeed be quite arbitrary and subject to large error. If the energy spectrum of a source similar in energy and thickness but considerably more intense is obtained, it is possible to extrapolate the counting rate from threshold to zero energy of this intense spectrum as mentioned above. From these data, the fraction of the activity below the threshold can be determined and applied to the data on the weak activity in order to obtain the total counting rate.

c. Resolution of the Effective Background from the Gross Activity

For each of the nuclides studied, the resolution of the background activity involved slightly different situations.

The most straightforward resolution was presented when the effective background above the alpha group(s) appeared to be the same as for the bare sample backing. This was true when no contaminating activities were present in the sample. The background activity was then resolved by subtracting the background spectrum for a bare sheet from the observed spectrum.

With a contaminating activity present at a significant level the background included not only the background for a bare sample backing but also the contribution from contaminants. Such was the case for Nd-144 where there was a nearly equal level of Sm-147 activity present. In these cases, each of the components of the background was resolved individually from the total spectrum which was observed.

d. Establishing An Upper Limit for the Specific Activity

In a number of nuclides studied, no alpha peaks were observed in the energy spectrum which could be attributed to that particular nuclide. To establish an upper limit for the specific activity the following procedure was used. The counting rate within the energy interval which should include the activity if it were present was obtained, and an average counting rate per channel for that region calculated. A conservative estimate was then made of the minimum counting rate above background in any one channel which would give a significant peak in this region. This was usually several times the standard deviation of the average counting rate per channel. The magnitude of this estimate was dependent upon the average counting rate per channel and on whether the counting rate per channel was approximately constant or if there was some variation due to tailing from a higher energy activity (e.g. Sm-147 activity in the Sm-148 and Sm-149 spectra). This estimate, which is an upper limit of the counting rate in one channel, was then converted to an upper limit for the absolute counting rate by determining the fraction of the total activity in one of the channels containing the peak of the spectrum of a known alpha emitter of approximately the same energy and sample thickness.

VI. RESULTS

A. Samarium-147

1. Experimental Details

Two separate experiments were run on a natural samarium sample, one to determine the specific activity of the samarium sample and the other to determine the alpha particle energy of Sm-147.

In the specific activity measurement, a 0.0070 g sample of natural samarium oxide giving a sample thickness of 0.00584 mg/cm^2 was counted for a period of 17.25 hours.

In the second experiment, designed to give an accurate measurement of the Sm-147 alpha energy, a mixed source containing 1.2 mg of Li as Li_2O and 0.5 mg of samarium oxide was counted for 4 hours in the presence of a thermal neutron flux from a Po-Be source.

Because of the high counting rate in both runs, anticoincidence cancellation would be insignificant. It, therefore, was not used.

2. Results

a. Specific Activity of Sm in Sample

(1) Gross Counting Rate- The total number of counts recorded between 1.5 and 2.4 Mev was 14,453 ± 120 in a period of 17.25 hours (See Figure **IXA**). The number of counts between 0 and 1.5 Mev was estimated to be 7500 ± 500 counts by a smooth extrapolation of the spectrum to zero energy. The gross number of counts was then 21,953 ± 510 and the gross counting rate 1273 ± 30 counts/hour or 0.353 ± 0.008 counts/sec.

(2) Background Counting Rate- The counting rate above 2.40 Mev in Figure **IXA** was extrapolated into the low energy region in order to obtain the effective background under the Sm-147 spectrum. It was determined to be 220 ± 22 counts which is equal to 12.75 ± 1.27 counts/hour or 0.0035 ± 0.003 counts/sec.

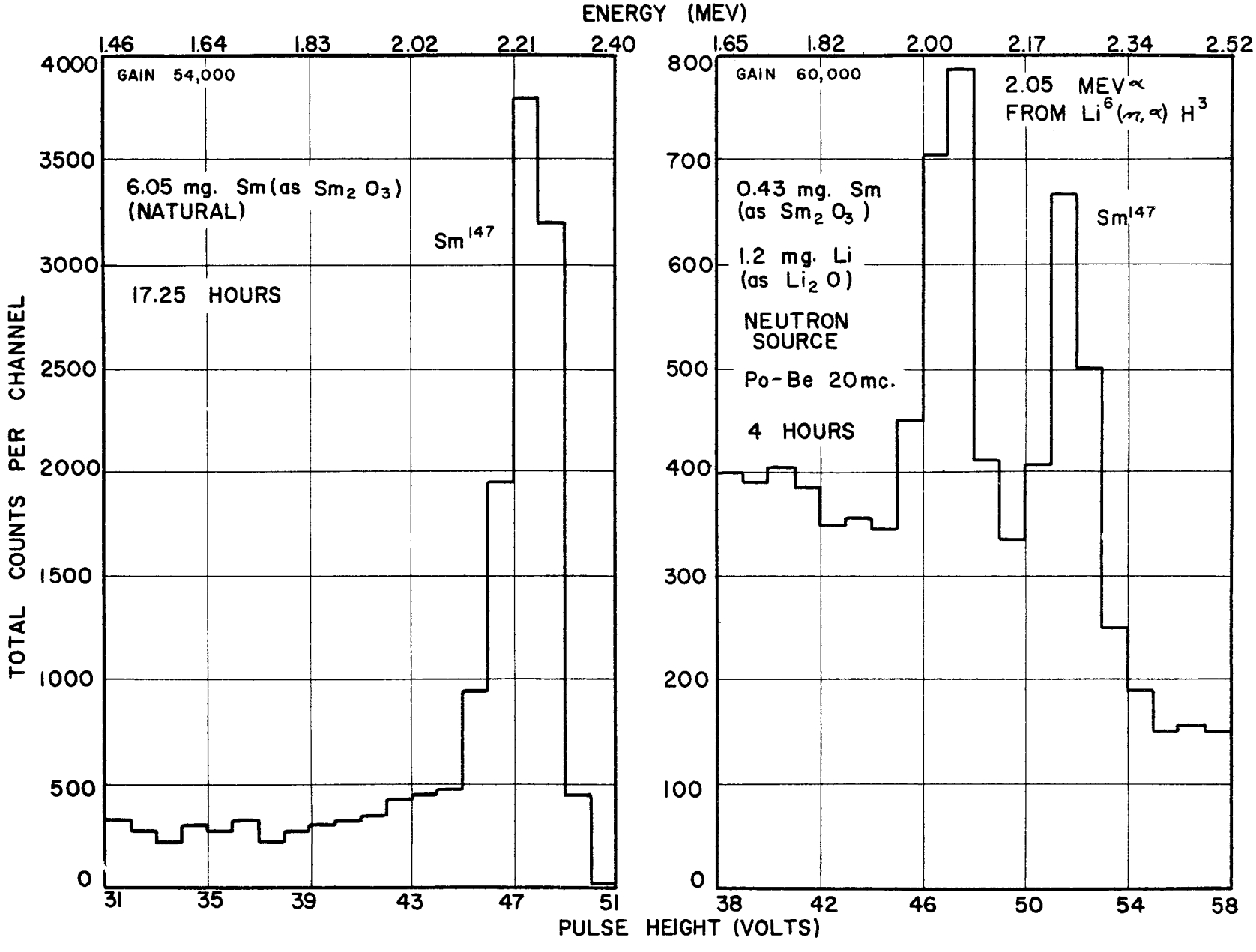

Figure IXA. Alpha Spectrum of Natural Sm

Figure IXB. Alpha Spectrum of Natural Sm and Li (with Neutron Source)

(3) Net Counting Rate (R_c) = (1) - (2)

(0.353 ± 0.008)c/sec - (0.0035 ± 0.0003)c/sec = 0.350 ± 0.008 c/sec

(4) Counting Yield

(a) Geometry Factor (G) = 0.500

(b) Self-Absorption Factor (S)- Using equation V-5, R_{Sm}/R_a can be calculated for Sm (Z = 62).

$$\frac{R_z}{R_a} = 0.053Z + 0.64 = 0.053(62) + 0.64 = 3.92$$

The range of a 2.24 Mev alpha in air (R_a) is 1.45 mg/cm^2 (Wil-49). The range of a 2.24 Mev alpha in Sm (R_{Sm}) is then 3.92 x 1.45 = 1.45 = 5.68 mg/cm^2. In order to obtain the range in Sm_2O_3, the Bragg sum rule is applied:

$$\frac{1}{R_{Sm_2O_3}} = \frac{f_{Sm}}{R_{Sm}} + \frac{f_O}{R_O}$$ where f_{Sm} and f_O are the fractions of Sm and O in Sm_2O_3, 0.864 and 0.136 respectively. R_O is considered to be the same as R_a. Substituting into the above equation then,

$$\frac{1}{R_{Sm_2O_3}} = \frac{0.864 \text{ g Sm/g } Sm_2O_3}{5.68 \text{ mg/cm}^2} + \frac{0.136 \text{ g O/g } Sm_2O_3}{1.45 \text{ mg/cm}^2}$$

$$R_{Sm_2O_3} = 4.08 \text{ mg/cm}^2$$

Using equation V-4, the self-absorption factor (S) can be calculated.

$$S = 1 - \frac{t}{2R} = 1 - \frac{0.00584 \text{ mg/cm}^2}{2 \times 4.08 \text{ mg/cm}^2} = 0.9993$$

(c) Backscattering Factor (B_s)- Because of the thinness of the Sm_2O_3 sample used, the backscattering surface was considered to be predominantly the stainless steel backing. The range of a 2.24 Mev alpha in Pt, the standard backing, is 6.6 mg/cm^2 (Gob-56). Using equation V-9, the backscattering factor can be calculated.

$$B_s = 1 + \frac{0.092}{(R_{E\alpha})_{Pt}^{1/2}} = 1 + \frac{0.092}{(6.6 \text{ mg/cm}^2)^{1/2}} = 1.0036$$

The counting yield is then:

$$Y = G \times S \times B_s = 0.500 \times 0.9993 \times 1.0036 = 0.5014$$

(5) Sample Weight (W_s)

The weight of Sm_2O_3 used was 0.0070 ± 0.0001 g. The fraction of Sm in the sample is 0.864 (f_{Sm}).

(6) Chemical Yield (C_y)- It was estimated that 0.97 ± 0.03 of the sample that was weighed was actually deposited on the sample backing.

From these above data, the specific activity of natural Sm can be calculated

$$S_A \text{ (natural Sm)} = \frac{R}{Y \times W_s \times f_{Sm} \times C_y} = \frac{(0.350 \pm 0.008) \text{ c/sec}}{0.5014 \text{ c/dis} \times (0.0070 \pm 0.0001)\text{g } Sm_2O_3 \times 0.864 \text{ g Sm/g } Sm_2O_3 \times (0.97 \pm 0.03)\text{g } Sm_2O_3 \text{ counted/g } Sm_2O_3 \text{ weighed}}$$

$$= (119 \pm 5)\text{dis/g Sm/sec}$$

b. Specific Activity of Sm-147

$$\alpha \text{ (natural Sm)} = 150.35 \text{ g Sm/mole}$$

$$\alpha \text{ (Sm-147)} = 147.0 \text{ g Sm-147/mole}$$

$$S_A \text{ (Sm-147)} = \frac{S_A(\text{natural Sm})}{i_{147} \text{ (natural Sm)}} \times \frac{\alpha \text{ (natural Sm)}}{\alpha \text{ (Sm-147)}}$$

$$= \frac{(119 \pm 5)\text{dis/g Sm/sec}}{(0.151 \text{ atom Sm-147/atom Sm})} \times \frac{150.35 \text{ g Sm/mole}}{147.0 \text{ g Sm-147/mole}}$$

$$= (806 \pm 31)\text{dis/g Sm-147/sec}$$

c. Decay Constant of Sm-147 (λ Sm-147)

$$\lambda \text{ (Sm-147)} = \frac{(806 \pm 31)\text{dis/g Sm-147/sec} \times 147.0 \text{ g Sm-147/mole} \times 3.155 \times 10^7 \text{sec/y}}{6.023 \times 10^{23} \text{ atom/mole}}$$

$$= (6.18 \pm 0.24) \times 10^{-12}/\text{y}$$

d. Half-life of Sm-147 (H_{Sm-147})

$$H_{Sm-147} = \frac{0.6931}{\lambda \text{ Sm-147}} \qquad \frac{0.6931}{(6.18 \pm 0.24) \times 10^{-12} \text{ y}^{-1}}$$

$$= (1.12 \pm 0.04) \times 10^{11} \text{ y}$$

It was possible to obtain independent measurements of the specific activity and half-life of Sm-147 from the data obtained with the enriched Sm-148 and Sm-149 samples. The Sm-148 sample contained 6.4 ± 0.21 % Sm-147 and the Sm-149 sample, 1.0.± 0.051 % Sm-147. The results of the calculations are summarized below.

(Sm-148 Sample - See Figure XIV)

Net Counting Rate (R)	(0.420 ± 0.003)c/sec
Sample Weight (W_s)	(0.0196 ± 0.0001)g Sm_2O_3
gravimetric factor (f_{Sm})	0.860 g Sm/g Sm_2O_3
atomic weight Sm - a (Sm sample)	148.13 g Sm/mole
isotopic abundance of Sm-147 - i_{147} (Sm Sample)	(0.64 ± 0.0006)atom Sm-147/atom Sm
Counting Yield - Y	0.5007 c/dis
Chemical Yield - C_y	0.97 ± 0.03
S_A (Sm Sample)	(51.0 ± 2.2)dis/g Sm/sec
S_A (Sm-147)	(805 ± 35)dis/g Sm-147/sec
S_A (natural Sm)	(119 ± 5)dis/g Sm/sec
λ (Sm-147)	(6.20 ± 0.27) x 10^{-12}/y
H (Sm-147)	(1.12 ± 0.05) x 10^{11} y

(Sm-149 Sample - See Figure XV)

Net Counting Rate (R)	(0.088 ± 0.001)c/sec
Sample Weight (W_s)	(0.0308 ± 0.0001)g Sm_2O_3
gravimetric factor (f_{Sm})	0.862 g Sm/g Sm_2O_3
atomic weight Sm - α (Sm Sample)	149.23 g Sm/mole
isotopic abundance of Sm-147 - i_{147} (Sm Sample)	0.010 ± 0.000 atom Sm-147/atom Sm
Counting Yield	0.50016 c/dis
Chemical Yield	0.97 ± 0.03
S_A (Sm Sample)	(6.35 ± .29)dis/g Sm/sec
S_A (Sm-147)	(694 ± 32)dis/g Sm-147/sec
S_A (natural Sm)	(102 ± 5)dis/g Sm/sec
λ (Sm-147)	(5.34 ± 0.25) x 10^{-12}/y
H_{Sm-147}	(1.29 ± 0.06) x 10^{11} y

The average values for the specific activity and half-life for the three runs are given below, together with the values of Beard and Wiedenbeck (Bea-54).

	This Work	Beard and Wiedenbeck Results
S_A (Sm-147)	769 ± 33 dis/g Sm-147/sec	719 ± 36 dis/g Sm-147/sec
S_A (natural Sm)	113 ± 5 dis/g Sm/sec	104 ± 5 dis/g Sm/sec
λ (Sm-147)	(5.88 ± 0.25) x 10^{-12}/y	5.54 ± 0.24 x 10^{-12}/y
H (Sm-147)	(1.18 ± 0.05) x 10^{11} y	(1.25 ± 0.06) x 10^{11} y

e. Alpha Particle Energy Measurement

Figure **IXB** shows the energy spectrum of the Sm-147 peak and the 2.05 Mev alpha from the $Li^6(n,\alpha)H^3$ reaction.

The pulse-height voltage of the 2.05 Mev alpha peak was estimated to fall at 47.2 ± .2 volts, and the Sm-147 alpha at 51.7 ± .2 volts.

Calculations

The alpha particle energy of Sm-147 was calculated using equation V-3.

$$E_{Sm-147} = E^* + [(E_{standard} - E^*)] \text{ Mev} \times \frac{V_{Sm-147}}{V_{standard}}$$

$$= (0.157 \pm 0.010) + [2.05 \pm 0.01) - (0.157 \pm 0.010)] \frac{51.7 \pm 0.2}{47.2 \pm 0.2}$$

$$= 2.24 \pm 0.02 \text{ Mev}$$

3. Discussion

The accurate evaluation of the alpha energy of Sm-147 was of considerable importance to this work because it was used as an energy standard in the determination of other alpha energies.

Rasmussen has calculated the Sm-147 and Eu-147 alpha half-lives using different modifications of the original Gamow-Gurney-Condon rate formula (Ras-52) and found in all cases an excessively long theoretical half-life compared to the experimental value. For the alpha energy of Sm-147, the value of 2.18 Mev obtained by Jesse and Sadauskis (Jes-50) was used in the calculation. The Eu-147 alpha energy was evaluated by Rasmussen using Sm-147 as an energy standard.

With this new value of the Sm-147 alpha energy, which is 60 kev higher than the Jesse and Sadauskis value (but probably within their uncertainty), the calculated value of the Sm-147 half-life is in agreement with the experimental value ($H_{calculated} = 1.57 \times 10^{11}$ y). A re-evaluation of the Eu-147 alpha energy brings its calculated half-life also into agreement with the experimental value.(See Section VII, part A).

The Q value for Sm-147 alpha decay calculated from the particle energy of 2.24 ± 0.02 Mev is 2.30 ± 0.02 Mev.

THERE IS NO PAGE 85 IN
THIS REPORT

B. Cerium-142

1. Experimental Details

A 58.0 mg sample of CeO_2 enriched in Ce-142 to 90.08% was deposited over an area of 1200 cm^2 on a stainless steel backing. This enrichment is 8.13 times the natural abundance of Ce-142. The sample thickness was 0.0483 mg/cm^2. The total counting time was 114.4 hours. Two-volt channels were used.

A small amount of natural Sm_2O_3 was mixed with the cerium sample giving a counting rate of ~ 3 counts per hour in the Sm-147 peak. The samarium was added for the purpose of obtaining an energy calibration for the Ce-142 peak.

2. Results

The spectrum which was obtained appears in Figure X. The Sm-147 peak appeared at the proper position but there was no definite indication of a second peak which could be attributed to Ce-142 activity. The expected peak height for Ce-142 is indicated in Figure X on the basis of the measurements of Riezler and Kauw (Rie-57). There is a slight indication of a peak in the region of 1.65 Mev which might be due to Ce-142.

Assuming the Ce-142 alpha particle energy to lie between 1.5 and 1.9 Mev (mass data gives 1.64 Mev), an upper limit for the specific activity of Ce-142 in the sample was calculated. The counting rate between 1.5 and 1.9 Mev was 2.81 ± 0.16 c/hour for an average counting rate per channel of 0.562 c/hour. It was estimated that a counting rate of 0.3 c/hour above this background in any one of the channels in the region would have given a significant peak. From an analysis of a Sm-147 spectrum of an equivalent thickness, it was found that the fraction of the counts in one channel covering the main part of the peak accounted for 12% of the total activity.

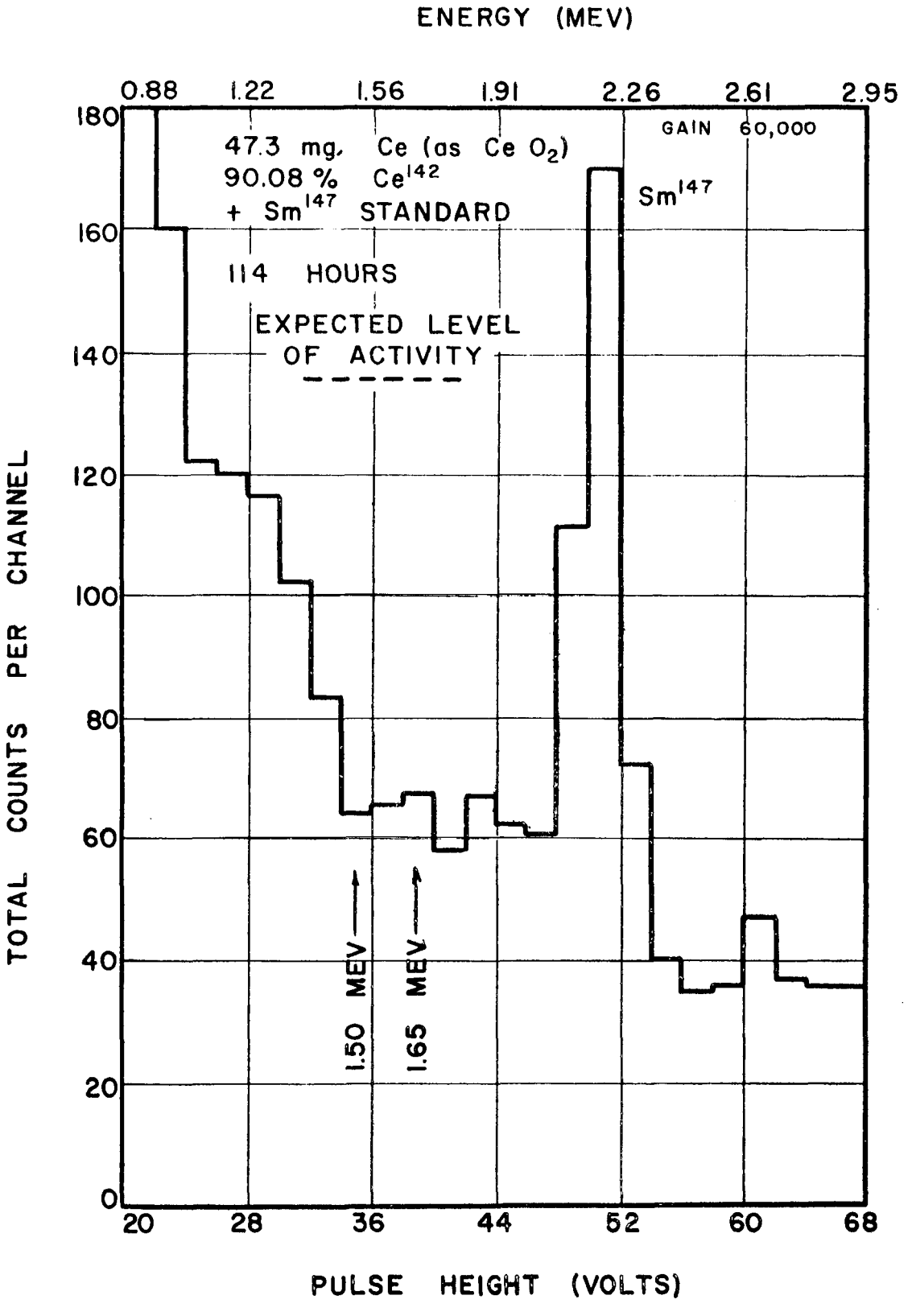

Figure X. Alpha Spectrum of Enriched Ce-142 Sample

The upper limit for the absolute counting rate of the cerium sample, then, is $\frac{0.3c/hour}{0.12/alpha}$ which is 2.5 alphas/hour or 0.000695 alphas/sec.

a. Upper Limit for Specific Activity of Sample

$$S_A \text{ (Ce sample)} < \frac{0.00069 \text{ a/sec.}}{0.0580 \text{ g } CeO_2 \times 0.815 \text{ g Ce/g } CeO_2}$$

$$< 0.0015 \text{ dis/g Ce/sec} \qquad (1.5 \leq E_\alpha \leq 1.9 \text{ Mev})$$

b. Upper Limit for Specific Activity of Ce-142

$$S_A \text{ (Ce-142)} < \frac{0.0015 \text{a/g Ce/sec}}{0.9008 \text{ atom Ce-142/atom Ce}} \times \frac{141.9 \text{ g Ce/mole}}{142.0 \text{ g Ce-142/mole}}$$

$$< 0.0017 \text{ dis/g Ce-142/sec} \qquad (1.5 \leq E_\alpha \leq 1.9 \text{ Mev})$$

c. Upper Limit for Specific Activity of Natural Ce

i_{142} (natural Ce) = 0.1108

$$S_A \text{ (Natural Ce)} < 0.0017 \text{ dis/g Ce-142/sec} \times 0.1108 \text{ atom Ce-142/atom Ce} \times \frac{142.0 \text{ g Ce-142/mole}}{140.13 \text{ g Ce/mole}}$$

$$< 0.00019 \text{ /g Ce/sec} \qquad (1.5 \leq E_\alpha \leq 1.9 \text{ Mev})$$

d. Upper Limit for Decay Constant λ Ce-142

$$\lambda_{\text{Ce-142}} < \frac{0.0017 \text{ dis/g Ce-142/sec} \times 142 \text{ g/mole Ce-142} \times 3.155 \times 10^7 \text{sec/yr}}{6.02 \times 10^{23} \text{ atom/mole}}$$

$$< 1.31 \times 10^{-17}/\text{yr} \qquad (1.5 \leq E_\alpha \leq 1.9 \text{ Mev})$$

e. Lower Limit for Half-Life

$$H_{\text{Ce-142}} > \frac{0.6931}{1.31 \times 10^{-17}/\text{yr}}$$

$$> 5.29 \times 10^{16} \text{ years} \qquad (1.5 \leq E_\alpha \leq 1.9 \text{ Mev})$$

3. Discussion

Since these results are in apparent disagreement with those of Riezler and Kauw ($H = 5 \times 10^{15}$ years) the experimental conditions were carefully checked. From the amount of Sm-147 observed in the spectrum and

the sharpness of the Sm-147 peak it appeared that the transfer of sample to the stainless steel backing was without significant loss of sample and that the deposit was uniform and thin enough to obtain good results. A small portion of the sample was returned to Oak Ridge in order to recheck the isotopic composition. The reanalysis agreed with the original determination. We can only conclude now that the half-life of Ce-142 is at least a factor of 10 larger than that reported by Riezler and Kauw. They reported in their paper that the identification of the very short Ce-142 alpha tracks was quite difficult because they could be confused with extraneous non-alpha produced tracks of approximately the same length. They reported that the Ce-142 alpha particle energy was 1.5 Mev, which on the basis of alpha rate theory corresponds to a very long half-life ($> 10^{20}$ years). It is possible that the reason why their reported energy was so low is that the peak they observed was composed not only of Ce-142 alpha tracks of $\sim$ 1.7 Mev energy but also of smaller length "background" tracks not due to Ce-142 alpha activity. This would, of course, also effect the calculation of the specific activity of the sample.

The energy available to Ce-142 for alpha decay is 1.69 $\pm$ 0.10 Mev based on calculations from mass data (Nie-57). The alpha half-life of Ce-142 corresponding to this energy is 1.45 x 10^{18} years using the Bethe formula. The uncertainty in the energy, however, could bring the half-life as low as 10^{16} years or as high as 10^{20} years.

C. Neodymium-144

1. Experimental Details

An 82.8 mg sample of neodymium oxide enriched in Nd-144 to 62.62% was counted in the ion chamber. This represents an enrichment of 2.8 times the normal abundance of Nd-144. The sample thickness was 0.069 mg/cm^2; the counting time, 145.3 hours.

2. Results

Figure XIA is a histogram of the spectrum which was obtained. Two peaks were observed; one at 42.3 ± .2 volts corresponding to the Nd-144 peak and the other at 52.3 ± .2 volts corresponding to a Sm-147 impurity activity in the sample. There was a good separation of the two activities (10 channels). The energy spectrum was taken in the interval 1.46 to 2.41 Mev.

a. Specific Activity of Nd in Sample

In order to obtain the specific activity of Nd-144, the activity due to Sm-147, high energy alpha emitters, and the background of the steel sheet had to be resolved from the activity due to Nd-144.

The Sm-147 activity was subtracted from the spectrum using a more intense alpha spectrum of Sm-147 of approximately the same sample thickness as a guide for determining the distribution of the Sm-147 activity over the channels (Figure XIIC). Figure XIB represents the spectrum minus the contribution from Sm-147 and Figure XIIA, the Sm-147 spectrum which was subtracted.

Next, the Nd-144 activity was resolved from the rest of the activity again using the same Sm-147 spectrum as a guide for determining the distribution of activity. (The fact that the Sm-147 spectrum will have a slightly different shape compared to the Nd-144 spectrum because of a difference in energies is recognized but no alternative approach has seemed any more reliable.) Figure XIC is the Nd-144 spectrum resolved from all the other activities.

What is left after the Nd-144 activity is removed from the spectrum is the effective background. This includes the activity from the sample backing, the contribution from high energy alpha emitters, or any other contribution to the background due to the presence of the sample in the counter (i.e. increased gamma sensitivity). Figure XID represents a spectrum

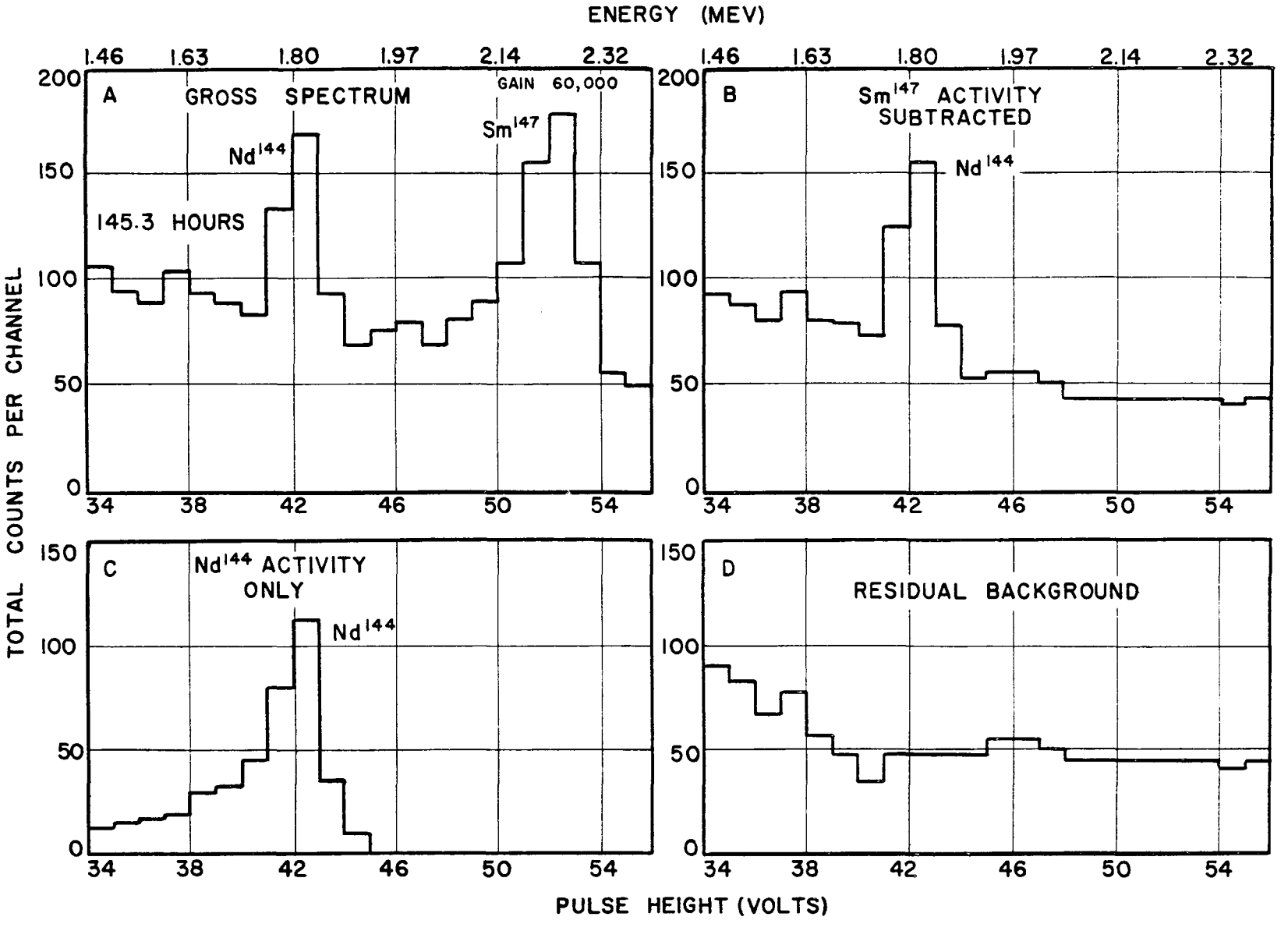

Figure XI. Alpha Spectrum of Enriched Nd-144 Sample

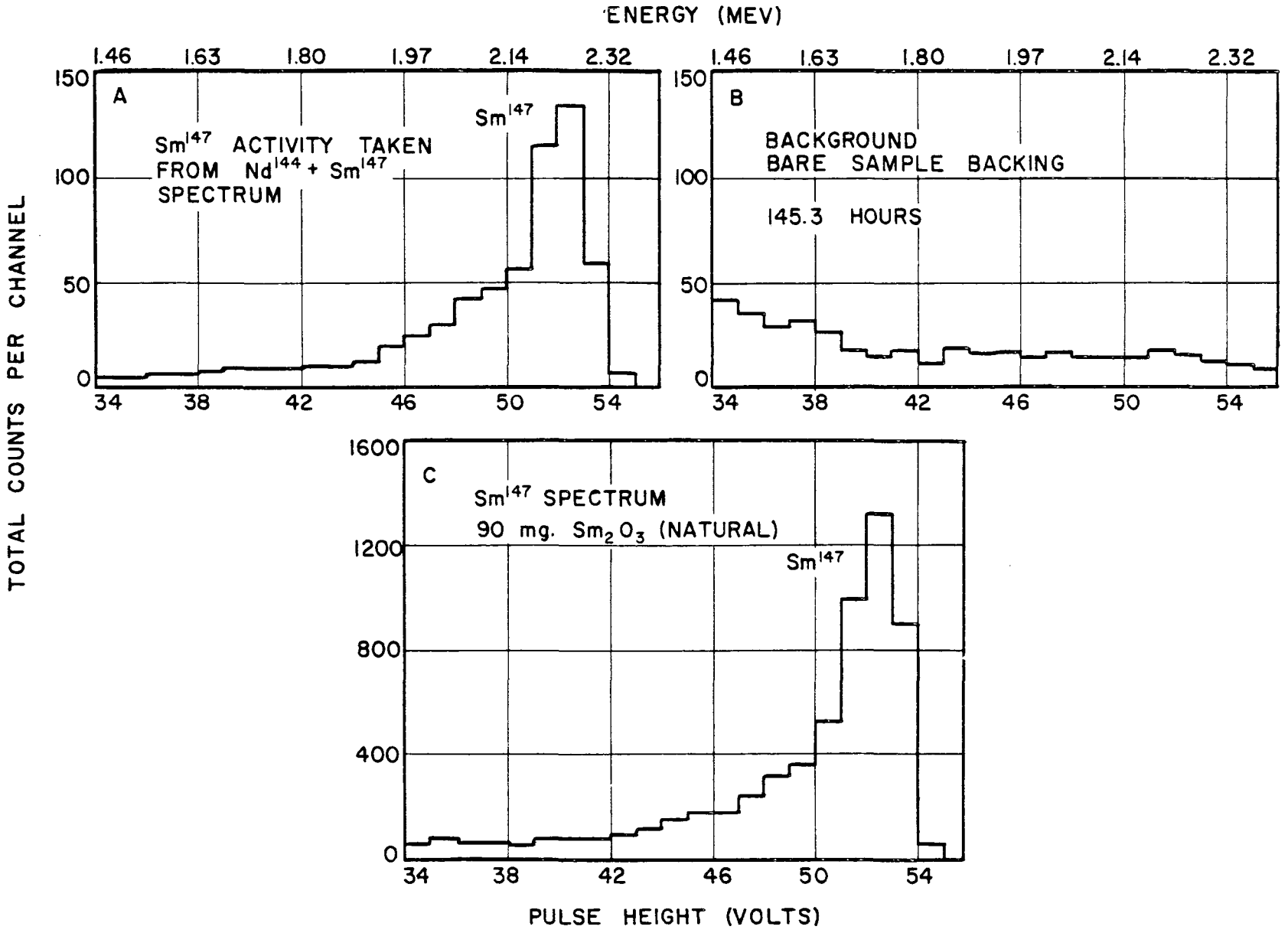

Figure XII. Alpha Spectra Used in Nd-144 Calculations

of the residual activity after the Nd-144 and Sm-147 activities were removed. The spectrum is essentially flat to about 1.8 Mev where it begins to rise with decreasing energy. The same sort of increase in background for low energies has also been observed with a bare sample backing, as is shown in Figure XIIB.

It appears that there are more counts in the low energy part of the background when a sample is in the counter. This can be explained by the fact that the samples are of a higher atomic number than the components of the sample backing and hence would increase the sensitivity of the counter for detecting gammas.

The overall increase in the effective background for the Nd-144 measurement (compare Figures XID and XIIB) is due to tailing of contaminating thorium activity into the low energy part of the spectrum.

1. Absolute Counting Rate (R)

The total number of counts due to Nd-144 between 1.45 and 1.95 Mev is 406 ± 40 giving a counting rate of 0.000776 ± 0.00008 c/sec. The low energy cut-off at 1.46 Mev is at an energy which is 0.647 times the alpha energy of Nd-144.

In an independent measurement of a sample of Sm_2O_3 of approximately the same thickness but considerably more intense than the neodymium (Figure XIIC) the fraction of the absolute counting rate appearing in the region above 0.647 times the alpha energy in the energy spectrum was determined. The counting rate due to Sm-147 between 1-46 and 2.32 Mev was determined to be (3.91 ± 0.05)c/sec. The specific activity of the sample was calculated using the method described in section VI-A and found to agree with the previously determined values, indicating that 91 mg of Sm_2O_3 were actually present. Assuming the specific activity of natural Sm to be 113 ± 5 dis/sec/g, the absolute counting rate of this sample should be 8.75 ± 0.43 dis/sec.

The fraction of the absolute counting rate detected is then

$\frac{(3.91 \pm 0.05)}{8.75 \pm 0.43} = 0.447 \pm 0.022$. This factor then can be used to obtain the absolute counting rate of the Nd-144 activity. This factor includes geometry, self-absorption, and backscattering factors. The absolute counting rate, then is $\frac{(0.000776 \pm 0.00008)\ c/sec}{(0.447 \pm 0.022)\ c/dis} = (0.001735 \pm 0.0002)$ dis/sec.

2. Sample Weight (W_s)

The weight of Nd_2O_3 used was 0.0828 ± 0.002 g. The fraction of Nd in the sample was 0.860 (f_{Nd}).

$$S_A \text{ (Nd sample)} = \frac{R}{W_s \times f_{Nd}} = \frac{(0.001735 \pm 0.0002) \text{ dis/sec}}{(0.0828 \pm 0.0020) \text{g } Nd_2O_3 \times 0.860 \text{ g Nd/g } Nd_2O_3}$$

$$= (0.0244 \pm 0.0030) \text{ dis/g Nd/sec}$$

b. Specific Activity of Nd-144

The isotopic abundance of Nd-144 in the sample was 0.6262. The atomic weight of Nd in the sample was 144.55.

$$S_A \text{ (Nd-144)} = \frac{S_A \text{ (Nd sample)}}{i_{144} \text{ (Nd sample)}} \times \frac{a \text{ (sample)}}{a \text{ (Nd-144)}}$$

$$= \frac{(0.0244 \pm 0.0030) \text{ dis/g Ne/sec}}{0.6262 \text{ atom Nd-144/atom Nd}} \times \frac{144.55 \text{ g Nd/mole}}{144.0 \text{ g Nd-144/mole}}$$

$$= (0.0389 \pm 0.0048) \text{dis/g Nd-144/sec}$$

c. Specific Activity of Natural Nd

The isotopic abundance of Nd-144 in natural Nd is 0.239. The atomic weight is 144.27.

$$S_A \text{ (natural Nd)} = S_A \text{ (Nd-144)} \times \frac{a \text{ (Nd-144)}}{a \text{ (natural Nd)}} \times i_{144} \text{ (natural Nd)}$$

$$= (0.0389 \pm 0.0048) \text{ dis/g Nd-144} \times \frac{144.0 \text{ g Nd-144/mole}}{144.27 \text{ g Nd/mole}} \times 0.239 \text{ atom Nd-144/atom Nd}$$

$$= (0.0093 \pm 0.0011) \text{ dis/g Nd/sec}$$

d. Decay Constant for Nd-144

$$\lambda_{(Nd\text{-}144)} = \frac{(0.0389 \pm 0.0048) \text{ dis/g Nd-144} \times 144.0 \text{ g Nd-144/mole} \times 3.155 \times 10^{7} \text{ sec/y}}{6.023 \times 10^{23} \text{ atom/mole}}$$

$$= (2.93 \pm 0.36) \times 10^{-16}/\text{y}$$

e. Half-life of Nd-144

$$H\,(Nd\text{-}144) = \frac{0.6931}{(Nd\text{-}144)} = \frac{0.6931}{(2.93 \pm 0.36) \times 10^{-16}/\text{y}}$$

$$= (2.36 \pm 0.29) \times 10^{15} \text{ y}$$

f. Alpha Particle Energy Measurement

From Figure XIA, it was estimated that the pulse-height voltage of the Nd-144 peak was 42.3 ± 0.3 volts and for Sm-147, the standard, 52.2 ± 0.3 volts. The Sm-147 alpha energy was taken to be 2.24 ± 0.02 Mev.

Calculations

The alpha particle energy of Nd-144 can be calculated using equation V-3. $E^* = 0.158 \pm 0.01$ Mev.

$$E_{Nd\text{-}144} = E^* + (E_{Sm\text{-}147} - E^*) \frac{V_{Nd\text{-}144}}{V_{Sm\text{-}147}}$$

$$= (0.158 \pm 0.010) \text{ Mev} + [(2.24 \pm 0.02) - (0.158 \pm 0.010)] \text{ Mev} \times \frac{(42.3 \pm 0.3) \text{ volts}}{(52.2 \pm .3) \text{ volts}}$$

$$= (1.84 \pm 0.02) \text{ Mev.}$$

3. Discussion

The results for the specific activity and alpha energy of Nd-144 are in reasonable agreement with the results of Waldron, Schultz, and Kohman (Wal-54) and Porschen and Riezler (Por-54, 56). Their results are summarized below.

Authors	E (Mev)	H (years)	Specific Activity Natural sample (α/g Nd/sec)
Waldron, Schuitz, Kohman, 1954	1.9 ± .1	1.5×10^{15}	0.015
Porschen and Riezler, 1954	1.8 ± .1	5×10^{15}	0.005
Porschen and Riezler, 1956	1.8 ± .1	2.2×10^{15}	0.010
This Work, 1959	1.84 ± .02	2.36×10^{15}	0.009

The Q value for Nd-144 corresponding to the measured alpha particle energy is 1.90 ± 0.02 Mev.

D. Samarium-146

1. Experimental Details

A 100.2 mg sample of natural samarium oxide was deposited on a stainless steel sheet and counted in the ion chamber for a period of 166 hours. The sample thickness was 0.083 mg/cm^2. The energy spectrum was run from 1.91 to 3.30 Mev.

2. Results

Figure XIII is a histogram of the differential counting rate spectrum which was obtained. That part of the spectrum in which the Sm-147 peak fell contained more than a million counts total while on the high energy side of the peak no more than 600 counts were recorded between 2.4 and 3 Mev.

There is a very slight indication of an activity at ~ 2.5 Mev which might be due to Sm-146 but the level of activity is within the statistical fluctuations of the counting rate per channel for that region.

Calculation of An Upper Limit to the Specific Activity

The counting rate from 2.4 to 2.8 Mev in the natural samarium spectrum was 3.5 ± .15 counts per hour for an average counting rate per

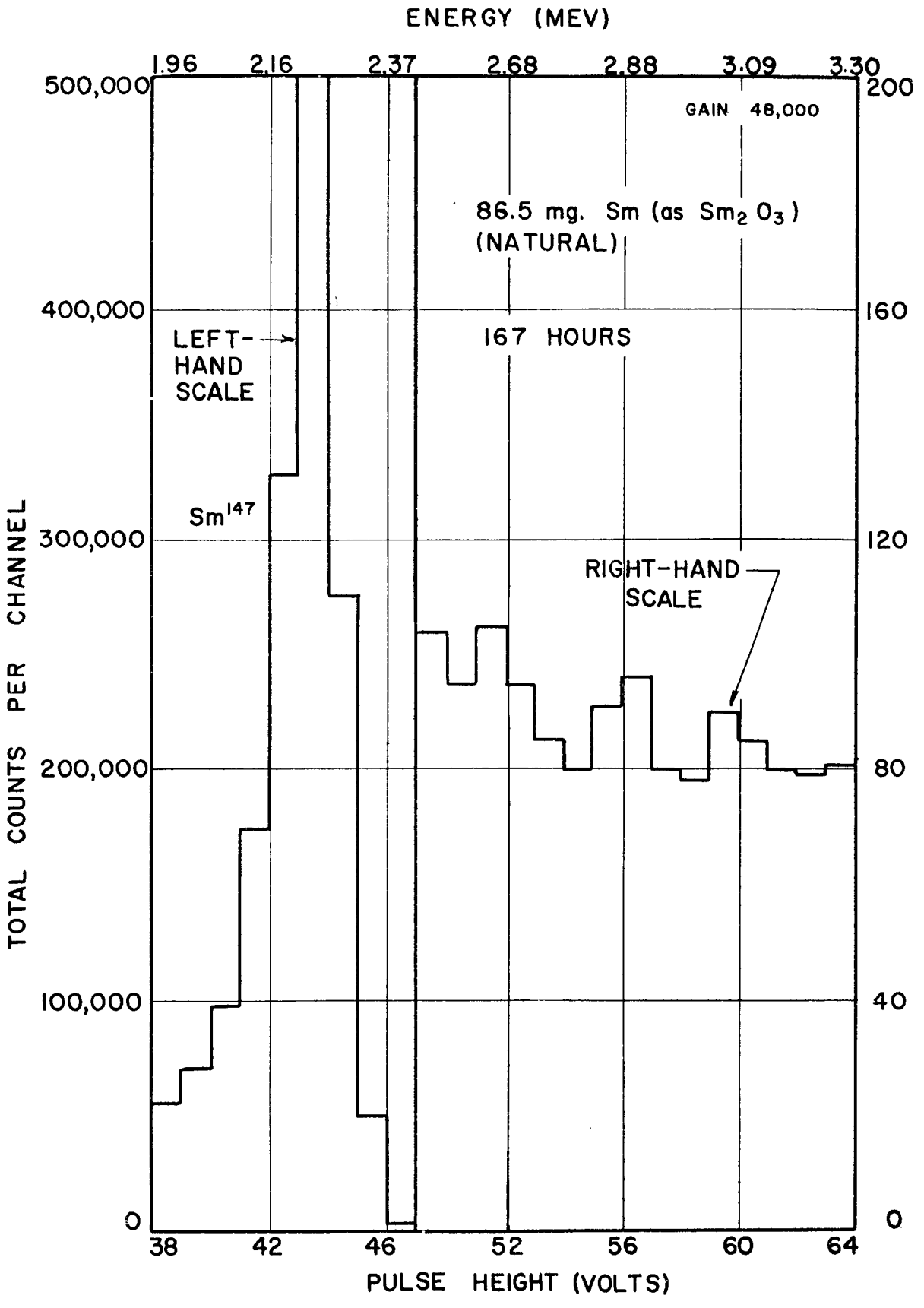

Figure XIII. Alpha Spectrum of Natural Sm (1.91-3.30 Mev)

channel of 0.50 ± .02 counts per hour. Below 2.4 Mev, the counting rate increased sharply due to Sm-147 activity.

It is estimated that a counting rate greater than 0.25 counts per hour above background in any one of the channels between 2.4 and 2.8 Mev would have given a significant Sm-146 spectrum. Since no spectrum was observed, this is an upper limit of the maximum counting rate due to Sm-146 in any one channel in this energy interval.

From the Sm-147 spectrum in the same sample, the maximum counting rate in the spectrum for one channel was found to account for 6% of the total disintegration rate. An upper limit for the Sm-146 absolute disintegration rate can be evaluated, then, and is simply $\frac{0.25 \text{ c/hr}}{0.06 \text{ c/dis}} = 4.2$ dis/hr or 0.00117 dis/sec (R). The sample weight is 0.1002 g (W_s) and the fraction of Sm in the sample (f_{Sm}), 0.864. The upper limit for the specific activity of Sm due to Sm-146 is:

$$(S_A)^{\text{natural}}_{Sm} < \frac{R}{W_s \times f_{Sm}} = \frac{0.0012 \text{ dis/sec}}{0.1002 \text{ g } Sm_2O_3 \times 0.864 \text{ g Sm/g } Sm_2O_3}$$

$$< 0.013 \text{ dis/g Sm/sec.}$$

3. Discussion

a. Determination of An Upper Limit for the Half-Life

With some assumptions as to the age of the elements and the primordial abundance of Sm-146, it is possible to calculate an upper limit for the half-life of Sm-146 on the basis of the upper limit of the specific activity established above.

First let us assume that the primordial abundance of Sm-146, i_o (Sm-146) was the same as for the stable isotope Sm-148: i_o(Sm-148) = i (Sm-148) = 0.112. Let us also assume that the age of the elements (T) is 6.6×10^9 years (Bur-57). Then the present isotopic abundance of Sm-146 is

$$i(\text{Sm-148}) = i_o(\text{Sm-146})\, e^{-\lambda \text{ Sm-146} \times T} = i(\text{Sm-148}) e^{-\lambda \text{ Sm-146} \times T}$$

The present specific activity of Sm due to Sm-146 we shall assume to be the upper limit calculated above, and

$$S_A \text{ (natural Sm)} = \frac{\text{(Sm-146) x i(Sm-146) N}}{\alpha \text{ (natural Sm)}}$$

where N = Avogadro Number = 6.023×10^{23} atom/mole and α(natural Sm) = the atomic weight of natural Sm = 150.35 g sm/mole. Making the substitution for i(Sm-146)

$$S_A \text{ (natural Sm)} = \frac{\text{(Sm-146) x i(Sm-148) x N } e^{-\lambda \text{ Sm-146 x T}}}{\alpha \text{ (natural Sm)}}$$

Substituting numerical values for the different quantities:

$$0.013 \text{ dis/g Sm/sec} \times 3.155 \times 10^7 \text{ sec/y} = \frac{\lambda \text{ (Sm-146)} \times 6.023 \times 10^{23} \text{ atom/mole} \times 0.112 \text{ atom Sm-148/atom Sm} \times e^{-\lambda \text{ (Sm-146)} \times 6.6 \times 10^9 \text{ y}}}{150.35 \text{ g Sm/mole}}$$

Taking logs, multiplying and regrouping,

$$\lambda \text{ (Sm-146)} = \frac{15.03 + \log \lambda \text{ (Sm-146)}}{2.86 \times 10^9}$$

This equation can be solved for λ (Sm-146) by a method of successive approximations giving λ (Sm-146) $\geq 2.2 \times 10^{-9}$/y and H(Sm-146) $\leq 3.1 \times 10^8$ y. The alpha decay energy according to the Bethe Formula would be $\geq$ 2.45 Mev. Seaborg and Dunlavey found the alpha particle energy of Sm-146 to be 2.55 $\pm$ 0.05 Mev (Dun-53). The theoretical half-life corresponding to 2.55 Mev is 4.0×10^7 y.

b. Determination of An Upper Limit to Present Isotopic Abundance

From these calculations, we can estimate an approximate limit to the present isotopic abundance of Sm-146. Assuming the primordial isotopic abundance of Sm-146 to be 11.2%, the present limit for the isotopic abundance is:

$$11.2\% \times e^{-(2.2 \times 10^{-9}/\text{y} \times 6.6 \times 10^9 \text{ y})} = 4.4 \times 10^{-6} \text{ y}$$

If the half-life obtained by Seaborg and Dunlavey (Dun-53) for an artificially prepared sample of Sm-146 is a correct value (5×10^7 years), then it will never be possible to detect Sm-146 in nature. With this half-life, the specific activity would be 10^{-207} α/g/sec! It would even be more extinct than the Ornithischia Iguanodon.

E. Samarium-148

1. Experimental Details

A 19.6 mg sample of samarium oxide enriched in Sm-148 to 83.1% was counted in the ion chamber. This represents an enrichment of 7.4 times the natural abundance of Sm-148. The sample also contained 6.4% Sm-147, a factor of 0.427 times the normal abundance of Sm-147. The sample thickness was 0.0167 mg/cm^2. Total counting time was 44.3 hours.

2. Results

Figure XIV shows a histogram of the result that was obtained. The energy interval was 1.54 to 2.54 Mev. Only the Sm-147 peak was evident. No other peak, which could be attributed to Sm-148, appeared.

In establishing an upper limit for the specific activity, the energy interval 1.54 to 2.0 Mev was first considered (mass data gives E_α(Sm-148) = 1.84 $\pm$ .15 Mev (Nie-56)). Between 2 and 2.4 Mev, the comparatively intense Sm-147 activity complicates the estimation of a limit to the specific activity.

The counting rate between 1.54 to 2.0 Mev was 167 $\pm$ 2 counts per hour giving an average counting rate per channel of 16.7 $\pm$ .2 counts per hour.

It is estimated that a counting rate of 2 counts per hour above background in any one of the channels between 1.5-2.0 Mev would have been enough to give a definite effect.

From the Sm-147 spectrum, it was determined that the maximum counting rate in one channel accounted for 10.5% of the total disintegration rate.

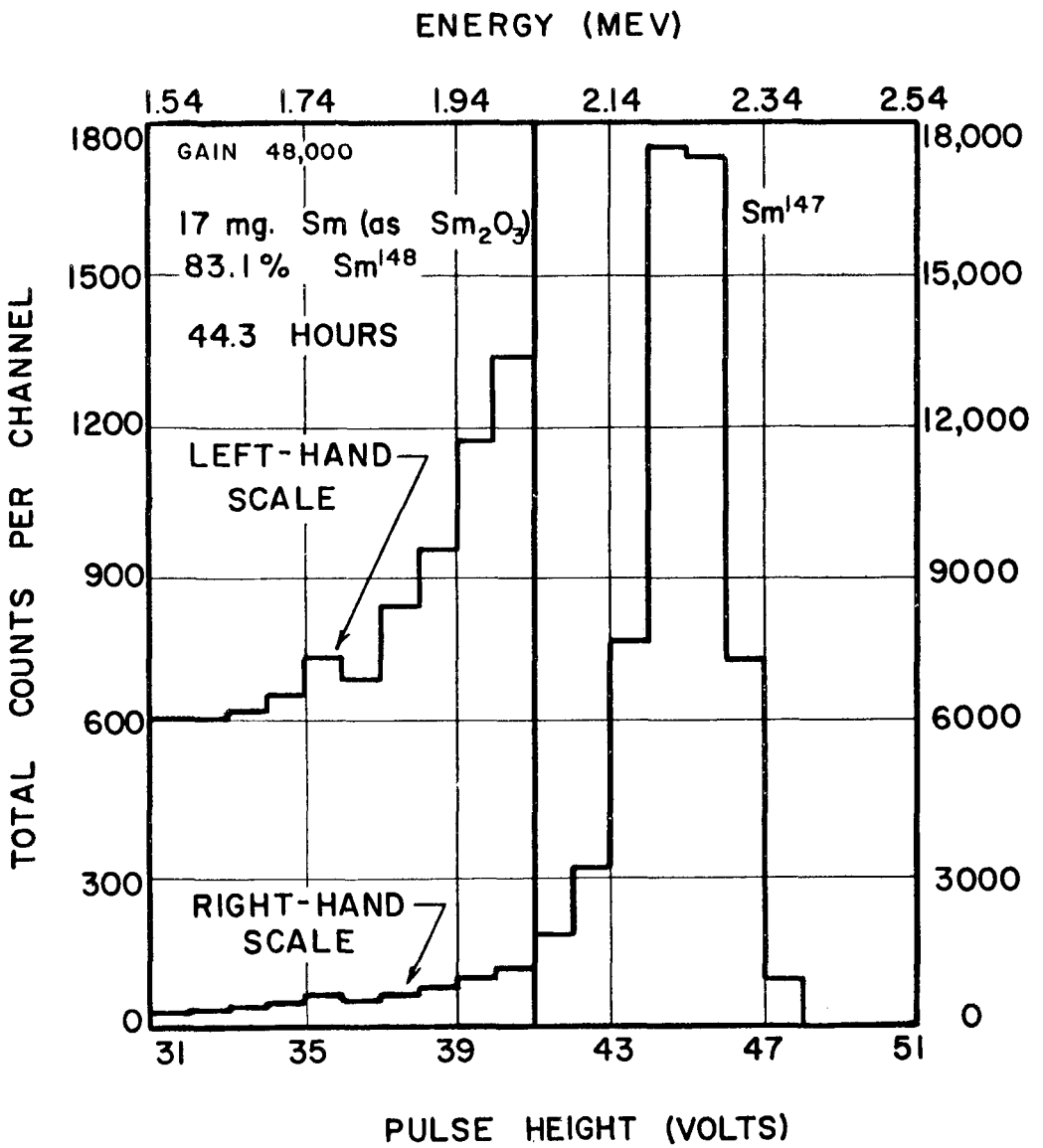

Figure XIV. Alpha Spectrum of Enriched Sm-148 Sample

The upper limit for the total disintegration rate is, then,

2/0.15 = 19 dis/hr or 0.0053 dis/sec

a. Specific Activity of Sample

$$S_A \text{ (Sm sample)} < \frac{0.0053 \text{ dis/sec}}{.019 \times 6 \text{ g } Sm_2O_3} \times 0.860 \text{ g Sm/g } Sm_2O_3$$

$$< 0.31 \text{ dis/g Sm/sec} \qquad (1.54 \leq E_\alpha \leq 2.0 \text{ Mev})$$

b. Specific Activity of Sm-148

$$S_A \text{ (Sm-148)} < \frac{S_A \text{ (Sm sample)}}{i_{148} \text{ (Sm sample)}} \times \frac{\alpha \text{ (Sm sample)}}{\alpha \text{ (Sm-148)}}$$

$$< \frac{0.314 \text{ dis/g Sm/sec}}{0.831 \text{ atom Sm-148/atom Sm}} \times \frac{148.13 \text{ g Sm/mole}}{148.0 \text{ g Sm-148/mole}}$$

$$< 0.38 \text{ dis/g Sm-148/sec} \qquad (1.54 \leq E_\alpha \leq 2.0 \text{ Mev})$$

c. Specific Activity of Natural Sm

$$S_A \text{ (natural Sm)} < S_A \text{ (Sm-148)} \times i_{148} \text{ (natural Sm)} \times \frac{\alpha \text{ (Sm-148)}}{\alpha \text{ (natural Sm)}}$$

$$< 0.377 \text{ dis/g Sm-148/sec} \times 0.112 \text{ atom Sm-148/atom Sm} \times \frac{148.0 \text{ g Sm-148/mole}}{150.35 \text{ g Sm/mole}}$$

$$< 0.041 \text{ dis/g Sm/sec} \qquad (1.54 \leq E_\alpha \leq 2.0 \text{ Mev})$$

d. Decay Constant of Sm-148

$$\lambda \text{ (Sm-148)} < \frac{0.38 \text{ dis/g Sm-148/sec} \times 148.0 \text{ g Sm-148/mole} \times 3.155 \times 10^7 \text{ sec/y}}{6.023 \times 10^{23} \text{ atom/mole}}$$

$$< 2.9 \times 10^{-15}/\text{y} \qquad (1.54 \leq E_\alpha \leq 2.0 \text{ Mev})$$

e. Half-life of Sm-148

$$H \text{ (Sm-148)} > \frac{0.6931}{2.9 \times 10^{-15}/\text{y}}$$

$$> 2.4 \times 10^{14} \text{ y} \qquad (1.54 \leq E_\alpha \leq 2.0 \text{ Mev})$$

The upper limit for the half-life in region between 2.0 and 2.14 Mev will be considerably lower because of the effect of the Sm-147 activity.

Using the same reasoning as above, it is estimated that a counting rate above background of 20 c/hr in one channel in this region would have given a significant peak. This is a factor of 10 larger than for the region between 1.54 and 2.0 Mev. The specific activities and half-life limits will also differ by a factor of 10.

S_A (Sm Sample)	< 3.1 dis/g Sm/sec	$(2.0 \leq E_\alpha \leq 2.14$ Mev)
S_A (Sm-148)	< 3.8 dis/g Sm-148/sec	$(2.0 \leq E_\alpha \leq 2.14$ Mev)
S_A (natural Sm)	< 0.41 dis/g Sm/sec	$(2.0 \leq E_\alpha \leq 2.14$ Mev)
λ (Sm-148)	$< 2.9 \times 10^{-14}$/y	$(2.0 \leq E_\alpha \leq 2.14$ Mev)
H (Sm-148)	$> 2.4 \times 10^{13}$ y	$(2.0 \leq E_\alpha \leq 2.14$ Mev)

3. Discussion

The half-life limit set for Sm-148 could have been better had the amount of Sm-147 in the sample been much less.

The Q value for Sm-148 alpha emission can be obtained from the mass measurements of Nier (Nie-56). A value of 1.90 ± 0.15 Mev has been calculated, about the same as for Nd-144. A difference of 2 in atomic number between Nd and Sm would make the half-life of Sm-148 a factor of 10 larger than Nd-144, or 2×10^{16} years. The uncertainty in the calculated energy, however, could bring the half-life as low as 2×10^{15} years ($Q = 2.05$ Mev).

If an enriched Sm-148 sample practically free from Sm-147 can be obtained, it should be possible to observe an alpha activity due to Sm-148.

F. Samarium-149

1. Experimental Details

A 30.8 mg sample of samarium oxide enriched in Sm-149 to 88.8% was counted in the ion chamber for a period of 78 hours. This represents an enrichment of 6.4 times the natural abundance of Sm-149. The sample also contained 1% Sm-147, a factor of 0.067 times the normal abundance of Sm-147. The sample thickness was 0.025 mg/cm^2.

2. Results

The spectrum obtained with the Sm-149 sample is shown in Figure XV. The Sm-147 peak was distinct and reasonably sharp giving good evidence that the sample preparation was satisfactory. No second peak, which might have been due to Sm-149 alpha activity, was observed.

The limit for the specific activity of Sm-149 was first calculated for the energy region 1.5 to 2.0 Mev, the energy where the Sm-147 alpha distribution begins to flatten out.

The counting rate between 1.5 and 2.0 Mev was 46.7 ± .78 counts per hour giving an average counting rate per channel of 3.88 ± 0.06 counts per hour.

It is estimated that a counting rate greater than 0.5 counts per hour above background in any one of the channels between 1.5-2.0 Mev would have been enough to give a definite peak.

From the Sm-147 peak, it was determined that the maximum counting rate in one channel accounted for 7.2% of the total disintegration rate.

The upper limit for the total disintegration rate due to Sm-149 in this sample is, then, 0.5/0.072 = 7.0 dis per hour, or 0.0019 dis/sec.

a. Specific Activity of Sample

$$S_A \text{ (Sm sample)} < \frac{0.0019 \text{ dis/sec}}{0.0308 \text{ g } Sm_2O_3} \times 0.862 \text{ g Sm/g } Sm_2O_3$$

$$< 0.072 \text{ dis/g Sm/sec} \qquad (1.5 \leq E_\alpha \leq 2.0 \text{ Mev})$$

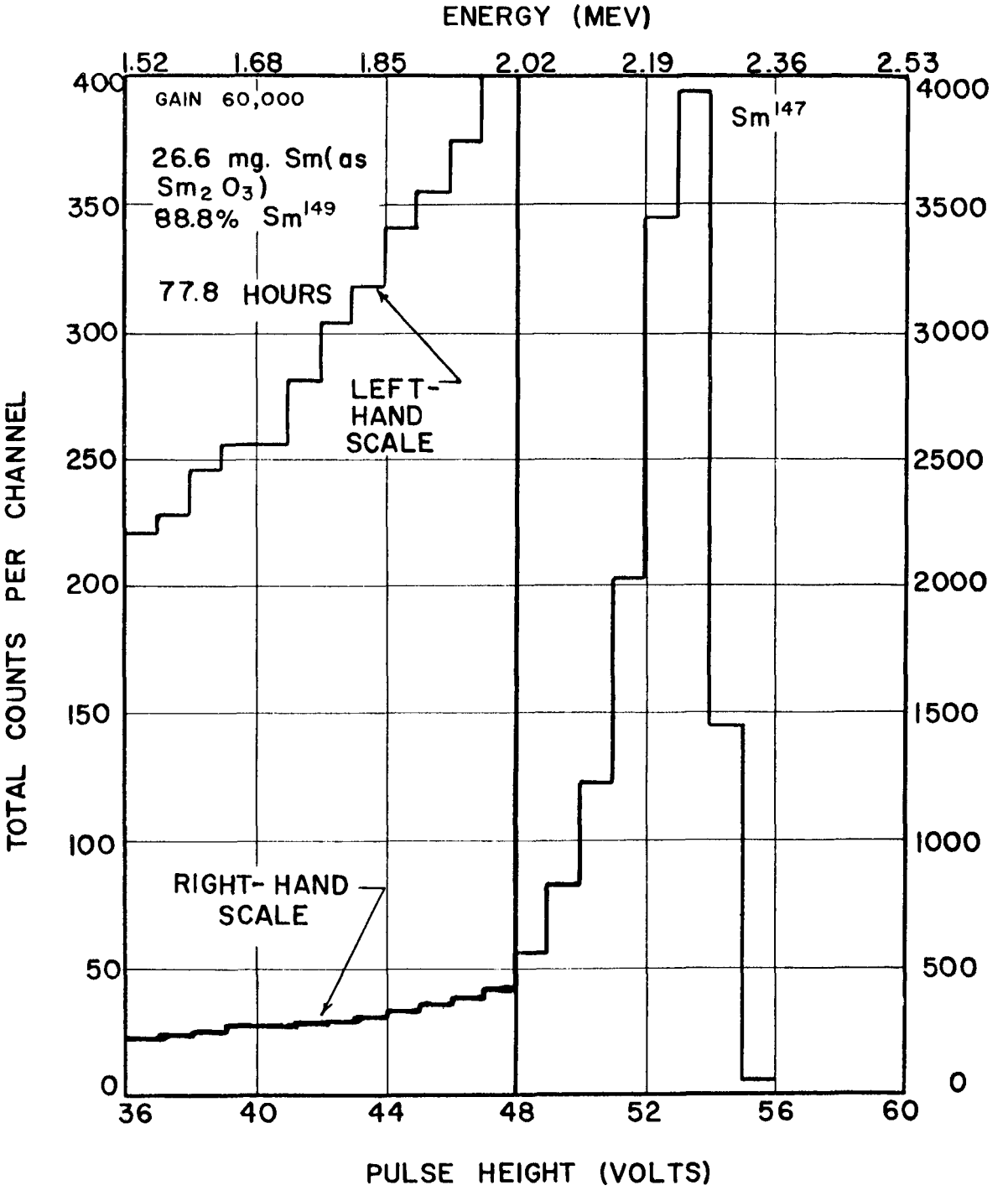

Figure XV. Alpha Spectrum of Enriched Sm-149 Sample

b. Specific Activity of Sm-149

$$S_A \text{ (Sm-149)} < \frac{S_A \text{ (Sm Sample)}}{i_{149} \text{ (Sm-sample)}} \times \frac{\alpha \text{ (Sm Sample)}}{\alpha \text{ (Sm-149)}}$$

$$< \frac{0.072 \text{ dis/g Sm/sec}}{0.888 \text{ atom Sm-149/atom Sm}} \times \frac{149.23 \text{ g Sm/mole}}{149.0 \text{ g Sm-149/mole}}$$

$$< 0.081 \text{ dis/g Sm-149/sec} \qquad (1.5 \leq E_\alpha \leq 2.0 \text{ Mev})$$

c. Specific Activity of Natural Sm

$$S_A \text{ (natural Sm)} < S_A \text{ (Sm-149)} \times i_{149} \text{ (natural Sm)} \times \frac{\alpha \text{ (Sm-149)}}{\alpha \text{ (natural Sm)}}$$

$$< 0.081 \text{ dis/g Sm-149/sec} \times 0.138 \text{ atom Sm-149/atom Sm} \times \frac{149.0 \text{ g Sm-149/mole}}{150.35 \text{ g Sm/mole}}$$

$$< 0.011 \text{ dis/g Sm/sec} \qquad (1.5 \leq E_\alpha \leq 2.0 \text{ Mev})$$

d. Decay Constant of Sm-149

$$\lambda_{(\text{Sm-149}} < \frac{0.081 \text{ dis/g Sm-149/sec} \times 149.0 \text{ g Sm-149/mole} \times 3.155 \times 10^7 \text{sec/y}}{6.023 \times 10^{23} \text{ atom/mole}}$$

$$< 6.3 \times 10^{-16}/\text{y} \qquad (1.5 \leq E_\alpha \leq 2.0 \text{ Mev})$$

e. Half-life of Sm-149

$$H = \frac{0.6931}{\lambda \text{ (Sm-149)}}$$

$$> \frac{0.6931}{6.3 \times 10^{-16}/\text{y}}$$

$$> 1.1 \times 10^{15} \text{ y} \qquad (1.5 \leq E_\alpha \leq 2.0 \text{ Mev})$$

In the region between 2.0 and 2.2 Mev it was estimated that a counting rate of 5 c/hr above background in any one channel in this region, would have produced a significant effect. This is a factor of 10 larger than the value for the region 1.5 to 2.0 Mev. The specific activity and half-life limit are then:

S_A (Sm Sample)	< 0.72 dis/g Sm/sec	$(2.0 \leq E_\alpha \leq 2.2$ Mev)
S_A (Sm-149)	< 0.81 dis/g Sm-149/sec	$(2.0 \leq E_\alpha \leq 2.2$ Mev)
S_A (natural Sm)	< 0.11 dis/g Sm-149/sec	$(2.0 \leq E_\alpha \leq 2.2$ Mev)
λ (Sm-149)	$< 6.3 \times 10^{-15}$/y	$(2.0 \leq E_\alpha \leq 2.2$ Mev)
H (Sm-149)	$> 1.1 \times 10^{14}$ y	$(2.0 \leq E_\alpha \leq 2.2$ Mev)

3. Discussion

From Nier's mass data, a value of Q for Sm-149 alpha emission can be obtained (Nie-56). Surprisingly, it is a little higher than that calculated for Sm-148, 2.00 ± .15 Mev. This apparent anamoly was the motivation for investigating this particular nuclide. Comparing with the Nd-144 half-life, this nuclide should have a half-life somewhere between 10^{14} and 10^{16} years if the Q is 2.00 ± 0.15 Mev.

If this slight break in alpha energy vs. mass number curve for Sm is real, it should present an interesting problem for explanation on a theoretical basis. Unfortunately, the upper limit on the half-life for Sm-149 calculated above does not prove or disprove the existence of this behavior.

Here, as in the case with Sm-148, it should be possible to detect alpha activity in Sm-149 if an enriched sample can be obtained containing a very small amount of Sm-147 ($<0.01\%$). This is assuming that Q_α determined from mass data is correct. If a discontinuity is not present, and a normal trend in the alpha energies of the Sm isotopes is followed, the Sm-149 alpha energy would be $\sim$ 1.6 Mev and the alpha half-life $\sim 10^{22}$ years, a half-life too long to enable detection of an activity.

G. Gadolinium-152

1. Experimental Details

A 15.5 mg sample of gadolinium oxide enriched in Gd-152 to 14.96% was counted in the ion chamber for a period of 109.3 hours. The enrichment

in Gd-152 is 75 times the normal abundance. The sample thickness was 0.0125 mg/cm^2.

In a second experiment, a small natural samarium oxide source was put on top of the gadolinium oxide deposit in the center of the counter. This Sm_2O_3 source was on a stainless steel backing 8 cm^2 in area and shaped to conform to the curvature of the counter wall. The counting rate of this source was 1 count per hour. The total time of the combined Gd and Sm run was 67.7 hours.

2. Results

Figure XVIA represents the spectrum which was obtained from the Gd-152 measurement. A distinct peak was observed at 48.3 volts. In order to find out whether this peak was due to Gd-152 or a Sm-147 impurity, a small samarium oxide source was placed on top of the gadolinium oxide and a second spectrum recorded. This is represented in Figure XVIB. In this second spectrum, two peaks were observed, one at 48.4 ± .3 volts and the other at 50.5 ± .3 volts.

The peak falling at 50.5 volts was at the approximate pulse-height voltage expected for the Sm-147 peak based on previous runs. The other peak, at 48.4 volts clearly at a voltage different from the Sm-147 peak was attributed to Gd-152, the lightest naturally occurring isotope of gadolinium.

a. Specific Activity of Sample

To obtain the absolute disintegration rate due to Gd-152 in the sample, the Gd-152 spectrum (Figure XVIA) was compared to an intense Sm-147 spectrum from a sample of Sm_2O_3 approximately the same thickness (Figure XVIID). From this, the distribution of the Gd-152 activity over the channels was determined and hence the Gd-152 activity resolved from the background.

Also, from the same Sm-147 spectrum, the fraction of the total activity above the low energy cut-off was obtained, and this value used to calculate the absolute disintegration rate of Gd-152.

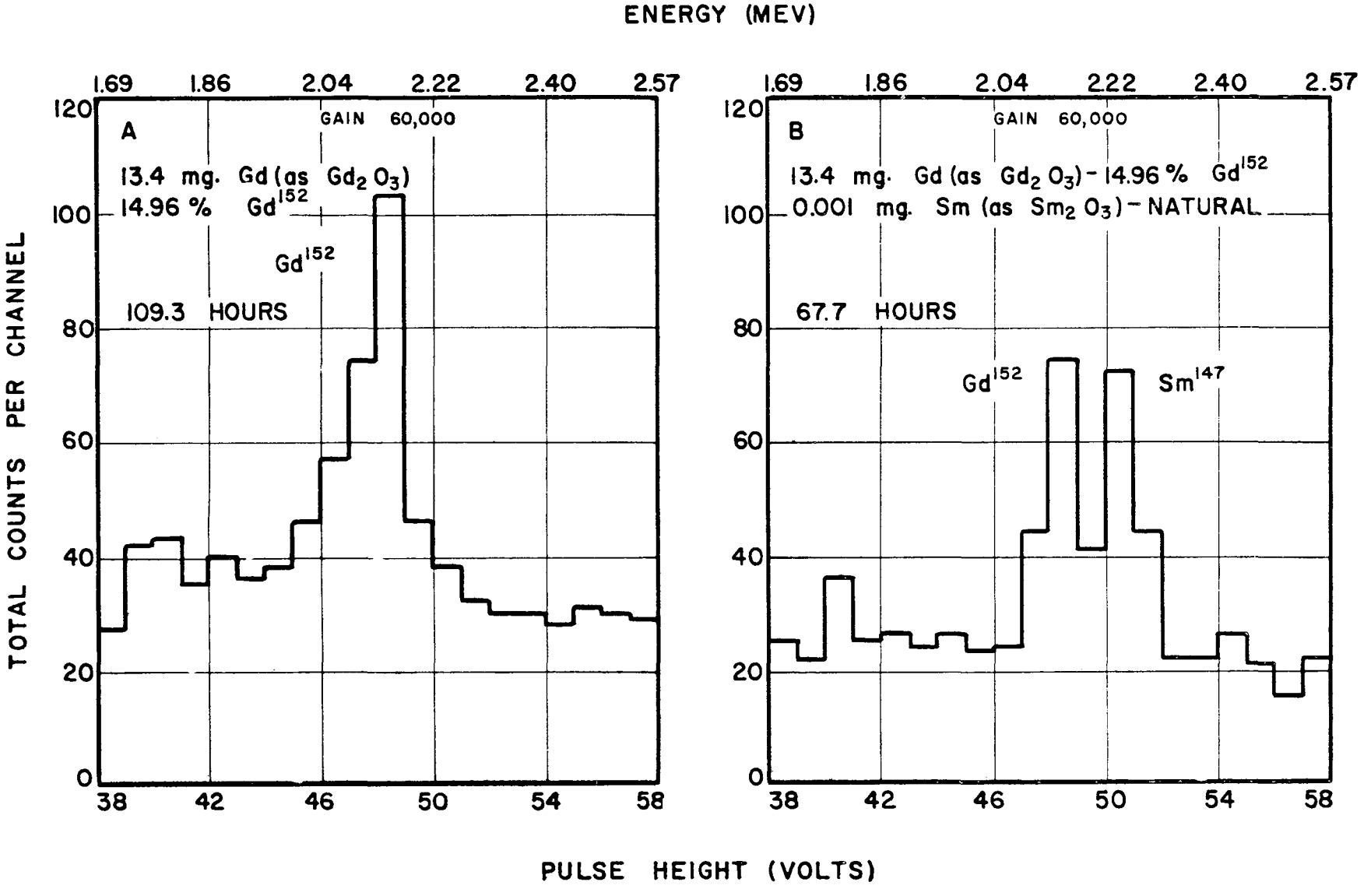

Figure XVIA. Alpha Spectrum of Enriched Gd-152 Sample

Figure XVIB. Alpha Spectrum of Enriched Gd-152 Sample and Sm_2O_3 Source

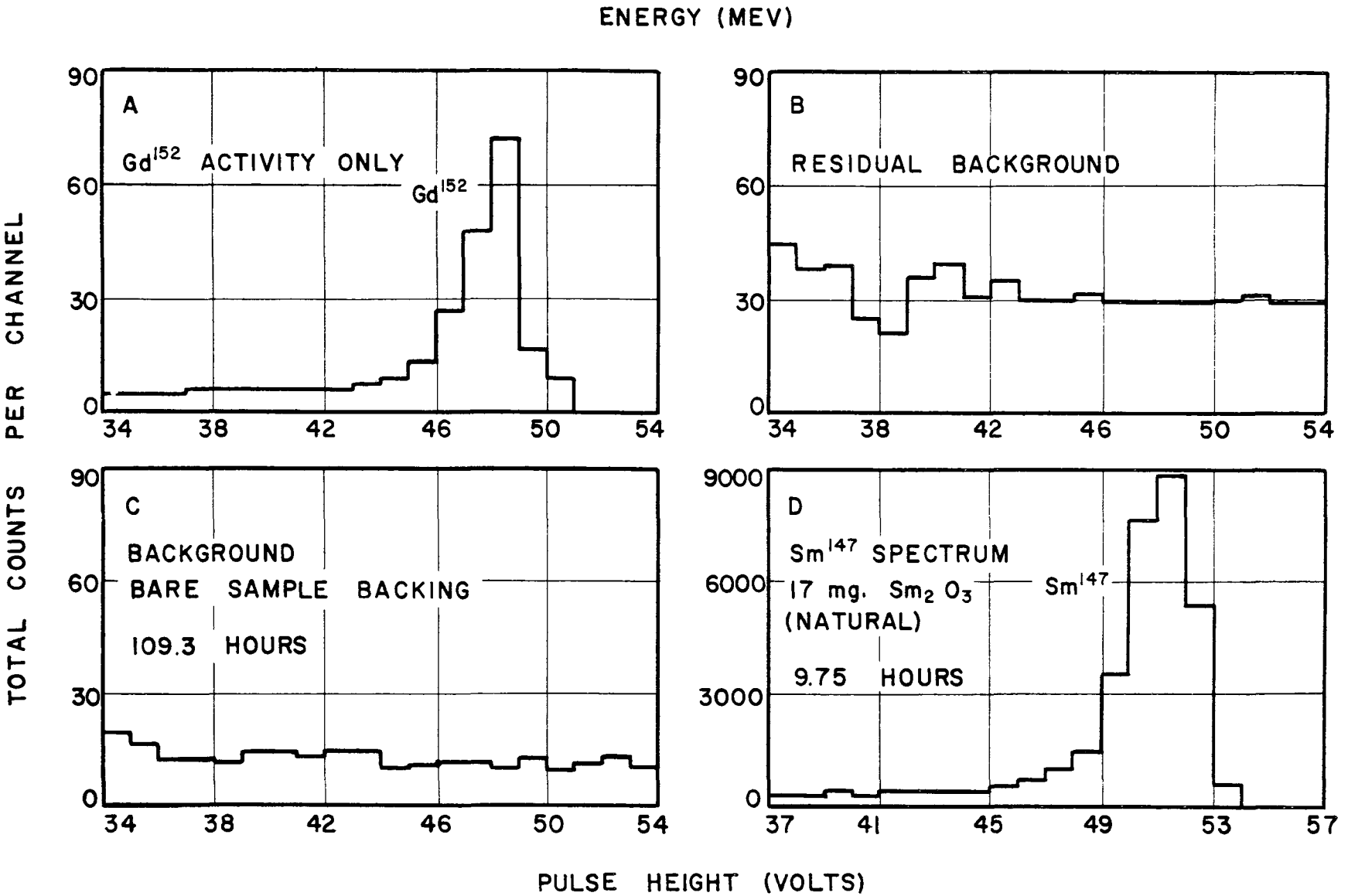

Figure XVII. Alpha Spectra Used in Gd-152 Calculations

Figure XVIIA is the spectrum of the Gd-152 activity with the background removed; Figure XVIIB is the residual background. Figure XVIIC is a background of a sample backing (not the same backing) over the same energy range and extrapolated to the same time. Figure XVIID is the Sm-147 spectrum which was used to estimate the distribution of the Gd-152 activity over the channels.

The residual background, Figure XVIIB, is higher than the background for the bare sample backing because of contamination by high energy alphas of U, Th, and their decay products. The large fluctuation in the relative number of counts per channel is the result of the statistics of the small number of counts which was present in the original spectrum.

The total number of counts due to Gd-152 above 1.51 Mev, the low energy cut-off, was 242 ± 16 giving a counting rate of 2.22 ± 0.01 c/hr or 0.000589 ± 0.0000028 c/sec.

In the intense Sm-147 spectrum, Figure XVIID, the counting rate between 1.6 and 2.3 Mev was determined to be 0.662 ± 0.0043 c/sec. Utilizing the method described previously for determining the specific activity of Sm (Section VI, A) a value was obtained which was in agreement with other values obtained indicating that 17 mg of Sm_2O_3 was actually present. Assuming the specific activity of natural Sm to be 113 ± 5 dis/g Sm/sec, the absolute counting rate should be 1.66 ± 0.07 d/sec. The fraction of the absolute counting rate detected is, then, $\frac{0.662 \pm 0.0043}{1.66 \pm 0.07} = 0.40 \pm 0.02$. Applying this value to the Gd-152 data, the absolute disintegration rate can be obtained.

The absolute disintegration rate is, then, $\frac{(0.000389 \pm 0.0000028)\text{c/sec}}{(0.40 \pm 0.02)\text{c/dis}}$ = (0.00147 ± 0.00009)dis/sec (R). W_s is the sample weight, 15.5 mg, f_{Gd}, the fraction of Gd in the sample, and C_y, an estimate of the fraction of the sample that was deposited on the sample backing.

$$S_A \text{ (Gd sample)} = \frac{R}{W_s \times f_{Gd} \text{ (Gd sample)} \times C_y}$$

$$= \frac{(0.00147 \pm 0.00009) \text{ dis/sec}}{0.0155 \text{ g } Gd_2O_3 \times 0.866 \text{ g Gd/g } Gd_2O_3 \times (0.97 \pm 0.03) \text{ g } Gd_2O_3 \text{ counted/g } Gd_2O_3 \text{ weighed}}$$

$$= 0.113 \pm 0.008 \text{ dis/g Gd/sec}$$

b. Specific Activity of Gd-152

$$S_A \text{ (Gd-152)} = \frac{S_A \text{ (Gd sample)}}{i_{152} \text{ (Gd sample)}} \times \frac{\alpha \text{ (Gd sample)}}{\alpha \text{ (Gd-152)}}$$

$$= \frac{(0.113 \pm 0.008 \text{ dis/g Gd/sec})}{0.1496 \text{ atom Gd-152/atom Gd}} \times \frac{155.55 \text{ g Gd/mole}}{152.0 \text{ g Gd-152/mole}}$$

$$= (0.772 \pm 0.052) \text{ dis/g Gd-152/sec}$$

c. Specific Activity of Natural Gd

$$S_A \text{ (natural Gd)} = S_A \text{ (Gd-152)} \times i_{152} \text{ (natural Gd)} \times \frac{\alpha(\text{Gd-152})}{\alpha(\text{natural Gd})}$$

$$= (0.772 \pm 0.052) \text{ dis/g Gd-152/sec} \times 0.002 \text{ atom Gd-152/atom Gd} \times \frac{152.0 \text{ g Gd-152/mole}}{157.26 \text{ g Gd/mole}}$$

$$= (0.00149 \pm 0.00010) \text{ dis/g Gd/sec}$$

d. Decay Constant of Gd-152

$$\lambda_{(\text{Gd-152})} = \frac{(0.772 \pm 0.052) \text{ dis/g Gd-152/sec} \times 152.0 \text{ g Gd/mole} \times 3.155 \times 10^7 \text{ sec/y}}{6.023 \times 10^{23} \text{ atom/mole}}$$

$$= (6.15 \pm 0.41) \times 10^{-15} \text{ /y}$$

e. Half-Life of Gd-152

$$H \text{ (Gd-152)} = \frac{0.6931}{(6.15 \pm 0.41) \times 10^{-15}/\text{y}}$$

$$= (1.13 \pm 0.08) \times 10^{14} \text{ y}$$

f. Alpha Particle Energy Measurement

From Figure XVIB, the pulse-height voltage of the Gd-152 peak was estimated to be 48.4 ± 0.3 volts, and the Sm-147 peak, 50.6 ± 0.3 volts. The Sm-147 alpha energy was taken as 2.24 ± 0.02 Mev. Formula V-3 given in

Section V, A was used.

$$E_\alpha \text{ (Gd-152)} = (0.158 \pm 0.010) \text{ Mev} + [E_\alpha(\text{Sm-147}) - (0.158 \pm 0.010) \text{ Mev}] \times \frac{V \text{ (Gd-152)}}{V \text{ (Sm-147)}}$$

$$= 0.158 \pm 0.010 + [(2.24 \pm 0.02) - (0.158 \pm 0.010)] \times \frac{48.4 \pm .3}{50.6 \pm 0.3}$$

$$= (2.15 \pm 0.03) \text{ Mev}$$

3. Is the Observed Activity Really Due to Gd-152?

With the measured alpha particle energy of Gd-152 being so close to the energy of Sm-147, it was necessary to prove without a doubt that the observed activity was due to Gd-152 and not to a Sm-147 impurity. The critical experiment, of course, was the one where a separate source of Sm_2O_3 was put in the counter with the gadolinium and two peaks observed.

In a preliminary experiment, the samarium source was mounted on a flat stainless steel disc and put in the counter without bending the disc to conform to the curvature of the counter wall. This resulted in a situation where most of the samarium lay a little closer to the center wire than the gadolinium. In the spectrum that was obtained, two peaks were observed, one at 48.1 volts and the other at 52.6 volts. The higher energy peak, presumably Sm-147, however, was a bit distorted and spread out. It was reasoned that the distortion of the peak was due to the effect of a distorted electric field around the center wire created by the presence of the stainless steel disc in the counter. It was also thought that a higher voltage would result for a given energy than if the source were at the counter wall.

To eliminate this difficulty, the Sm source was replaced by another which was smaller (8 cm^2 compared to 16 cm^2) and was bent to conform to the curvature of the counter wall. The spectrum obtained with this arrangement also showed two peaks (Figure XVIB) but they were only separated by 2.2 volts rather than 4.5 as before. What if the Sm were intimately mixed together with

the gadolinium? Would the two peaks come even closer together so that there would be only one peak, Sm-147, in the spectrum? Experimental difficulties prohibited the performance of an experiment where the Sm and Gd were intimately mixed together but an alternative experiment was devised which gave the same information.

The technique of using a separate calibrating source on top of the sample being studiedhas been used frequently in this work for obtaining energy calibrations. It was, therefore, important to know if there is any shift in the pulse-height voltage of the standard when it is a separate source on top of the sample compared to when it is intimately mixed with the sample.

a. Experimental Details

Two separate Sm-147 sources were prepared, one a 15 mg natural gadolinium sample spiked with samarium to give a counting rate of 0.5 counts per minute and deposited on a stainless steel sheet over an area of 1200 cm^2. The other source was natural samarium oxide on a stainless steel plate having an area of 25 cm^2 and bent to conform to the curvature of the counter wall. Its counting rate was approximately 0.5 counts per minute, also.

A spectrum of the source on the large sample backing was first obtained and then the smaller source put on the sheet and a second spectrum recorded.

b. Results

Figure XVIIIA is a plot of the spectrum obtained with the 15 mg natural Gd_2O_3 sample spiked with samarium. Figure XVIIIB is the spectrum of the combined effect of the samarium spiked gadolinium oxide sample and the separate samarium oxide source.

In both cases, only one peak was observed with no distortion of the peaks.

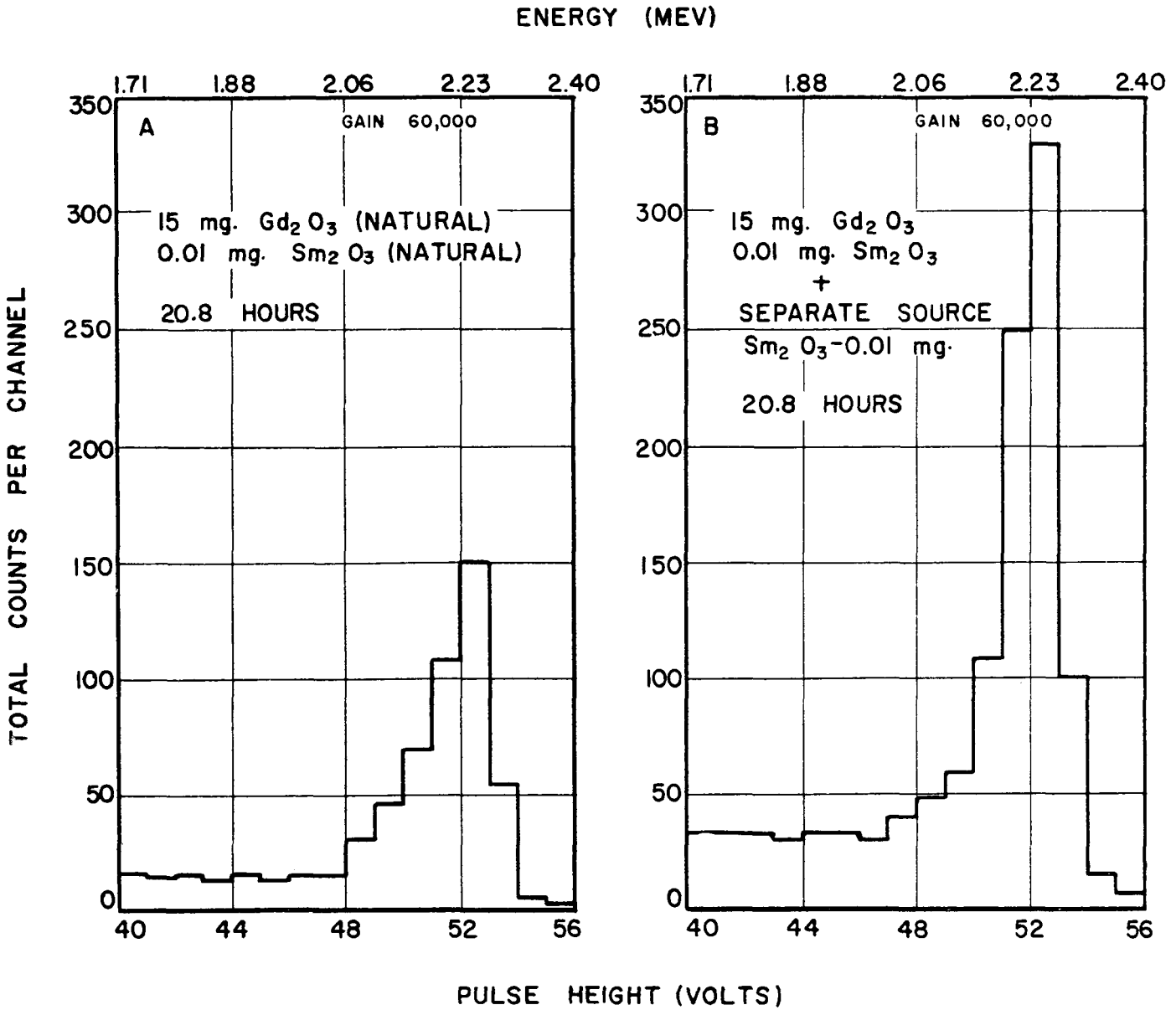

Figure XVIIIA. Alpha Spectrum of Natural Gd Spiked with Natural Sm

Figure XVIIIB. Alpha Spectrum of Natural Gd Spiked with Natural Sm plus a Separate Sm Source

It is evident from this result that the technique of using a separate calibrating source on top of the sample gives the same result as if the calibrating source were intimately mixed with the sample. One precaution must be adhered to however; the calibrating source must be at nearly the same distance from the center wire as the sample being measured. In these experiments, this difference amounted to the thickness of the sample backing of the calibrating source, 0.45 mm. Based on the measurements described above, this is apparently a tolerable difference.

4. Discussion

The alpha activity of Gd-152 would surely have been detected earlier by the nuclear emulsion technique were it not for the fact that its energy lies so close to the Sm-147 alpha energy. That its detection and resolution from Sm-147 was at all possible in this work is attributed to the distinct advantage enjoyed by the ionization chamber method in resolving alpha groups of similar energy.

The Q value for Gd-152 alpha emission, based on the measured alpha particle energy is 2.21 ± 0.03 Mev.

The experimental half-life of $(1.13 \pm 0.08) \times 10^{14}$ years is in agreement with the theoretical value (1.57×10^{14} years) by the Bethe formula using the experimental value of Q. It is just a little longer than the best lower limit which was set by Porschen and Riezler, 8×10^{13} years (Por-56).

H. Hafnium-174

1. Experimental Details

In the first experiment, a 123.9 mg sample of hafnium oxide enriched in Hf-174 to 10.14% was counted in the ion chamber. This represents an enrichment of 56.3 times the normal abundance of Hf-174. Placed on top of the HfO_2 sample was a separate Po-210 source having a counting rate of ~ 15 c/hr. Total counting time was 236 hours.

In the second experiment, a 40.5 mg sample of the same sample was counted. A small amount of natural Sm_2O_3 was mixed with the sample giving a counting rate for the samarium activity of ~ 10 c/hr. This experiment was run in order to obtain an accurate measurement of the Hf-174 alpha energy. Total counting time was 696 hours.

2. Results

The spectrum obtained with the 123.9 mg sample is plotted in Figure XIXA. A small peak is apparent in the region of 2.5 Mev which is attributed to the natural alpha activity of Hf-174.

This run was made in the early stages of the work when the optimum counting conditions were not realized. As a result the resolution of the alpha peaks is poorer than with subsequent runs. Also, the pulse-height voltage vs. energy curve is slightly different, the curve intercepting the energy axis at 500 kev compared to 158 kev for the later runs. This run was used mainly to establish the specific activity of the Hf-174 activity.

In Figure XX, the components of the gross spectrum are resolved: the Po-210 activity,Figure XXB, Hf-174 activity, Figure XXC, and the residual background, Figure XXD. The shapes of the Po-210 and Hf-174 spectra were estimated because no standard spectra were available which could accurately give the shape of the distribution of the activities under the conditions which were used.

From Figure XXC, the total number of counts above 9 volts due to Hf-147 was found to be 146 counts. The total number of counts between 9 and zero volts was obtained by a smooth extrapolation of the curve to zero volts and determined to be 20 counts. The total number of counts due to Hf-174 was then 166. Considering the uncertainties involved in the resolution of the Hf-174 activity from the gross spectrum, the uncertainty in this number was estimated to be at least 20%. The net counting rate of the Hf-174 activity

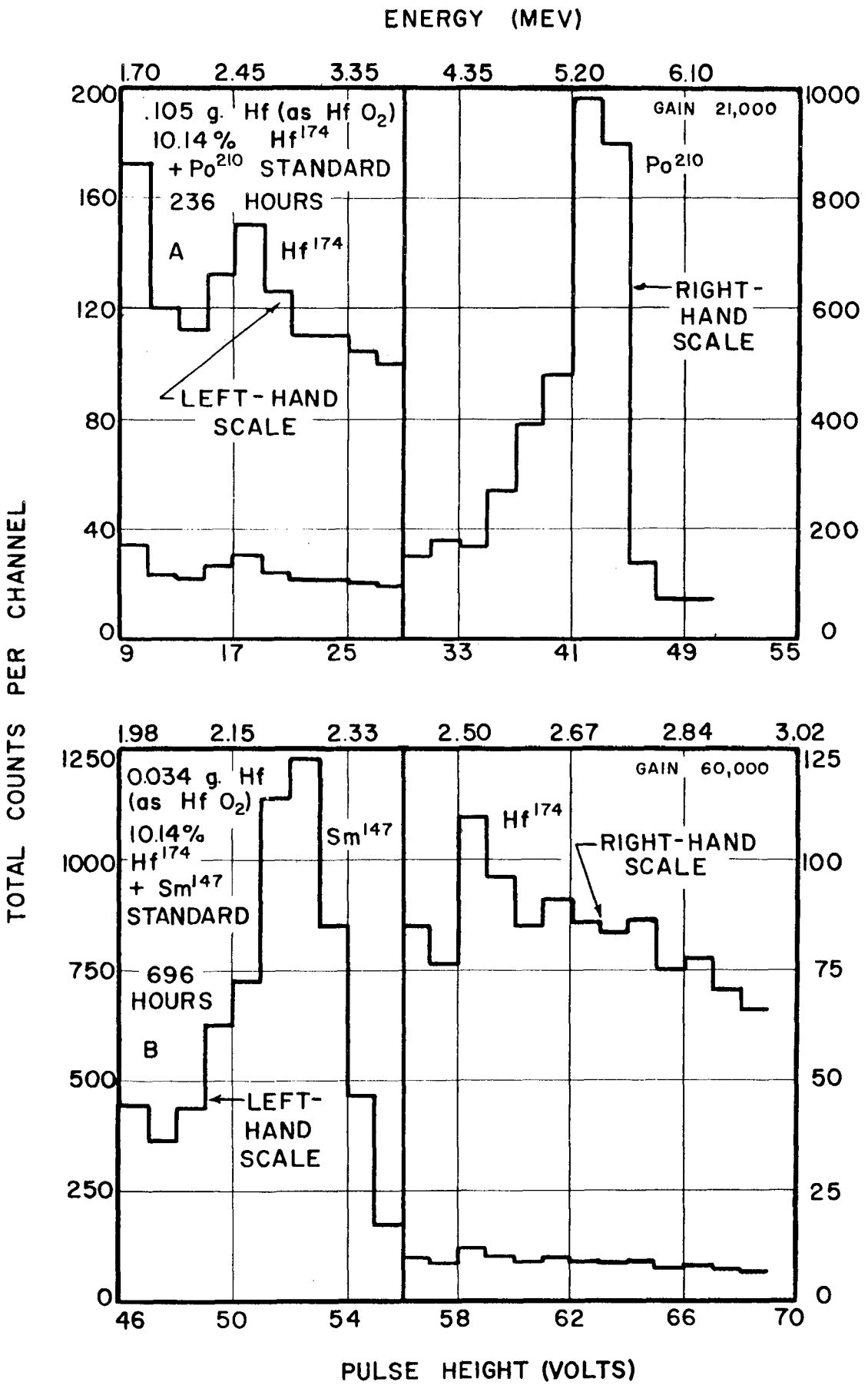

Figure XIX. Alpha Spectra of Enriched Hf-174 Sample

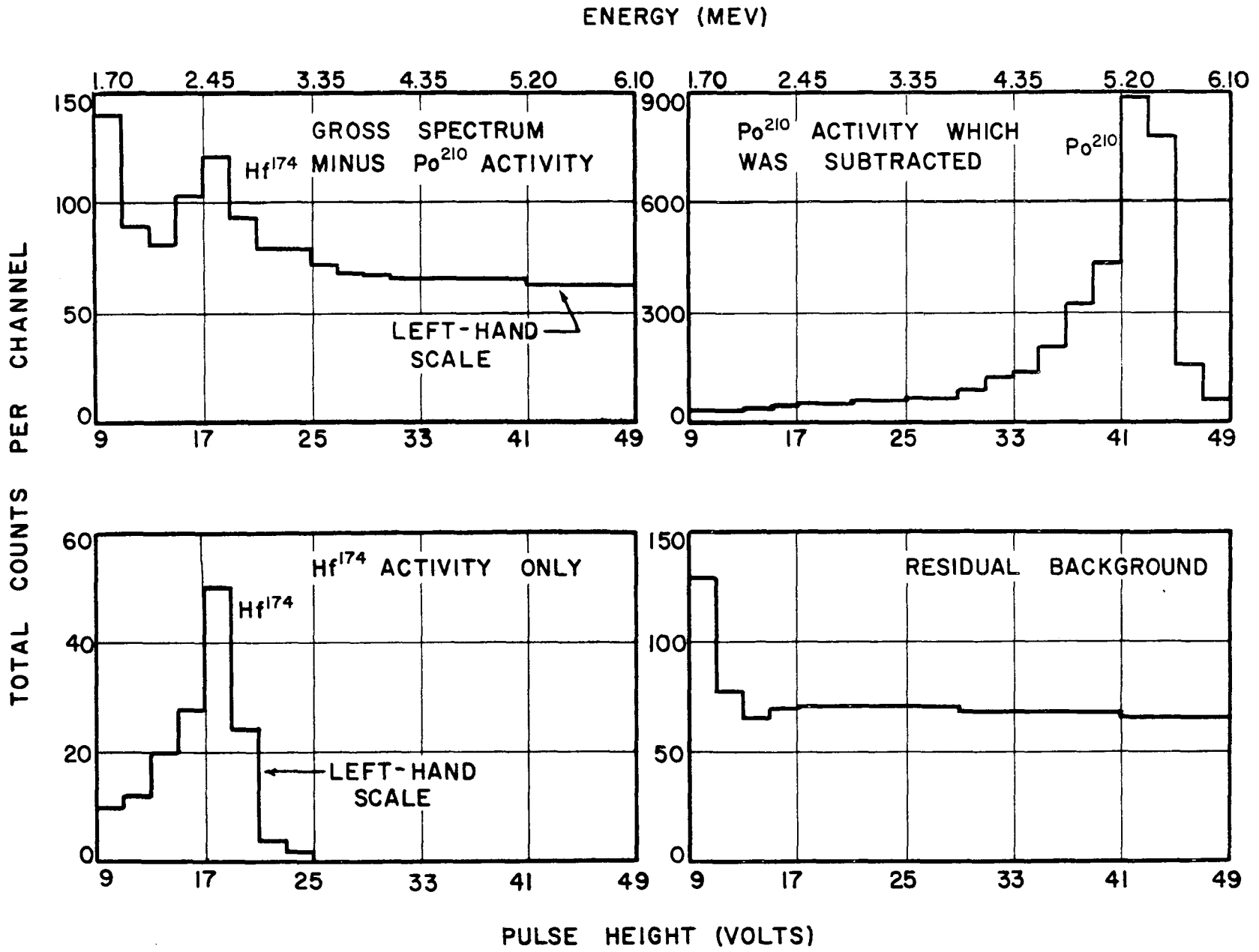

Figure XX. Alpha Spectra Used in Hf-174 Calculations

is $\frac{166 \pm 33 \text{ c}}{236 \text{ hours}} = 0.71 \pm 0.14$ c/hr or 0.0002 ± 0.00004 c/sec (R).

a. Specific Activity of Sample

The backscattering factor (B_s) was calculated using equation V-9. The range of a 2.5 Mev α in Pt is 7.5 mg/cm^2 (Gob-56).

$$B_s = 1 + \frac{0.092 \text{ mg}^{1/2}/\text{cm}}{(7.5 \text{ mg/cm}^2)^{1/2}}$$

$$= 1.033$$

The self-absorption factor (S) can be calculated using equations V-4 and V-5.

$$\frac{R(Hf)}{R_a} = 0.053 \times 72 + 0.64$$

$$= 4.45$$

The range of a 2.5 Mev α in air (R_a) is 1.65 mg/cm^2 (Wil-49). The range of a 2.5 Mev α in Hf is then

$$R_{2.5}\,(Hf) = 4.45 \times 1.65 \text{ mg/cm}^2$$

$$= 7.34 \text{ mg/cm}^2$$

Using the Bragg Sum Rule to obtain the range in HfO_2,

$$\frac{1}{R_{2.5}(Hf)} = \frac{f(Hf)}{R_{2.5}(Hf)} + \frac{f(O)}{R_{2.5}(O)}$$

$$= \frac{0.847}{7.34 \text{ mg/cm}^2} + \frac{0.153}{1.65 \text{ mg/cm}^2}$$

$$R\,(HfO_2) = 4.81 \text{ mg/cm}^2$$

The sample thickness (t) is $\frac{123.9 \text{ mg}}{1200 \text{ cm}^2} = 0.10$ mg/cm^2. The self-absorption factor is, then,

$$S = 1 - \frac{1}{2} \times \frac{t}{R(HfO_2)}$$

$$= 1 - \frac{1}{2} \times \frac{0.10 \text{ mg/cm}^2}{4.81 \text{ mg/cm}^2}$$

$$= 0.989$$

The counting yield is

$$Y = G \times B_s \times S$$

$$= 0.500 \times 1.033 \times 0.989$$

$$= 0.501$$

The chemical yield (C_y) was estimated to be 0.97 ± 0.03, i.e. 0.97 ± 0.03 of the sample that was weighed was actually counted in the chamber.

The sample weight, W_s, was 123.9 mg; the fraction of Hf in the sample, 0.847.

With these data given above, the specific activity of the sample can be calculated.

$$S_A \text{ (Hf sample)} = \frac{R}{Y \times C_y \times W_s \times f(\text{Hf sample})}$$

$$= \frac{(0.0002 \pm 0.00004) \text{ c/sec}}{0.501 \text{ c/dis} \times (0.97 \pm 0.03) \times 0.1239 \text{ g } HfO_2 \times 0.847 \text{ g Hf/g } HfO_2}$$

$$= (0.0039 \pm 0.0008) \text{ dis/g Hf/sec}$$

b. Specific Activity of Hf-174

$$S_A \text{ (Hf-174)} = \frac{S_A(\text{Hf sample})}{i_{174}(\text{Hf sample}} \times \frac{\alpha \text{ (Hf sample)}}{\alpha \text{ (Hf-174)}}$$

$$= \frac{(0.0039 \pm 0.0008) \text{ dis/g Hf/sec}}{0.1014 \text{ atom Hf-174/atom Hf}} \times \frac{177.25 \text{ g Hf/mole}}{174.00 \text{ g Hf-174/mole}}$$

$$= (0.039 \pm 0.008) \text{ dis/g Hf-174/sec}$$

c. Specific Activity of Natural Hf

$$S_A \text{ (natural Hf)} = S_A \text{ (Hf-174)} \times i_{174}(\text{natural Hf}) \times \frac{\alpha \text{ (Hf-174)}}{\alpha \text{ (natural Hf)}}$$

$$= (0.039 \pm 0.008) \text{ dis/g Hf-174/sec} \times 0.0018 \text{ atom Hf-174/atom Hf}$$

$$\times \frac{174.0 \text{ g Hf-174/mole}}{178.50 \text{ g Hf/mole}}$$

$$= (0.000068 \pm 0.000013) \text{ dis/g Hf/sec}$$

d. Decay Constant of Hf-174

$$\lambda_{(Hf-174)} = \frac{(0.039 \pm 0.008)\text{dis/g Hf-174/sec} \times 174\text{ g Hf-174/mole} \times 3.155 \times 10^{7}\text{ sec/y}}{6.023 \times 10^{23}\text{ atom/mole}}$$

$$= (3.5 \pm 0.7) \times 10^{-16}/\text{y}$$

e. Half-life of Hf-174

$$H\,(Hf-174) = \frac{0.6931}{(3.5 \pm 0.7) \times 10^{-16}}$$

$$= (2.0 \pm 0.4) \times 10^{15}\text{ y}$$

f. Alpha Particle Energy Measurement

From Figure XIXB, the data required to calculate the alpha particle energy of Hf-174 can be obtained. The Sm-147 peak was determined to fall at 52.1 ± 0.3 volts and the Hf-174 peak at 58.7 ± 0.5 volts. The alpha particle energy of Sm-147 was taken to be 2.24 ± 0.02 Mev. Using equation V-3,

$$E\,(Hf-174) = E^{*} + [E(Sm-147) - E^{*}] \times \frac{V(Hf-174)}{V(Sm-147)}$$

$$= (0.158 \pm 0.010) + [(2.24 \pm 0.02) - (0.158 \pm 0.010)] \times \frac{58.7 \pm 0.5}{52.1 \pm 0.3}$$

$$= (2.50 \pm 0.03)\text{ Mev}$$

3. Discussion

The alpha particle energy calculated above gives a Q_{α} of 2.56 ± 0.03 Mev for the decay energy of Hf-174. Using this value to calculate a theoretical half-life employing the Bethe formula, a half-life of 2.69×10^{15} years was obtained which is in agreement with t he experimental value of $(2.0 \pm 0.4) \times 10^{15}$ years determined above.

I. Tungsten-180

1. Experimental Details

A 99.5 mg sample of WO_3 containing W-180 enriched to 6.95% was counted in the ion chamber for a period of 66.7 hours. This represents an

enrichment of 49.6 times the normal abundance of W-180. The sample thickness was 0.083 mg/cm^2.

A separate source (8 cm^2 area) containing Po-210 to give a counting rate of 1.5 counts per hour was put on top of the tungsten sample to provide an energy calibration.

2. Results

Figure XXI is a histogram of the spectrum which was obtained. The Po-210 activity gave a prominent peak in the spectrum but no other peak was observed which could be attributed to W-180. There was an indication of a small peak at ~2.7 Mev but there was not a significant number of counts to establish a definite activity.

The counting rate of the bare sample backing for the region 2 to 3.5 Mev was 1.11 ± 0.12 counts per hour compared to 1.14 ± 0.12 counts per hour with the tungsten sample for the same energy interval.

It is estimated that a counting rate of 0.5 counts per hour above background would have given a significant spectrum. Further, from an extrapolation of the Sm-147 data for a 100 mg sample of samarium oxide, at least 30% of the total disintegration rate would have been recorded in the energy interval 2-3.5 Mev. The limit of the total disintegration rate is, then, 0.5/0.30 = 1.7 alphas per hour or 0.0005 dis/sec.

a. Specific Activity of Sample

$$S_A \text{ (W sample)} < \frac{0.0005 \text{ dis/sec}}{0.0995 \text{ g } WO_3 \times 0.793 \text{ g W/g } WO_3}$$

$$< 0.006 \text{ dis/g W/sec}$$

b. Specific Activity of W-180

$$S_A \text{ (W-180)} < \frac{S_A \text{ (W sample)}}{i_{180} \text{ (W sample)}} \times \frac{\alpha \text{ (W sample)}}{\alpha \text{ (W-180)}}$$

$$< \frac{0.006 \text{ dis/g W/sec}}{0.0695 \text{ atom W-180/atom W}} \times \frac{183.01 \text{ g W/mole}}{180.0 \text{ g W-180/mole}}$$

$$< 0.08 \text{ dis/g W-180/sec}$$

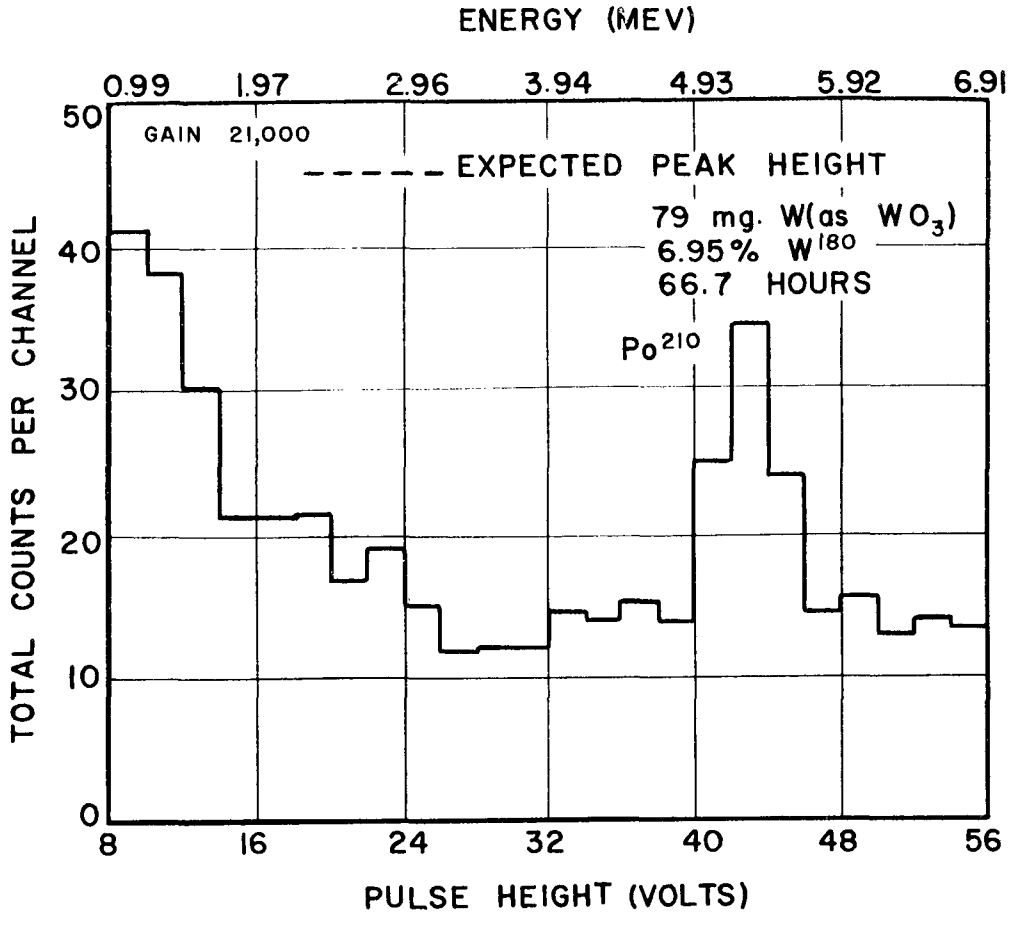

Figure XXI. Alpha Spectrum of Enriched W-180 Sample

c. Specific Activity of Natural W

$$S_A \text{ (natural W)} \quad S_A \text{ (W-180)} \times i_{180} \text{ (natural W)} \times \frac{\alpha \text{ (W-180}}{\alpha \text{ (natural W)}}$$

$$< 0.08 \text{ dis/g W-180.sec} \times 0.0014 \text{ atom W-180/atom W} \times \frac{180.0 \text{ g W-180/mole}}{183.86 \text{ g W/mole}}$$

$$< 0.0001 \text{ dis/g W/sec}$$

d. Decay Constant of W-180

$$\lambda_{(W-180)} < \frac{S_A \text{ (W-180)} \times \alpha \text{ (W-180)} \times 3.155 \times 10^7 \text{ sec/y}}{6.023 \times 10^{23} \text{ atom/mole}}$$

$$< \frac{0.08 \text{ dis/g W-180/sec} \times 180 \text{ g W-180/mole} \times 3.155 \times 10^7 \text{ sec/y}}{6.023 \times 10^{23} \text{ atom/mole}}$$

$$< 7.9 \times 10^{-15}/\text{y}$$

e. Half-Life of W-180

$$H \text{ (W-180)} > \frac{0.6931}{\lambda \text{(W-180)}}$$

$$> \frac{0.6931}{7.9 \times 10^{-15}/\text{y}}$$

$$> 8.8 \times 10^{14} \text{ y} \qquad 2.5 \leq E_\alpha \leq 3.5 \text{ Mev}$$

3. Discussion

The negative result obtained for W-180 was indeed surprising. If the alpha activity observed by Porschen and Riezler in natural tungsten (Por-53) had been due to W-180, supposedly the lightest naturally occurring isotope of tungsten, a pronounced peak would have been observed. (See Figure XXI for the expected peak height).

This leaves the situation open to two possible explanations. Either the activity is due to some isotope of tungsten other than W-180, such as W-178 or W-179, whose abundance is so low that it has gone undetected; or the original observation of activity in the natural sample

was in error (See Section I, p. 16). Before any investigations are directed to the possibility of the existence of an extremely rare isotope of tungsten, it would seem advisable to recheck the natural tungsten result of Porschen and Riezler.

According to a private communication from Riezler and Kauw in July, 1958 (Rie-58b), they have also made measurements with enriched W-180 using nuclear emulsions. They too could not find activity at the level to be expected assuming W-180 to be the active isotope, in agreement with our results communicated to them at the same time.

J. Platinum-190

1. Experimental Details

In the first experiment, a 1.602 gm sample of natural platinum was plated on the sample backing and counted for a period of 34.5 hours. The sample thickness was 1.602 mg/cm^2.

In the second experiment, a 45.3 mg sample of platinum enriched in Pt-190 was counted for the same time, 34.5 hours. The sample thickness was 0.045 mg/cm^2. The fraction of Pt-190 in the sample was 0.0076, representing an enrichment to 63.3 times the normal abundance of Pt-190.

The third experiment, whose purpose was to obtain an accurate measurement of the Pt-190 alpha particle energy, involved the counting of 25 mg of the enriched Pt-190 sample on which had been placed a small Sm-147 and Th-232 calibration source. Counting time for this run was 12 hours with the Sm-147 and Pt-190 peaks and 12 hours with the Th-232 and Pt-190 peaks. The sample thickness was 0.025 mg/cm^2.

2. Results

a. Natural Platinum

Figure XVIIA is a histogram obtained from the natural platinum sample. A strong peak was observed in the neighborhood of 3 Mev and another

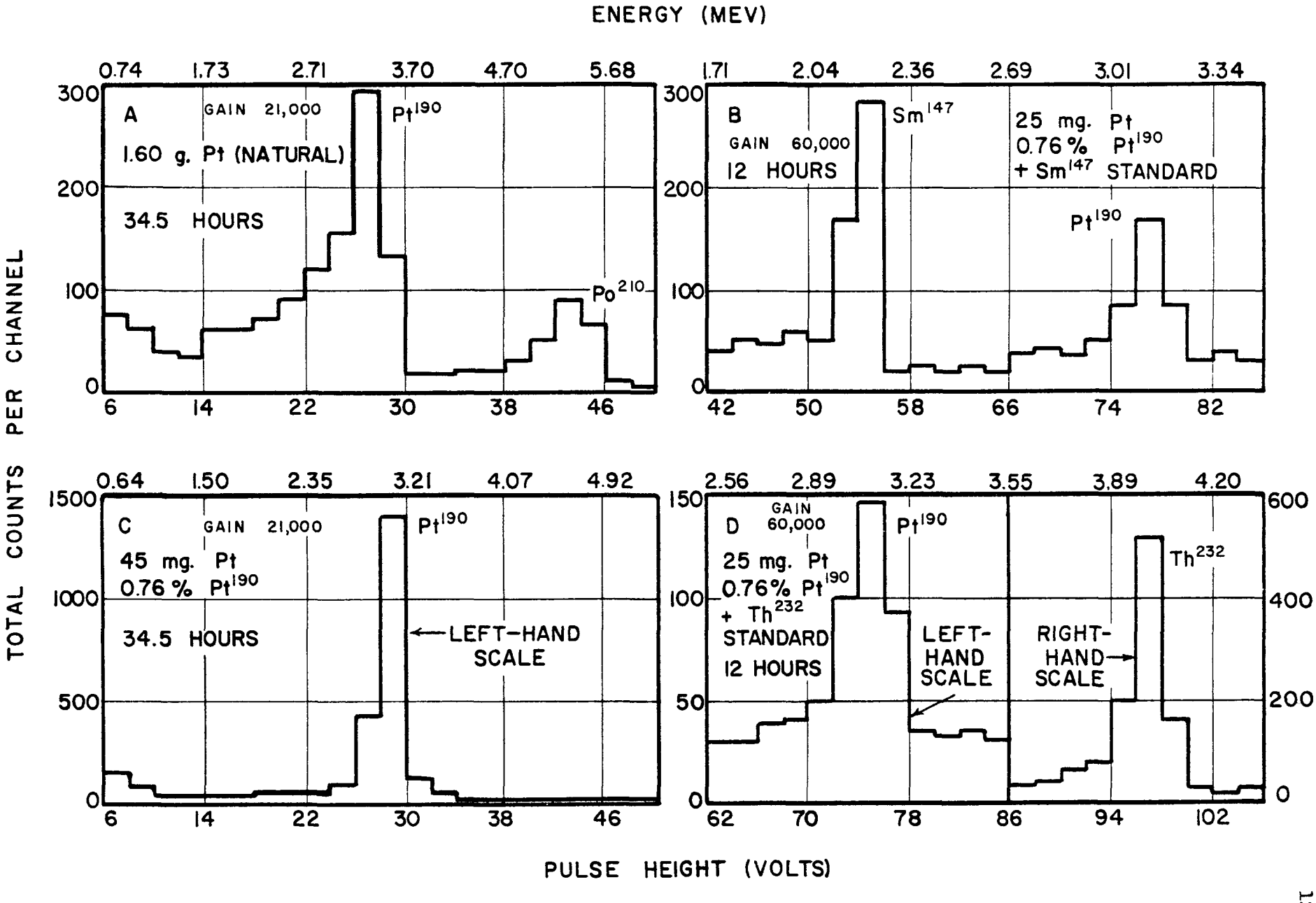

Figure XXII. Alpha Spectra of Natural Pt and Enriched Pt-190 Sample

at 5.3 Mev. The latter peak was attributed to Po-210 contamination, and the former to Pt-190.

The total activity due to Pt-190 only was easily obtained by extrapolating the spectrum to zero volts, and subtracting the Pt-190 activity from background, which was much lower than the level of the Pt-190 activity.

1. Specific Activity of Sample.

The total number of counts from 0 to 30 volts was 1441 ± 144, or 0.0126 ± 0.001 counts per second. Of this total, 430 ± 43 counts or 0.0034 ± 0.0003 c/sec were attributed to the background. The total counting rate due to Pt-190 is, then, 0.0082 ± 0.0008 c/sec (R).

The backscattering surface was considered to be the sample itself because of the thickness of the sample. The backscattering factor, B_s, can be calculated using equation V-8.

$$B_s = 1 + 2 \times \left[\frac{R\ (4.76\ \text{Mev})}{R\ (3.10\ \text{Mev})}\right]_{Pt}^{1/2} \times \left[\frac{a\ (Pt)}{a\ (Pt)}\right]^{3/2} \times 0.03$$

The range of a 4.76 Mev α in Pt is 15.2 mg/cm^2 and of a 3.10 Mev α, 9.4 mg/cm^2 (Gob-56). The backscattering factor, then, is

$$B_s = 1 + 2 \times \left(\frac{15.2\ \text{mg/cm}^2}{9.4\ \text{mg/cm}^2}\right)^{1/2} \times 0.03$$

$$= 1.076$$

The self-absorption factor S, can be calculated using equation V-4

$$S = 1 - \frac{1}{2} \times \frac{t}{R}$$

$$= 1 - \frac{1}{2} \times \frac{1.602\ \text{mg/cm}^2}{9.4\ \text{mg/cm}^2}$$

$$= 0.915$$

The counting yield is then,

$$Y = G \times B_s \times S$$

$$= 0.500 \times 1.076 \times 0.915$$

$$= 0.492$$

The chemical yield C_y, is equal to unity because the Pt was analyzed after the run was made (See Section IV, p. 57). Using the above data, the specific activity of natural Pt can be calculated.

$$S_A \text{ (natural Pt)} = \frac{R}{Y \times C_y \times W_s}$$

$$= \frac{0.0082 \pm 0.0008 \text{ c/sec}}{0.492 \text{ c/dis} \times 1 \times 1.602 \text{ g Pt}}$$

$$= (0.010 \pm 0.001) \text{ dis/g Pt/sec}$$

2. Specific Activity of Pt-190

$$S_A \text{ (Pt-190)} = \frac{S_A \text{ (natural Pt)}}{i_{190} \text{ (natural Pt)}} \times \frac{\alpha \text{ (natural Pt)}}{\alpha \text{ (Pt-190)}}$$

$$= \frac{(0.0104 \pm 0.001) \text{ dis/g Pt/sec}}{0.00012 \text{ atom Pt-190/atom Pt}} \times \frac{195.09 \text{ g Pt/mole}}{190 \text{ g Pt-190/mole}}$$

$$= (89 \pm 4) \text{ dis/g Pt-190/sec}$$

3. Decay Constant of Pt-190

$$\lambda(\text{Pt-190}) = \frac{S_A \text{ (Pt-190)} \times \alpha \text{ (Pt-190)} \times 3.155 \times 10^7 \text{ sec/y}}{6.023 \times 10^{23} \text{ atom/mole}}$$

$$= \frac{(89 \pm 9) \text{ dis/g Pt-190/sec} \times 190 \text{ g Pt-190/mole} \times 3.155 \times 10^7 \text{sec/y}}{6.023 \times 10^{23} \text{ atom/mole}}$$

$$= (8.9 \pm 0.9) \times 10^{-13}/\text{y}$$

4. Half-Life of Pt-190

$$H = \frac{0.6931}{\lambda(\text{Pt-190})}$$

$$= \frac{0.6931}{(8.9 \pm 0.4) \times 10^{-13}/\text{y}}$$

$$= (7.8 \pm 0.8) \times 10^{11} \text{ y}$$

b. Enriched Platinum-190

Figure XXIIC represents the spectrum obtained with 45.3 mg of the enriched Pt-190 sample. Figure XXIIB is a spectrum of the combined effect of Pt-190 and Sm-147 and Figure XXIID, Pt-190 and Th-232. Both of these spectra were used to determine the alpha particle energy of Pt-190.

1. Specific Activity of Sample

The high counting rate (compared to background) in the Pt-190 pulse distribution (Figure XXIIC) made the determination of the total number of counts due to Pt-190 quite straightforward and devoid of a large number of the uncertainties present with the other samples studied.

The total number of counts from 0 to 32 volts was 2459 ± 120 or 0.0198 ± 0.0009 counts per second. The background was estimated to be 240 ± 24 counts or 0.0019 ± 0.0002 c/sec. The net counting rate due to Pt-190 then is 0.0179 ± 0.0009 c/sec (R).

Because of the thinness of the sample used the backscattering surface was considered to be the copper surface on top of the stainless steel backing. The backscattering factor can be calculated using equation V-8.

$$B_s = 1 + 2 \times \left[\frac{R\ (4.76\ \text{Mev}\ \alpha)}{R\ (3.10\ \text{Mev}\ \alpha)} \right]_{Pt}^{1/2} \times \left[\frac{\alpha\ (Cu)}{\alpha\ (Pt)} \right]^{3/2} \times 0.03$$

$$= 1 + 2 \times \left(\frac{15.2\ \text{mg/cm}^2}{9.4\ \text{mg/cm}^2} \right)^{1/2} \times \left(\frac{63.57\ \text{g Cu/mole}}{195.09\ \text{g Pt/mole}} \right)^{3/2} \times 0.03$$

$$= 1.014$$

The self-absorption factor (S), can be calculated using equation V-4.

$$S = 1 - \frac{1}{2} \times \frac{t}{R}$$

$$= 1 - \frac{1}{2} \times \frac{0.025\ \text{mg/cm}^2}{9.4\ \text{mg/cm}^2}$$

$$= 0.986$$

The chemical yield (C_y), as in the case with natural Pt, is unity because the sample was analyzed after the run was made.

The counting yield is then,

$$Y = G \times S \times B_s$$

$$= 0.500 \times 0.986 \times 1.014$$

$$= 0.500$$

The specific activity of the sample can then be calculated using the above data

$$S_A \text{ (Pt sample)} = \frac{R}{Y \times C_y \times W_s}$$

$$= \frac{(0.0179 \pm 0.0004) \text{ c/sec}}{0.500 \text{ c/dis} \times 1 \times 0.0453 \text{ g Pt}}$$

$$= (0.790 \pm 0.017) \text{ dis/g Pt/sec}$$

2. Specific Activity of Pt-190

$$S_A \text{ (Pt-190} = \frac{S_A \text{ (Pt sample)}}{i_{190} \text{ (Pt sample}} \times \frac{a \text{ (Pt sample)}}{a \text{ (Pt-190)}}$$

$$= \frac{(0.790 \pm 0.017) \text{ dis/g Pt/sec}}{0.0076 \text{ atom Pt-190/atom Pt}} \times \frac{194.56 \text{ g Pt/mole}}{190.0 \text{ g Pt-190/mole}}$$

$$= (106 \pm 5) \text{ dis/g Pt-190/sec}$$

3. Specific Activity of Natural Pt

$$S_A \text{ (Natural Pt)} = S_A \text{ (Pt-190)} \times i_{190}\text{(natural Pt)} \times \frac{a \text{ (Pt-190)}}{a \text{ (natural Pt)}}$$

$$= (106 \pm 5) \text{ dis/g Pt-190/sec} \times 0.00012 \text{ atom Pt-190/atom Pt} \times \frac{190.0 \text{ g Pt-190/mole}}{195.09 \text{ g Pt/mole}}$$

$$= (0.013 \pm 0.0005 \text{ dis/g Pt/sec}$$

4. Decay Constant of Pt-190

$$\lambda \text{ (Pt-190)} = \frac{S_A \text{ (Pt-190)} \times a \text{ (Pt-190)} \times 3.155 \times 10^7 \text{ sec/y}}{6.023 \times 10^{23} \text{ atom/mole}}$$

$$= (1.06 \pm 0.05) \times 10^{-12}/\text{y}$$

5. Half-Life of Pt-190

$$H = \frac{0.6931}{\lambda \text{ (Pt-190)}}$$

$$= \frac{0.693}{(1.06 \pm 0.05) \times 10^{-12}/\text{y}}$$

$$= (6.5 \pm 0.3) \times 10^{11} \text{ y}$$

The average values for the specific activity and half-life of Pt-190 obtained from natural and enriched Pt are summarized below. The values obtained with the enriched Pt-190 were weighed a factor of 3 relative to the natural Pt results because fewer uncertainties were involved with the enriched Pt-190 result.

S_A (natural Pt)	(0.012 ± 0.001) dis/g Pt/sec
S_A (Pt-190)	(100 ± 7) dis/g Pt-190/sec
λ (Pt-190)	(1.0 ± 0.07) x 10^{-12}/y
H (Pt-190)	(6.9 ± 0.5) x 10^{11} y

6. Alpha Particle Energy Determination

From Figure XXIIB, the Sm-147 alpha peak was estimated to fall at 54.7 ± 0.2 volts and the Pt-190 alpha at 77.0 ± 0.2 volts. The Sm-147 alpha energy was taken to be 2.24 ± 0.02 Mev. Using equations V-3, the Pt-190 alpha particle energy can be calculated.

$$E\ (Pt\text{-}190) = E^* + [E(Sm\text{-}147) - E^*] \times \frac{V\ (Pt\text{-}190)}{V\ (Sm\text{-}147)}$$

$$= (0.158 \pm 0.010) + [(2.24 \pm 0.02) - (0.158 \pm 0.010] \times \frac{77.0 \pm 0.2}{54.7 \pm 0.2}$$

$$= (3.09 \pm 0.03)\ \text{Mev.}$$

The Pt-190 peak was also compared with Th-232 in order to obtain an independent measurement of the alpha particle energy (Figure XXIID). The Pt-190 alpha peak was estimated to fall at 74.8 ± 0.4 volts and the Th-232 peak at 96.8 ± 0.4 volts. The Th-232 alpha energy was taken to be 4.01 ± 0.005 Mev (Har-57). See Table VI.

$$E\ (Pt\text{-}190) = E^* + [E\ (Th\text{-}232) - E^*] \times \frac{V\ (Pt\text{-}190)}{V\ (Th\text{-}232)}$$

$$= (0.158 \pm 0.010) + [(4.01 \pm 0.005) - (0.158 \pm 0.010)] \times \frac{74.8 \pm 0.4}{96.8 \pm 0.4}$$

$$= (3.13 \pm 0.02)\ \text{Mev}$$

The average of the two determinations is 3.11 ± 0.03 Mev.

3. Discussion

The fact that approximately the same specific activity (correcting for isotope enrichment) was obtained for both the natural platinum and enriched platinum-190 sample gives experimental proof to the mass assignment of 190 as the naturally alpha active isotope of platinum.

The experimental values of the alpha energy and half-life of Pt-190 are in agreement with those determined by Porschen and Riezler (Por-54). Their results gave 3.3 ± .2 Mev for the alpha energy and 1×10^{12} (± 50%) for the half-life.

They also had indication of a second peak in their spectrum at about 2.7 Mev which might be due to Pt-192. However, in our results, it was not possible to either confirm or dispute the possibility. This was mainly due to the fact that the effect was so weak that it was swamped out by the more intense Pt-190 spectrum.

The alpha decay energy of Pt-190 obtained from the experimental particle energy obtained above is calculated to be 3.18 ± 0.03 Mev. Using this value, the theoretical half-life using the Bethe formula is found to be 6.25×10^{11} years which is in good agreement with the observed experimental values.

There is a possibility of fine structure in the Pt-190 spectrum due to alpha decay to the first excited state of Os-186, lying 137 kev above the ground state. (Ptr-56). An attempt was made to detect a fine structure in the Pt-190 spectrum but it was not possible to resolve it from the main peak. An alternative approach would be to study the excited state transition through the emitted gammas or internal conversion electrons or coincidences between gammas and alphas.

K. Mercury-196

1. Experimental Details

A 121.4 mg sample of HgS enriched in Hg-196 to 1.46% was counted in the ion chamber for a period of 23.9 hours. This represents an enrichment of 9.75 times the natural abundance of Hg-196. The sample was 0.105 mg thick.

A separate Po-210 standard was placed on top of the HgS sample to give the energy calibration.

2. Results

Figure XXIII is a histogram of the spectrum obtained. The Po-210 calibration peak was observed but no second peak which could be attributed to Hg-196.

The specific activity limit for Hg-196 was referred to the region 2.5 - 3.5 Mev. On the basis of the energy dependence on the half-life of Hg-196, it is doubtful whether its alpha will appear out of this region.

The total counting rate in this region was 2.50 ± 0.07 counts per hour. It is estimated that 1 count per hour above background from Hg-196 would have given a significant spectrum. Further, from the Sm-147 results, it was estimated that 40% of the absolute disintegration rate would have fallen in this interval. This includes the geometry factor.

The limit to the absolute disintegration rate is, then, 1/0.4 2.5 alphas per hour or 0.00069 dis/sec.

a. Specific Activity of Sample

$$S_A \text{ (Hg Sample)} < \frac{0.00069 \text{ dis/sec}}{0.1214 \text{ g HgS} \times 0.863 \text{ g Hg/g HgS}}$$

$$< 0.007 \text{ dis/g Hg/sec}$$

b. Specific Activity of Hg-196

$$S_A \text{ (Hg-196)} < \frac{S_A \text{ (Hg Sample)}}{i_{196} \text{ (Hg Sample)}} \times \frac{\alpha \text{ (Hg Sample)}}{\alpha \text{ (Hg-196)}}$$

$$< \frac{0.007 \text{ dis/g Hg/sec}}{0.0146 \text{ atom Hg-196/atom Hg}} \times \frac{201.73 \text{ g Hg/mole}}{196.0 \text{ g Hg-196/mole}}$$

$$< 0.5 \text{ dis/g Hg-196/sec}$$

c. Specific Activity of Natural Hg

$$S_A \text{ (natural Hg)} < S_A \text{ (Hg-196)} \times i_{196} \text{ (natural Hg)} \times \frac{\alpha \text{ (Hg-196)}}{\alpha \text{ (natural Hg)}}$$

$$< 0.5 \text{ dis/g Hg-196/sec} \times 0.0005 \text{ atom Hg-196/atom Hg}$$

$$\times \frac{196.0 \text{ g Hg-196/mole}}{200.61 \text{ g Hg/mole}}$$

$$< 0.0007 \text{ dis/sec/g Hg}$$

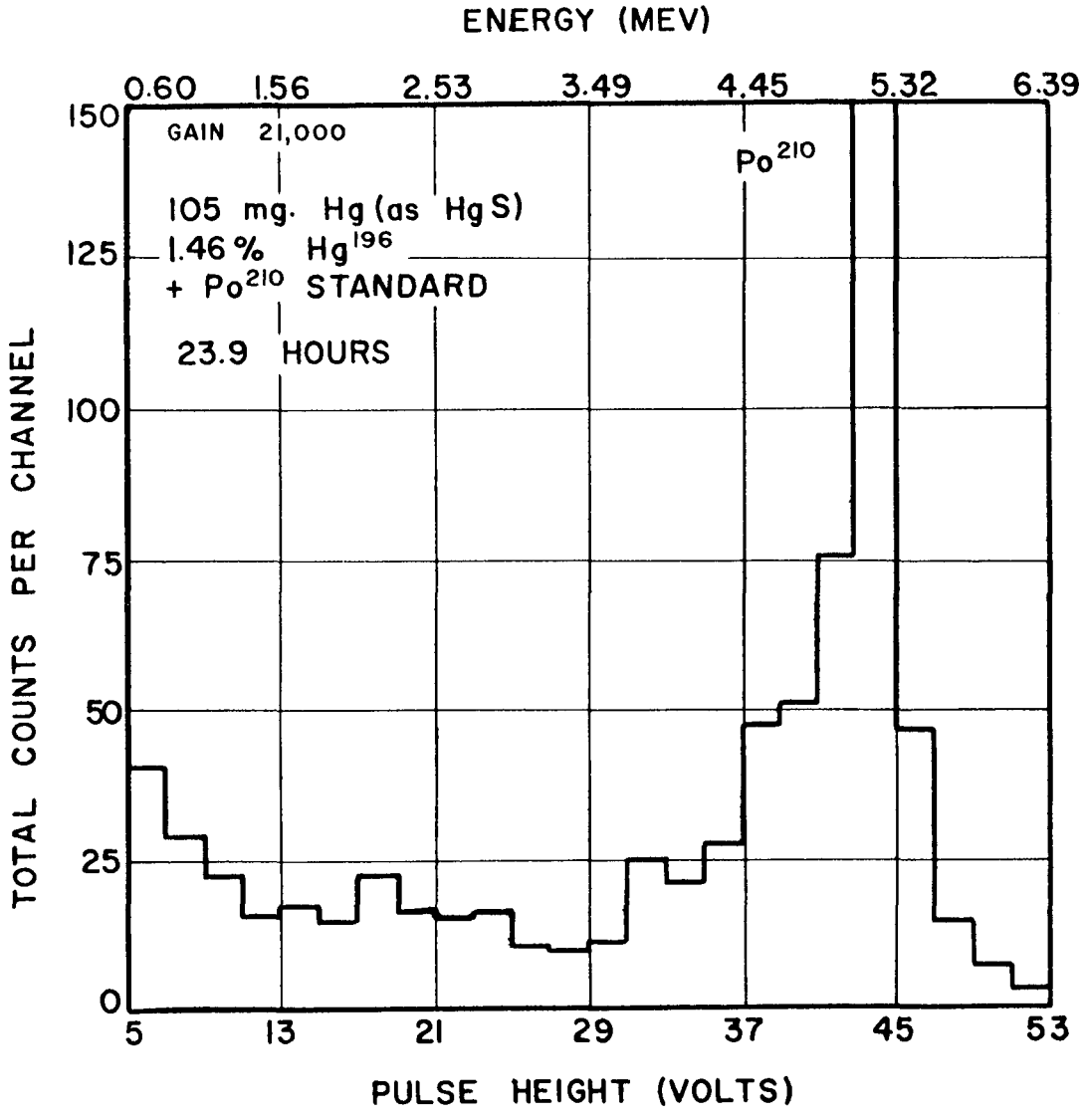

Figure XXIII. Alpha Spectrum of Enriched Hg-196 Sample

d. Decay Constant of Hg-196

$$\lambda(\text{Hg-196}) < \frac{0.5 \text{ dis/g Hg-196/sec} \times 196.0 \text{ g Hg-196/mole} \times 3.155 \times 10^{7} \text{sec/y}}{6.023 \times 10^{23} \text{ atom/mole}}$$

$$< 5 \times 10^{-15}/\text{y}$$

e. Half-life of Hg-196

$$H(\text{Hg-196}) > \frac{0.6931}{5 \times 10^{-15}/\text{y}}$$

$$> 1.4 \times 10^{14} \text{ y} \qquad 2.5 \quad E \quad 3.5$$

3. Discussion

The natural alpha activity of mercury is one of those activities which cannot be studied by nuclear emulsions with the usual high degree of sensitivity. The reason for this is that mercury salts desensitize the emulsion. Counters, of course, do not suffer from this disadvantage. The limit for the half-life of Hg-196 which was set was greater by a factor of 5000 than that set by Porschen and Riezler using nuclear emulsions.

On the basis of the systematics of alpha decay which is discussed in Section VII, the alpha decay energy of Hg-196 is estimated to be 2.90 Mev. The theoretical half-life, using the Bethe Formula, and this value for the alpha energy, is 1×10^{17} years. With a highly enriched Hg-196 sample, it should be possible to observe a natural alpha activity in Hg.

TABLE VIII

Summary of Results

Nuclide	E_α (Mev)	Q (Mev)	Specific Activity (dis/g/sec) natural	Specific Activity (dis/g/sec) nuclide	Decay Constant ($years^{-1}$)	Half-Life (years)	Energy Interval (Mev)
Ce-142	-	-	< 0.00019	< 0.0017	$< 1.31 \times 10^{-17}$	$> 5.3 \times 10^{16}$	$1.5 \leq E_\alpha \leq 1.9$
Nd-144	1.84 ± 0.02	1.90 ± 0.02	0.0093 ± 0.0011	0.0389 ± 0.0048	$(2.93 \pm 0.36) \times 10^{-16}$	$(2.36 \pm 0.29) \times 10^{15}$	-
Sm-146	-		$\leqslant 0.013$	-	$\geqslant 2.2 \times 10^{-9}$	$\leq 3 \times 10^{8}$	$2.4 \leq E_\alpha \leq 2.8$
Sm-147	2.24 ± 0.02	2.30 ± 0.02	113 ± 5	769 ± 33	$(5.88 \pm 0.25) \times 10^{-12}$	$(1.18 \pm 0.05) \times 10^{11}$	-
Sm-148	-	-	< 0.041	< 0.38	$< 2.9 \times 10^{-15}$	$> 2.4 \times 10^{14}$	$1.5 \leq E_\alpha \leq 2.0$
Sm-148	-	-	< 4.1	< 3.8	$< 2.9 \times 10^{-14}$	$> 2.4 \times 10^{13}$	$2.0 \leq E_\alpha \leq 2.14$
Sm-149	-	-	< 0.011	< 0.081	$< 6.3 \times 10^{-16}$	$> 1.1 \times 10^{15}$	$1.5 \leq E_\alpha \leq 2.0$
Sm-149	-	-	< 0.11	< 0.81	$< 6.3 \times 10^{-15}$	$> 1.1 \times 10^{14}$	$2.0 \leq E_\alpha \leq 2.2$
*Gd-152	2.15 ± 0.03	2.21 ± 0.03	0.00149 ± 0.00010	0.772 ± 0.052	$(6.15 \pm 0.41) \times 10^{-15}$	$(1.13 \pm 0.08) \times 10^{14}$	-
*Hf-174	2.50 ± 0.03	2.56 ± 0.03	0.000068 ± 0.000013	0.039 ± 0.008	$(3.5 \pm 0.7) \times 10^{-16}$	$(2.0 \pm 0.4) \times 10^{15}$	-
W-180	-	-	< 0.00012	< 0.084	$< 7.9 \times 10^{-15}$	$> 8.8 \times 10^{14}$	$2.5 \leq E_\alpha \leq 3.5$
Pt-190 (av. val.)	3.11 ± 0.03	3.17 ± 0.03	0.012 ± 0.001	100 ± 7	$(1.0 \pm 0.07) \times 10^{-12}$	$(6.9 \pm 0.5) \times 10^{11}$	-
Hg-196	-	-	< 0.0007	< 0.5	$< 5 \times 10^{-15}$	$> 1 \times 10^{14}$	$2.5 \leq E_\alpha \leq 3.5$

*new activity

VII. GENERAL DISCUSSION

A. Comparison of Experimental Alpha Half-Lives of the Medium-Heavy Alpha Emitters with Theory

1. General Comments

As was mentioned in the introduction of this thesis (Section I, E), the kinetics of alpha decay for the even-even heavy-element alpha emitters is satisfactorily described by the Gamow-Gurney-Condon theory. The radius parameter r_o is fairly constant, having an average value of 1.54×10^{-13} cm when the Bethe solution of the formula is used.(Bet-37). There is no reason to believe that the medium-heavy alpha emitters will behave any differently. Rasmussen, in 1952, using the same r_o as for the heavy elements, showed that with the data available at that time, the theoretical and experimental half-lives were in fair agreement. With more and improved data available now, it is possible to obtain a better comparison of experimental and theoretical alpha half-lives for the medium-heavy alpha emitters.

For these calculations, the Bethe Formula (Section I, E) was used. Corrections for electron screening were made using the following formula: (Per-56)

$$\Delta E_{Sc} = [65.3 (Z + 2)^{2/5} - 80(Z + 2)^{2/5}] \text{ e.v.}$$

where Z is the atomic number of the daughter nucleus. For the rare earth nuclides, this effect amounts to the addition of 0.02 Mev to the Q value; for Pt, Hf, and Pb, 0.03 Mev.

Also, a radius parameter of 1.54×10^{-13} cm was used.

2. Results

In Table IX, the experimental and theoretical half-lives are listed for those alpha emitters among the medium-heavy elements where energies and half-lives have been experimentally determined.

TABLE IX

Comparison of Experimental and Calculated Half-Lives of the Medium-Heavy Alpha Emitters

Nuclide	Q^t (includes electron screening correction)	Alpha Half-Life Experimental	Theoretical	Reference
Bi-209	3.10 Mev***	2×10^{17} y***	1.2×10^{14}y	Far-51,Por-52,56
Pb-204	2.65 ***	1.4×10^{17}y***	1×10^{23}y	Rie-58
Pt-190	3.21	6.54×10^{11}	6.25×10^{11}y	*
W-180	3.10***	1×10^{14}y***	1.2×10^{10}y	Por-53,56
Hf-174	2.58	2.0×10^{15}y	2.69×10^{15}y	*
Tb-151	3.51	754 y	7.42 y	Ras-53
Tb-149	4.08	27.3 h	7.09 h	Ras-53
Gd-152	2.23	1.13×10^{14}y	1.57×10^{14}y	*
Gd-149	3.10	3.64×10^{3}y	5.73×10^{3}y	Ras-53
Gd-148	3.27	130 y	176 y	Ras-53
Eu-147	3.06**	6×10^{3}y	3.04×10^{3}	Ras-53
Sm-147	2.32	1.18×10^{11}y	1.57×10^{11}y	*
Sm-146	2.60	5×10^{7}y	3.97×10^{7}y	Dun-53
Nd-144	1.92	2.36×10^{15}	7.36×10^{15}y	*
Ce-142	1.70****	5×10^{15}y***	1.45×10^{18}y	Rie-57

* Value of half-life and alpha energy obtained in this work.

** Corrected from 3.00 to 3.06 Mev. See following discussion.

*** Value in doubt.

**** Determined from mass data (Nie-56); Porschen and Riezler value, 1.55 Mev.

3. Discussion

The calculated half-lives are generally in agreement with the experimental values where the activity is certain, thus showing that the same radius parameter can be used for the medium-heavy as well as the heavy elements.

There is considerable disagreement with the Pb-204 calculated and experimental half-life but this might be explained by an error in the experimental value of the alpha energy. An energy 0.25 Mev higher would bring the theoretical and experimental half-lives into agreement. However, recent mass measurements give values for the Q_α of Pb-204 which indicate that the alpha energy is actually lower than 2.65 Mev. From the data of Demirkhanov, Gutkin, and Dorokhov a value of 2.4 ± 0.1 Mev is obtained (Dem-58), and very recently Benson, Damerow, and Ries give mass data from which a value of 2.00 ± 0.02 Mev is obtained (Ben-59). If the later Q_α value, which has a very low precision index, is correct, the alpha half-life of Pb-204 would be $\sim 10^{31}$ years, a half-life much too long to enable the detection of alpha activity in Pb-204.

The calculated half-life of Nd-144 is a factor of 3 larger than the experimental half-life but this too could be due to uncertainty in the value of the alpha energy. An energy 0.02 Mev higher would be enough to give agreement. For very long half-lives such as these, the energy dependence on the half-life is extremely sensitive. (See Figure I, section I)

The Eu-147 alpha energy was originally determined by Rasmussen using Sm-147 as an energy standard (Ras-53). It was adjusted from 3.00 to 3.06 Mev to correspond to the 60 kev difference in the Sm-147 alpha particle energy determined in this work compared to the Jesse and Sadauskis value (Jes-50) which Rasmussen used. The calculated alpha half-lives of Sm-147 and

Eu-147 are now in agreement with the experimental values.

The theoretical half-life for Bi-209 is expected to be much lower than the experimental value because this nuclide decays by alpha emission across the closed proton shell of 82. Decay across closed shells by other nuclides has been shown to have a hindering effect on the rate of alpha emission.

The experimental and theoretical half-lives for W-180 and Ce-142 are in strong disagreement indicating that either their experimental alpha energies or alpha lives are in error (See Section VI B, I).

4. Theoretical Alpha Half-lives of Alpha Emitters for which only the Alpha Energy is Known

Listed below are those artificial medium-heavy alpha emitters for which only a limit to the half-life can be set. They either possess a relatively long half-life or a small and as yet undetermined alpha branching ratio.

Nuclide	Q'(includes electron screening	Half-Life Experimental	Theoretical(Alpha H)	Ref.
Dy-154	3.48	$>$ 13 h	51.9 y	Tot-58
-153	3.60	$>$ 5 h	6.1 y	Tot-58
-152	3.75	$>$2.3 h	0.49 y	Tot-58
Gd-150	2.80	$>10^5$ y	6.6×10^6 y	Ras-53

B. Alpha Energy Systematics in the Medium-Heavy Nuclides

1. General Comments

Very precise measurement of atomic masses in the medium-heavy elements give a means of obtaining reliable alpha decay energies in this region for nuclides having half-lives much too long to be experimentally observed. Information can even be obtained for nuclides which are completely alpha stable ($Q \leq 0$).

By combining Q values determined through direct observation of alpha activity or by mass differences with beta decay energies it is possible to calculate alpha decay energies for a number of beta labile nuclides as well.

The usual representation of alpha energy systematics is to plot alpha decay energy vs. mass number for each element. This type of plot has been used to describe the alpha energy systematics of the heavy elements (Per-50).

Combining the somewhat meager alpha decay data of the medium-heavy nuclides with alpha energies determined by mass differences and beta energies and utilizing the Cameron Mass Formula (Cam-57) and some reasonable estimates to fill in the gaps, a fairly complete picture of alpha energy systematics for this region can be constructed. This picture is represented in Figure XXIV.

2. Methods Used to Determine Alpha Energy

a. Alpha Decay Data

Alpha activity has now been observed in 16 nuclides in the medium-heavy elements with a definite determination of mass number, alpha energy and half-life and in 7 others for which the mass numbers and/or alpha half-lives are not known. Q values were taken from the latest Table of Isotopes (Sea-57) with the exception of those nuclides for which new values were determined in this work.

b. Atomic Mass Differences

A large number of alpha decay energies were determined by this method in the region between tin and dysprosium. Q values were determined from the data in terms of mass differences in millimass units and converted to energy in Mev by multiplying by the mass-energy conversion factor 0.93114 Mev/mmu (Coh-55). The mass of the He atom was taken to be 4.00388 (Mat-56) and the atomic mass of the hydrogen atom, 1.0081442 (Nie-56).

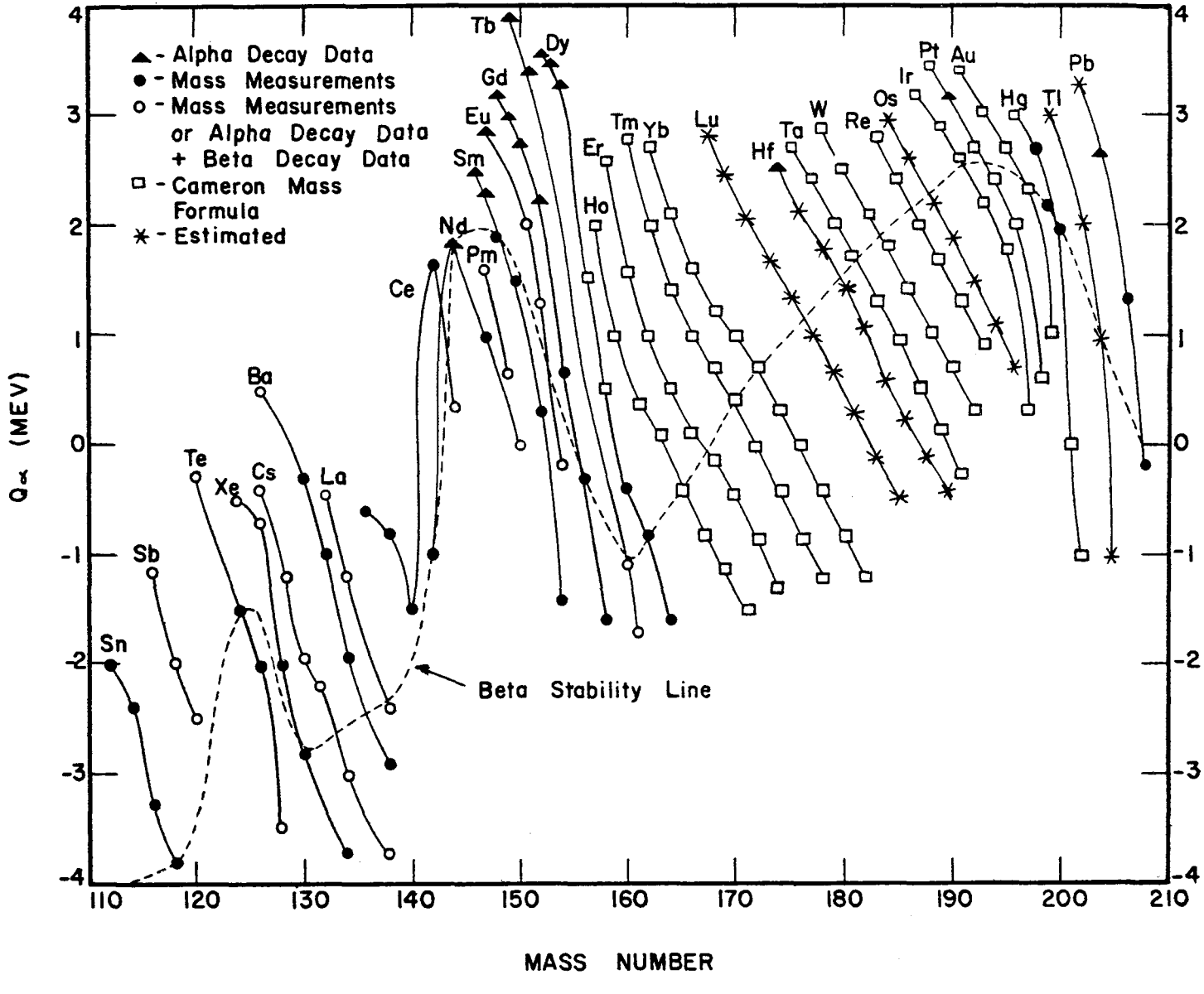

Figure XXIV. Alpha Decay Systematics of the Medium-Heavy Elements

The tables of mass spectroscopic mass difference compiled by H. E. Duckworth were used as a major source of the mass data (Duc-54,57).

c. Beta Decay Data

The use of beta decay data in conjunction with alpha decay and mass data gave alpha decay energies for a large number of beta-labile nuclides.

Beta disintegration energies were taken from a table compiled by R. W. King (Kin-54), from a later table compiled by L. J. Lidofsky (Lid-57) and from the Table of Isotopes (Sea-58).

d. Cameron Mass Formula

For the elements between dysprosium and lead, practically no data are available for the determination of alpha energies. A few isolated alpha active nuclides are known and there are a small number of energies which can be calculated from mass data. (A large fraction of the available mass data between Dy-Pb are not precise enough to obtain meaningful alpha decay energies.) In order to get enough points to observe a trend in this region another means of determining alpha energies had to be used.

The Cameron Mass Formula (Cam-57) gives generally good agreement with the alpha energies determined by direct measurement or mass differences in the region from Sn-Dy where a number of experimentally determined points are available. Listed in Table X are the experimental alpha energies which are available in the region of elements between Sn and Pb and the energies which are calculated from the Cameron Mass Formula.

TABLE X

Comparison of Experimental Alpha Decay Energies with Values Obtained from the Cameron Mass Formula

Nuclide	Experimental Alpha Decay Energy (Mev)	Method	Cameron Value (Mev)	Difference (Mev) $E_{exp}-E_{Cam}$
Sn-112	-2.0	b	-1.7	-0.3
114	-2.4	b	-2.5	+0.1
116	-3.3	b	-3.5	+0.2
118	-3.8	b	-4.3	+0.5

Sb-116	-1.2	c	-1.2	0.0
118	-2.0	c	-2.0	0.0
120	-2.5	c	-3.0	+0.5
Te-120	-0.8	b	+0.1	-0.9
124	-1.5	b	-1.4	-0.1
126	-2.0	b	-2.4	+0.4
128	-3.5	c	-2.9	-0.6
Xe-124	-0.5	c	-0.1	-0.4
126	-0.7	c	-0.5	-0.2
128	-2.0	b	-1.5	-0.5
130	-2.8	b	-1.9	-0.9
134	-3.5	c	-4.4	+0.9
Cs-126	-0.4	c	+0.4	-0.8
128	-1.2	c	-0.3	-0.9
130	-2.0	c	-1.2	-0.8
132	-2.2	c	-1.8	-0.4
134	-3.0	c	-3.0	0.0
138	-3.7	c	-2.2	-1.5
Ba-126	+0.5	c	+1.2	-0.7
130	-0.3	b	-0.1	-0.2
132	-1.0	b	-0.5	-0.5
134	-1.9	b	-1.7	-0.2
138	-2.9	b	-2.7	-0.2
La-132	-0.5	c	+0.1	-0.6
134	-1.2	c	-0.4	-0.8
138	-2.4	c	-2.8	+0.4
Ce-136	-0.6	b	-0.7	+0.1
138	-0.8	b	-1.8	+1.0
140	-1.5	b	-1.6	+0.1
142	+1.7	b	+1.1	+0.6
144	+0.3	c	+1.0	-0.7
Nd-142	-1.0	b	-1.0	0.0
144	+1.9	a	+1.8	+0.1
147	+1.0	b	+1.4	-0.4
150	0.0	c	-0.8	+0.8
Pm-147	+1.6	c	+2.0	-0.4
149	+0.6	c	+1.1	-0.5
Sm-146	+2.6	a	+2.4	+0.2
147	+2.3	a	+2.8	-0.5
148	+1.9	b	+2.4	-0.5
149	+2.0	b	+2.1	-0.1
150	+1.5	b	+1.5	0.0
152	+0.3	b	-0.1	+0.4
154	-0.4	b	-1.1	-0.3

Eu-147	+3.0	a	+2.4	+0.6
151	+2.0	c	+1.5	+0.5
152	+1.3	c	+0.8	+0.5
154	-0.2	c	-0.5	+0.3
Gd-148	+3.3	a	+3.0	+0.3
149	+3.1	a	+3.4	-0.3
150	+2.8	a	+3.0	-0.2
152	+2.2	a	+2.2	0.0
154	+0.7	b	+0.6	+0.1
156	-0.3	b	-0.4	+0.1
158	-1.6	b	-1.1	-0.5
Tb-149	+4.1	a	+3.3	+0.8
151	+3.5	a	+3.4	+0.1
160	-1.1	c	-1.0	-0.1
161	-1.7	c	-1.3	+0.4
Dy-152	+3.7	a	+3.9	-0.2
153	+3.6	a	+3.6	0.0
154	+3.5	a	+3.1	+0.4
160	-0.4	b	-0.1	-0.3
164	-1.6	b	-1.0	-0.6
Hf-174	+2.6	a	+2.0	+0.6
Pt-190	+3.2	a	+3.1	+0.1
Hg-198	+2.7	b	+2.6	+0.1
199	+2.2	b	+2.2	0.0
200	+2.0	b	+1.2	+0.8
Pb-204	+2.7,2.5,2.0	a,b,b	-0.4	+3.1, 2.9
206	+1.3	b	+0.1	+1.2
208	-0.2	b	0.0	-0.2

a - Alpha Decay Data
b - Mass Data
c - Alpha Decay and/or Mass Data and Beta Decay Data

Except for a few scattered cases, the Cameron Formula does reasonably well in predicting alpha energies. It was felt that this was the best method available for determining the alpha energies of these nuclides for which no experimental data are available.

e. Estimated Alpha Energies

There are a few experimental alpha energies available in the region between Ho and Pb which can be used to test the accuracy of the Cameron

formula for certain elements. Also, lower limits to the alpha half-lives established by the work of Porschen and Riezler (Por-56) and in this work, can be used to obtain upper limits in the alpha decay energy.

The Pt-190 alpha energy (3.18 Mev), for example, is in agreement with the value given by the Cameron formula (3.10 Mev) as are the alpha energies of Hg-198, 199 which were determined by mass differences. The calculated value of 2.51 Mev for the alpha energy of W-180 is also in line with the lower limit of the half-life of this nuclide obtained in this work. However, some of the energies calculated by the Cameron formula are contrary to the experimental facts.

The experimental alpha energy of Hf-174, for example, is 2.58 Mev. while the Cameron formula gives 2.01 Mev. Accordingly, the Cameron values of the other Hf isotopes were increased by 0.6 Mev so as not to show a discontinuity in the curve for the Hf isotopes.

The calculated alpha energy of Os-184 is 3.58 Mev while the lower limit for the half-life of Os-184 (Por-56)gives the information that the alpha energy is $\leq$ 3.0 Mev. Accordingly, the calculated value of the Os isotopes were decreased by 0.6 Mev for the same reason as for the Hf isotopes. Because the Hf curve was shifted the Lu curve was also shifted to a position midway between Yb and Hf so that a large gap between the Lu and Hf curves would not be created.

It was the intention in Figure XXIV to present as accurate a picture of the systematics of alpha decay in the medium-heavy elements as possible utilizing the latest available information. The situation between Dy and Pb which is represented in Figure XXIV is by no means well-defined. The Cameron formula was used as a guide in establishing the basic trend, (the slope of the curves) and experimental alpha decay energies or upper limits for the energies plus mass data used in estimating the position of the curves where possible.

3. Discussion

The region between tin and lead is a very interesting one from a nuclear structure standpoint. A closed shell of protons is in evidence at 50 (tin), a closed shell of neutrons at 82, and a double closed shell at 82 protons and 126 neutrons.

The effect of the closed proton shell at 50 on the alpha decay systematics is to give the tellurium isotopes (Z = 52) an enhanced alpha energy and to depress the Q_α's for the tin isotopes.

The effect of the 82 neutron shell is also to enhance the alpha decay energies of nuclides containing 84-88 neutrons and to stabilize the elements below Ce against alpha decay. This enhancement is responsible for the observation of alpha activity in a number of nuclides in this region.

Beyond 88 neutrons the effect of proximity to the closed neutron shell rapidly disappears and the alpha energy falls off very quickly. Dy-154, for example, containing 88 neutrons, has an alpha energy of 3.3 Mev. Adding two more neutrons to give Dy-156 decreases the energy available for alpha emission to 1.5 Mev.

It has been postulated that this rapid drop in alpha energy is related to nuclear structure changes in going from 88-90 neutrons.(Ras-58). This same rapid drop is also found between Gd-152 and Gd-154 and Sm-150 and Sm-152 although to a progressively lesser extent.

Once beyond the effects of the 82 neutron shell, the overall trend of alpha energies shows a slow rise with increasing atomic number reaching a maximum at platinum whereupon the proximity to the 82 proton and 126 neutron shell begins to have its effects and the alpha energy quickly drops to a minimum at Pb-208.

The fact that the maximum is reached at Pt is reflected in the detection of natural alpha activity in this element. The two elements

lying on either side of the maximum, Os and Hg, should also reveal the presence of natural alpha activity under careful examination.

C. Prediction of the Alpha Half-Lives of Certain Naturally-Occurring Medium-Heavy Nuclides

1. General Comments

From the alpha energy systematics represented in Figure XXIV, the alpha energies of some naturally-occurring nuclides can be obtained and the alpha half-life calculated using the Bethe Formula.

With the exception of the elements effected by closed shells, the most alpha labile of the stable isotopes is the most neutron deficient. Therefore, the half-life of the most neutron deficient stable isotope of Dy, Er, Yb, W, Os, and Hg were calculated. Also, the half-life of Sm-148 and Sm-149 was included because these nuclides have an enhanced alpha energy due to the 82-neutron effect.

The odd Z elements were not considered for two reasons. First, they possess at most two naturally-occurring nuclides, and these lie very close to the beta stability curve. Hence, the energy available for alpha emission is very low, meaning that the alpha half-life is extremely long. Secondly, it is uncertain whether the calculated alpha half-lives for these odd Z elements would have much meaning, since it is quite possible that alpha decay would be hindered by an odd nucleon effect.

2. Results

The alpha decay energies for the nuclides were taken from Figure XXIV except for the following nuclides: the alpha energy of Dy-156 was increased from 1.58 Mev as given by the Cameron formula to 1.9 Mev, the alpha energy of Er-162 from 1.0 to 1.8 Mev and for Yb-168, from 1.3 to 2.2 Mev. The reason for these changes is that the calculated half-lives for each of these nuclides is so astronomically high using energies calculated from the Cameron formula

(The IBM-650 stopped on an overflow error when given the problem to evaluate the half-life of Er-162 corresponding to an alpha energy of 1.0 Mev). It is quite possible that the error in the alpha energy for these nuclides calculated by the Cameron formula can be as large as 1 Mev but it is not expected to be much larger than that. Taking the optimistic viewpoint that the actual energy is higher than the Cameron value by these estimated amounts gives an optimistic value for the half-life of these nuclides which, as is shown in the table below, is still very large.

TABLE XI

Predicted Half-Lives for Certain Naturally-Occurring Nuclides Among the Medium-Heavy Elements

Nuclide	Q (Mev) From Figure XXIV	Calculated Half-Life (years) (from Bethe Formula)	Experimental Lower Limit (years)	Reference
Hg-196	2.9	1.0×10^{17}	1.0×10^{14}	this work
Pt-192	2.8	2.5×10^{17}	1×10^{15}	Por-56
Os-184	2.9	1.4×10^{14}	1.8×10^{13}	Por-56
W-180	2.7	1.8×10^{15}	8.8×10^{14}	this work
Yb-168	$<$ 2.2	$>$ 6.1×10^{19}	1.4×10^{14}	Por-56
Er-162	$\leq$ 1.8	$>$ 9.7×10^{25}	1.4×10^{14}	Por-56
Dy-156	$<$ 1.9	$>$ 3.4×10^{22}	1.0×10^{18}	Por-56
Sm-149	2.0	1.5×10^{16}	1.1×10^{15}	this work
Sm-148	1.9	1.2×10^{18}	2.4×10^{14}	this work
Ce-142	1.7	1.4×10^{18}	5.3×10^{15}	this work

3. Discussion

Because of the uncertainties in the alpha energies of these nuclides, and the very sensitive dependence of energy on long half-lives, the calculated values of the half-life are very approximate. At best, this table only serves

as a guide in pointing out the most likely possibilities for detecting new natural alpha activities.

It is apparent from this table that there is a very good chance that natural alpha activity can be observed in Os-184. With very sensitive detection techniques it should also be possible to observe natural alpha activity in W-180, Pt-192, and Hg-196. (Porschen and Riezler had an indication of a second peak in their platinum energy spectrum which might be due to Pt-192) (Por-54,56).

It appears that with Dy-156, Er-162, and Yb-168, the alpha half-life is much too long to enable the detection of natural alpha activity in these nuclides.

Both Sm-148 and Sm-149 are possibilities, Sm-149 especially, if the Q calculated from mass data for this nuclide is correct. (See section VI, discussion of Sm-149 results) Here, as stated previously, the big problem is Sm-147 contamination.

D. Possibilities for Producing New Artificial Alpha Emitters in the Medium-Heavy Elements

If Figure XXIV is an accurate representation of alpha decay systematics in the medium-heavy nuclides, then it should be possible to extrapolate these curves to very neutron deficient nuclides and predict which of these will be sufficiently alpha labile to enable detection.

If a highly neutron deficient nuclide is produced it will be quite unstable toward positron emission and probably will decay with a half-life of a few hours at most. Let us assume that the smallest alpha branching fraction which can be detected is 10^{-6} so that the maximum alpha half-life giving a detectible alpha activity is $\sim 10^3$ years.

Using the relationship between Q and half-life plotted for various values of Z in Figure I, Section I which was calculated using the Bethe formula, the alpha energy required to give a half-life of 10^3 years for each element can be obtained. Figure XXIV can be used to determine the mass number corresponding to this energy. Any mass number less than this value will, of course, have a half-life shorter than 10^3 years (barring closed shell effects). The results are given in Table XII. Also included is the α, xn reaction required to produce each of these nuclides. The target nuclide in each case is the most neutron deficient naturally-occurring isotope of the element two atomic numbers less than the product nuclide.

TABLE XII

Predicted Maximum Mass Number for Producing Detectable Artificial Alpha Activity in the Medium-Heavy Elements

Element	Q (Mev) corresponding to H of 10^3 years	Mass Number corresponding to Q (from Figure XXIV)	A Feasible Mode of Production
Sn	2.3	101	$Cd^{106}(\alpha,9n)Sn^{101}$
Te	2.4	111	$Sn^{112}(\alpha,5n)Te^{111}$
Xe	2.6	116	$Te^{120}(\alpha,8n)Xe^{116}$
Ba	2.7	120	$Xe^{124}(\alpha,8n)Ba^{120}$
Ce	2.9	125	$Ba^{130}(\alpha,9n)Ce^{125}$
Nd	3.0	130	$Ce^{136}(\alpha,10n)Nd^{130}$
Er	3.5	156	$Dy^{156}(\alpha,4n)Er^{156}$
Yb	3.6	160	$Er^{162}(\alpha,6n)Yb^{160}$
Hf	3.8	168	$Yb^{168}(\alpha,4n)Hf^{168}$
W	4.0	172	$Hf^{174}(\alpha,6n)W^{172}$
Os	4.2	178	$W^{180}(\alpha,6n)Os^{178}$
Pt	4.3	184	$Os^{184}(\alpha,4n)Pt^{184}$
Hg	4.5	190	$Pt^{190}(\alpha,4n)Hg^{190}$
Pb	4.7	198	$Hg^{196}(\alpha,2n)Pb^{198}$

According to Rasmussen, (Ras-52) the α, xn reaction is a convenient reaction for producing very neutron deficient nuclides (without producing a large number of bothersome intermediate neutron deficient beta emitters.) With bombarding alpha particle energies of 200-400 Mev, Rasmussen expects it is possible to evaporate as many as 12 neutrons from the nucleus.

Clearly, on the basis of the above predictions, it should be possible to produce a large number of new alpha emitters in the medium-heavy elements without too much trouble. Such a study should be a worthwhile contribution to our understanding of alpha decay theory and nuclear structure.

E. An Evaluation of the Methods Used to Detect Weak Alpha Activities

One can say now that all of the nuclides possessing a comparatively high natural alpha specific activity ($\leq$ 0.001 α/g/sec) have been found. Any new discoveries will require a most sensitive means of detection.

It has become apparent during the course of this work that the method giving the highest degree of sensitivity is still the nuclear emulsion technique.

There are two difficulties with solid sample counting using internal sample ion chambers. One is the background, which, although reducable to a low value does, not nearly compare with the extremely low effective background of a nuclear emulsion plate. Secondly, in order to reduce self-absorption, which tends to smear out the energy spectrum, only very thin samples can be counted. This difficulty is not encountered in the nuclear emulsion technique because the sample is distributed throughout the ionizing medium (the photosensitive emulsion) in a manner analogous to a sample being present as a gas in an ion chamber.

There are, of course, some attractive properties of electronic counting techniques which provide distinct advantages over nuclear emulsions. The most important is the ability to measure alpha energies with greater

precision (probably a factor of 10 greater) which also means that alphas of similar energy can be more easily resolved. Resolution of the Gd-152 and Nd-144 alphas from Sm-147 in this work are good examples of this.

Being able to use more sample for counting (in this work up to 1 gm compared to 1 mg for nuclear emulsion work) means that counting time can be greatly reduced and better counting statistics achieved. And, to say the least, there is much less eye strain in reading the numbers off a pulse analyzer than in measuring the length of tracks in a nuclear emulsion.

There are some possibilities for increasing the sensitivity of counters to the point where they might be able to compete with or even improve on the sensitivity of nuclear emulsions. A distinct improvement would be realized if one could avoid the problem of self-absorption, reduce the effective background, increase the counting geometry from 50% to 100%, and count larger samples.

Gas Counting

One possibility for satisfying most of these factors mentioned above is gas sample counting. Some preliminary work was actually done in the early stages of this work which involved the construction of a giant ionization chamber (50 liters capacity) for the purpose of counting gas samples of elements in the medium-heavy nuclides. (This was referred to as Project Sewer Pipe.) Conditions were developed to the point where it was possible to obtain Sm-147 and Po-210 spectra in this chamber using a counting gas comprised of 0.5 atm of argon-nitrogen-ethylene mixture and 10 mm of $Hg(CH_3)$ (5 gms). Difficulties were encountered which resulted in the abandonment of this project, but it is felt that with more work these difficulties can be resolved and the method used with high sensitivity for studying weak alpha activities. (The main difficulties encountered were due to sample

impurity, mainly water, which effected the counting characteristics of the ion chamber, and drift in stability.) A number of low-boiling compounds are available which can be used. Among these are WF_6, ReF_6, OsF_8, IrF_6, $Hg(CH_3)_2$, $Pb(CH_3)_4$, and $Bi(CH_3)_3$.

Scintillation Counting

Some work has been done recently by Beard and Wiedenbeck (Bea-58) which involved the determination of the specific activity of samarium using a scintillation counter where the scintillant was a liquid containing a small amount of a samarium salt. Although the energy resolution of the spectrum was poor (25%), they nevertheless obtained a value for the specific activity in good agreement with those determined by other methods.

Another possibility for scintillation counting applied to low level alpha activity is to use for the scintillating material crystals of compounds containing the element being studied. A good example of this would be $CaWO_4$ for studying the alpha activity of tungsten.

With this method, a comparatively large sample (at least 10 gms) could be studied with good counting efficiency, and no self-absorption problems. There would be a problem of a relatively high background, but by using thin crystals and an anticoincidence arrangement with massive shielding, it might be possible to lower the background sufficiently to detect weak alpha activities.

VIII BIBLIOGRAPHY

Asa-53 F. Asaro, F. Stephens, Jr., I. Perlman, Phys. Rev. 107, 1091 (1957)

Bas-53 G. Bastin-Scoffier, J. Sant'ana-Dionisic, Compt. rend. 236, 1016 (1953)

Bea-54 G. Beard, M.L. Wiedenbeck, Phys. Rev. 95, 1245 (1954)

Bea-58 G. Beard, W.H. Kelly, Nuclear Phys. 8, 207 (1958)

Bel-50 W. A. Bell, L.O. Love, Oak Ridge National Laboratory Report AECD-3502 (1950)

Ben-59 J.L. Benson, R.A. Damerow, R.R. Ries, Phys. Rev. 113, 1105 (1959)

Ber-53 G. Bertolini, M. Beltoni, A. Bisi, Phys. Rev. 92, 1586 (1953)

Bes-49 F. Bestenreiner, E. Broda, Nature 164, 919 (1949)

Bet-36 H. Bethe, R.F. Bacher, Revs. Mod. Phys. 8, 165 (1936)

Bet-37 H. Bethe, Revs. Mod. Phys. 9, 263 (1937)

Bla-39 M. Blau, Arch. Math. Naturvidenskab B42, 1 (1939)

Boh-39 N. Bohr, J.A. Wheeler, Phys. Rev. 56, 426 (1939)

Bri-54 G.H. Briggs, Revs. Mod. Phys. 26, 1 (1954)

Bur-57 E.M. Burbidge, G.R. Burbidge, W.A. Fowler, F. Hoyle, Revs. Mod. Phys. 29, 547 (1957)

Cam-57 A.G.W. Cameron, Can. J. Phys. 35, 1021 (1957)

Coh-55 E.R. Cohen, J.W.M. Du Mond, T.W. Layton, J.S. Rollett, Revs. Mod. Phys. 27, 363 (1955)

Cra-48 T.E. Cranshaw, J.A. Harvey, Can. J. Res. A26, 243 (1948)

Cra-49 J.A. Crawford, The Transuranium Elements, G.T. Seaborg, J.J. Katz, W.M. Manning, editors, Vol 14B, Div IV, Paper 16.55, (Mc-Graw-Hill, New York, 1949)

Cue-46 P. Cuer, C.M.G. Lattes, Nature 158, 197 (1946)

Col-57 T.L. Collins, F.M. Rourke, F.A. White, Phys. Rev. 105, 196 (1957)

Cun-49a B.B. Cunningham, A. Ghiorso, A.H. Jaffey, The Transuranium Elements, G.T. Seaborg, J.J. Katz, W.M. Manning, editors, Vol 14B, Div IV, Paper 16.6 (McGraw-Hill, New York, 1949)

Cun-49b B.B. Cunningham, A. Ghiorso, A.H. Jaffey, ibid, Paper 16.3

Cur-33 M. Curie, S. Takvorian, Comt. rend. 196, 923 (1933)

Cur-34 M. Curie, F. Joliot, Compt rend. 198, 360 (1934)

Dan-56 E.W. McDaniel, H.J. Schaefer, J.K. Colehour, Rev. Sci. Inst. 27, 864 (1956)

Das-50 R.K. Das, Ind. J. Phys. 24, 525 (1950)

Dem-48 A.J. Dempster, Phys. Rev. 73, 1125 (1948)

Dem-49 A.J. Dempster, Argonne National Laboratory Report, ANL-4355 (1949)

Dem-58 R.A. Demirkhanow, T.I. Gutkin, V.V. Dorokhov, J. Exptl. Theoret. Phys. 35, 917 (1958)

Duc-54 H.E. Duckworth, B.G. Hogg, E.M. Pennington, Revs. Mod. Phys. 26, 463 (1954)

Duc-57 H.E. Duckworth, Revs. Mod. Phys. 29, 767 (1957)

Dun-53 D.C. Dunlavey, G.T. Seaborg, Phys. Rev. 92, 206 (1953)

Elm-49 W.C. Elmore, M. Sands, Electronics, McGraw-Hill, New York (1949)

Fac-56 U. Facchini, M. Forte, A. Malvicini, T. Rossini, Energia Nucleare 3, 182 (1956)

Far-51 H. Faraggi, A. Berthelot, Compt. rend. 232, 2093 (1951)

Fee-47 E. Feenberg, Revs. Mod. Phys. 19, 239 (1947)

Fer-47 E. Fermi, unpublished, Quoted in C. Goodman, The Science and Engineering of Nuclear Power, Vol I (Addison-Wesley, Cambridge, Mass. 1947)

Fis-52 V.K. Fisher, Phys. Rev. 87, 859 (1952)

Fow-49 W.A. Fowler, unpublished, Quoted in W.E. Siri, Isotopic Tracers and Nuclear Radiations, (McGraw-Hill, New York 1949)

Fro-47 G. Frongia, N. Margoniu, Rend. seminar facolta sci. univ. Cagliani 17, 98 (1947)

Gam-28 G. Gamow, Z. Physik 51, 204 (1928)

Gob-56 G.W. Gobeli, Phys. Rev. 103, 275 (1956)

Gra-53 A.G. Gray, editor, Modern Electroplating, (J. Wiley and Sons, New York 1953)

Gre-54 A.E.S. Green, Phys. Rev. 95, 1006 (1954)

Gru-56 W.E. Grummitt, R.M. Brown, A.J. Cruikshank, I.L. Fowler, Can. J. Chem. 34, 206 (1956)

Gur-28 R.W. Gurney, E.U. Condon, Nature 122, 439 (1928)

Gys-44 B. Gysae, Naturwissenschaften 32, 219 (1944)

Hae-49 Ch. Haenny, M. Najar, M. Gaillourd, Helv. Phys. Acta 22, 611 (1949)

Hal-52 R.E. Halstead, Phys. Rev. 88, 666 (1952)

Han-50 G.C. Hanna, Phys. Rev. 80, 530 (1950)

Har-57 B.G. Harvey, H.G. Jackson, T.A. Eastwood, G.C. Hanna, Can. J. Phys. 35, 258 (1957)

Her-34 M. Herzfinkiel, A. Wronberg, Compt. rend. 199, 133 (1934)

Hes-48 D.C. Hess, Phys. Rev. 74, 773 (1948)

Hev-32 G. v Hevesy, M. Pahl, Nature 130, 846 (1932)

Hev-33 G. v Hevesy, M. Pahl, R. Hosemann, Z. Physik 83, 43 (1933)

Hev-34 G. v Hevesy, M. Pahl, Z. Phys. Chem. 169A, 147 (1934)

Hin-52 E.P. Hincks, C.H. Millar, Proc. Roy. Soc.(Canada) 46, 143 (1952)

Hin-58 E.P. Hincks, C.H. Millar, G.C. Hanna, Can. J. Phys. 36, 231 (1958)

Hof-21 G. Hoffmann, Z. Physik, 7, 254 (1921)

Hos-36 R. Hosemann, Z. Physik 90, 405 (1936)

Hum-56 J.P. Hummel, PhD Thesis, University of California Radiation Laboratory Report UCRL-3456 (1956)

Ing-48 M.G. Inghram, D.C. Hess, R.J. Hayden, Phys. Rev. 73, 780 (1948)

Jen-49 K. Jenkner, E. Broda, Nature 164, 412 (1949)

Jen-51 K. Jenkner, E. Broda, Experientia, 7, 121 (1951)

Jes-50 W.P. Jesse, J. Sadauskis, H. Forstat, Phys. Rev. 77, 782 (1950)

Jes-55 W.P. Jesse, J. Sadauskis, Phys. Rev. 100, 1755 (1955)

Joh-57 W.H. Johnson, V.B. Bhanot, Phys. Rev. 107, 1669 (1957)

Kel-48 K.K. Kellar, K.B. Mather, Phys. Rev. 74, 624 (1948)

Kin-54 R.W. King, Revs. Mod. Phys. 26, 327 (1954)

Koh-48 T.P. Kohman, Phys. Rev. 73, 20 (1948)

Koh-49 T.P. Kohman, Phys. Rev. 76, 448 (1949)

Koh-54 T.P. Kohman, N. Saito, Ann. Rev. Nucl. Sci. 4, 401 (1954)

Lel-50 W.L. Leland, Phys. Rev. 77, 634 (1950)

Les-56 G.E. Leslie, Thesis, North Carolina State College, AD-37749 (1954)

Lew-36 L. Lewin, Nature 138, 326 (1936)

Lib-33 W.F. Libby, W.M. Latimer, J. Amer. Chem. Soc. 55, 433 (1933)

Lib-34 W.F. Libby, Phys. Rev. 46, 196 (1934)

Lid-57 L.J. Lidofsky, Revs. Mod. Phys. 29, 773 (1957)

Lon-52 J.K. Long, M.L. Pool, D.M. Kunder, Phys. Rev. 88, 171 (1952)

Lyf-34 D. Lyford, J.H. Bearden, Phys. Rev. 45, 743 (1934)

Mac-53 R.C. Mack, J.J. Neuer, M.L. Pool, Phys. Rev. 91, 903 (1953)

Mad-34 M. Mader, Z. Physik 88, 601 (1934)

Mat-42 J. Mattauch, S. Flugge, Nuclear Physics Tables, (Verlag Julius Springer, Berlin 1942)

Mat-46 J. Mattauch, S. Flugge, Introduction to Nuclear Physics, (Interscience Publishers, Inc. New York, 1946)

Mat-56 J. Mattauch, L. Waldmann, R. Bieri, F. Everling, Ann. Rev. Nucl. Sci. 6, 179 (1956)

Mel-54 C.E. Melton, G.S. Hurst, T.E. Bortner, Phys. Rev. 96, 643 (1954)

Mul-52 G. I. Mulholland, T.P. Kohman, Phys. Rev. 85, 144 (1952)

Maz-33 L. Mazza, L. Rolla, Atti accad. Lincei 18, 472 (1933)

Nie-57 A.O. Nier, W.H. Johnson, Phys. Rev. 105, 1014 (1957)

Ort-34 G. Ortner, J. Schintlmeister, Z. Physik 90, 698 (1934)

Per-50 I. Perlman, A. Ghiorso, G.T. Seaborg, Phys. Rev. 77, 26 (1950)

Pic-49 E. Picciotto, Compt. rend. 229, 117 (1949)

Por-52 W. Porschen, W. Riezler, Z. Naturforsch. 7a, 634 (1952)

Por-53 W. Porschen, W. Riezler, Z. Naturforsch. 8a, 502 (1953)

Por-54 W. Porschen, W. Riezler, Z. Naturforsch. 9a, 701 (1954)

Por-56 W. Porschen, W. Riezler, Z. Naturforsch. 11a, 143 (1956)

Ptr-56 F.T. Porter, M.S. Freedman, T.B. Novey, F. Wagner, Jr., Phys. Rev. 103, 921 (1956)

Pry-50 M.H.L. Pryce, Proc. Phys. Soc. (London) A63, 692 (1950)

Qui-56 K.S. Quisenberry, T.T. Scolman, A.O. Nier, Phys. Rev. 102, 1071 (1956)

Ras-50 J.O. Rasmussen, F.L. Reynolds, S.G. Thompson, Phys. Rev. 80, 475 (1950)

Ras-51 J.O. Rasmussen, R.W. Hoff, S.G. Thompson, Phys. Rev. 83, 1068 (1951)

Ras-52 J.O. Rasmussen, Thesis, University of California Radiation Laboratory Report, UCRL-1473 Rev. (1952)

Ras-53 J.O. Rasmussen, S.G. Thompson, A. Ghiorso, Phys. Rev. 89, 33 (1953)

Rie-57 W. Riezler, G. Kauw, Z. Naturforsch. 12a, 665 (1957)

Rie-58a W. Riezler, G. Kauw, Z. Naturforsch. 13a, 904 (1958)

Rie-58b W. Riezler, G. Kauw, private communication with T.P. Kohman (1958)

Ret-50 G. Reitweiser, W. Metropolis, Table of Atomic Masses, U.S. Atomic Energy Commission, NP-1980 (1950)

Sah-46 Saha, Saha, Trans. Natl. Inst. Sci. India 2, 193 (1946)

Sch-35 J. Schintlmeister, Sitzber. Akad. Wiss. Wien Math.-naturw. Klasse, Abt IIa, 144, 449 (1935)

Sch-36 J. Schintlmeister, ibid 145, 475 (1936)

Ste-57 F.S. Stephens, Jr. F. Asaro, I. Perlman, Phys. Rev. 107, 1091 (1957)

Swa-56 N.K. Rama Swamy, Nuovo Cimento 4, 1570 (1956)

Str-58 D. Strominger, J.M. Hollander, G.T. Seaborg, Revs. Mod. Phys. 30, Part II (1958)

Szt-53 D. Szteinsznaider, J. phys. rad. 14, 465 (1953)

Tay-35 H.J. Taylor, Nature 136, 719 (1935)

Tay-36 H.J. Taylor, V.D. Dabholkar, Proc. Phys. Soc. (London) 48, 285 (1936)

Tho-49 S.G. Thompson, A. Ghiorso, J.O. Rasmussen, G.T. Seaborg, Phys. Rev. 76, 406 (1949)

Tot-58 K.S. Toth, J.O. Rasmussen, Phys. Rev. 109, 121 (1958)

Var-56 Y. Pal Varshini, Nuovo Cimento 3, 1148 (1956)

Wal-53 E.C. Waldron, V. Schultz, T.P. Kohman, NYO-3621 (1953)

Wal-54 E.C. Waldron, V.A. Schultz, T.P. Kohman, Phys. Rev. 93, 254 (1954)

Wea-50 B. Weaver, Phys. Rev. 80, 301 (1950)

Wei-37 C.F. v Weizacker, Z. Physik 96, 431 (1935)

Wil-38 T.R. Wilkins, A.J. Dempster, Phys. Rev. 54, 315 (1938)

Wil-49 F.C. Williams, W.A. Aron, B.G. Hoffman, University of California Radiation Laboratory Report, UCRL-121 (1949)

Wil-50 G. Wilkinson, Phys. Rev. 80, 495 (1950)

Yeh-33 W. Yeh, Compt. rend. 197, 142 (1933)